Seton Hall University Dissertations and Theses (ETDs)

Seton Hall University Dissertations and Theses

Spring 5-1999

Insight into the Selectivity of Molecular Imprinted Polymers

Thomas Patrick O'Brien
Seton Hall University

Follow this and additional works at: https://scholarship.shu.edu/dissertations

Part of the Polymer Chemistry Commons

Insight into the Selectivity of Molecular Imprinted Polymers

By:

Thomas Patrick O'Brien

Dissertation submitted to the Department of Chemistry of Seton Hall University in partial fulfillment of the requirements for the degree of

DOCTOR OF PHILOSOPHY

in

Chemistry

May, 1999

South Orange, New Jersey

We certify that we have read this thesis and that, in our opinion, it is adequate in scope and

quality as a dissertation for the degree of Doctor of Philosophy.

APPROVED:
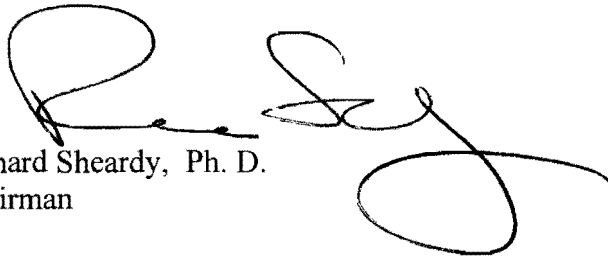
Nicholás H. Snow, Ph. D.
Research Mentor, Associate Chairman

Yuri Kazakevich, Ph. D.
Member of the Dissertation Committee

Nelu Grinberg, Ph. D.
Member of the Dissertation Committee

Richard Sheardy, Ph. D.
Chairman

Abstract

Insight into the Selectivity of Molecular

Imprinted Polymer Phases

Molecular imprinting is a relatively new technique used to prepare a polymer that selectively binds a particular target molecule. A molecular imprint is formed by placing a template molecule into a solution of monomers and initiating a polymerization. As the reaction proceeds, an 'impression' of the template is molded into the backbone of the growing polymer. When the polymerization is complete and the template is removed, the polymer can selectively rebind the template compound from a solution containing several related compounds. Preparing an imprinted polymer requires careful selection of monomer(s) that will interact with the template molecule during the polymerization and the selectivity of the polymer is sensitive to the number and strength of these interactions. In this work, we explore the interactions responsible for the selectivity of molecular imprinted polymers (MIP's) from two standpoints. First, the interactions governing the rebinding of a template to its imprint are characterized for a simple template-MIP system. It is shown that the template rebinds to the imprinted site by a cooperative process involving both complementary hydrogen bonding and steric interactions. Secondly, by Infrared (IR) Spectroscopy, we explore the interactions leading to a successful imprint of a sophisticated pharmaceutical molecule. In this study, the selectivity of the imprint is predicted based on the strength and number of the hydrogen bonding interactions observed between the template and monomers in solution prior to the polymerization. For both studies, the imprinted polymers are used as stationary phases in High-Performance Liquid Chromatography (HPLC) to evaluate their selectivity.

Acknowledgments

For the five years of my graduate school career, I have had the unique opportunity to grow as a scientist in both the academic and industrial worlds. This has been the perfect route for me to complete my doctoral degree, as the work I have pursued in this dissertation directly relates to my career interests. For this, I have to thank both of my advisors, Dr. Nicholas Snow and Dr. Nelu Grinberg for their expert tutelage, advice, and friendship.

I further acknowledge my research group at Seton Hall University and the several chemistry faculty members who encouraged and advised me in numerous ways: Dr. Yuri Kazakevich, Dr. Jerry Hirsch, Dr. Matthew Petersheim, Dr. James Hanson, and Dr. Richard Sheardy.

From Merck, I want to thank Charles Moeder, who was my supervisor for the past five years and is also my friend. He has made tremendous contributions to this work and my development as a scientist at Merck. There are countless others from Merck that deserve acknowledgment for their contributions, here are just a few: Dr. David Conlon, Dr. Thomas Dowling, Gary Bicker, Dr. Richard Thompson, and Thomas Loughlin. I also have to thank Merck and Company for providing me with this extraordinary opportunity and the financial support that went along with it.

As important to these contributions has been the support I have received from my family and friends. I appreciate the help from my brother and sisters. I also want to thank my father-in-law, Sal, for his help and unique perspective as both a father and a Ph.D. scientist. I especially want to thank my mother and father for their tremendous support over my entire 22 years of education. This would not have been achievable without them. Finally, I want to thank my wife, Karen, for her companionship and patience throughout my graduate career, something that I will always cherish.

Table of Contents

.

viii.

List of Figures

List of Tables

Chapter 1.

Introduction – Development of Chiral Chromatography

Chromatography

Chromatography is a process used to separate a mixture of compounds by distributing the compounds between two phases: a mobile phase and a stationary phase. This technique was invented nearly a century ago by a botanist named Michail S. Tswett, whose interest in the separation and purification of plant pigments lead to the first separation of these materials using a stationary phase made of paper [1-2]. A typical chromatographic system consists of a gas or liquid mobile phase that is passed over a solid or liquid stationary phase. These chromatographic techniques have thus been coined gas chromatography (GSC for a solid and GLC for a liquid stationary phase) and liquid chromatography (LSC for a solid and LLC for a liquid stationary phase) respectively. To achieve a separation, a mixture is introduced to one end of a chromatographic system composed of a mobile phase flowing through (or over) a stationary phase. The flowing mobile phase forces the components of the mixture to move toward the opposite end of the chromatographic system where detection occurs. In the process of traversing the chromatographic system, each component is distributed differently between the stationary and mobile phases. A component that interacts strongly with the stationary phase will spend more time in the stationary phase and, as a result, will be retained longer than a weakly interacting component that primarily remains in the mobile phase. Because each component arrives at the opposite side of the chromatographic system and is detected at a different time, a separation is achieved. For a chromatographic process controlled by thermodynamics, the separation of two components is achieved *only* when the free energy change (ΔG) upon

1

transferring from the mobile phase to the stationary phase is different for each component (see below). This free energy difference exists because the range of chemical interactions governing the distribution of a mixture of components between the mobile phase and stationary phase (i.e. electrostatic, dipole, and hydrophobic forces [3]) are often different for each component.

The development of High-Performance Liquid Chromatography (HPLC) in the late 1960's transformed Liquid Chromatography into a modern, efficient separation technique [4]. HPLC utilizes a chromatographic column packed with a small particles (μm dimensions) of stationary phase. The mobile phase is passed through the column using a high pressure pump and the sample is introduced to one end of the column through an injection valve. This technique achieves rapid, high resolution separations of components of a mixture. A block diagram of a typical HPLC system is given in Figure 1-1 [5].

Two major classes of liquid chromatography are characterized by the relative polarity of the stationary and mobile phases. 'Normal' phase liquid chromatography (NPLC) utilizes non-polar organic solvents as the mobile phase to foster interaction of the analyte with a relatively polar stationary phase [6]. Solute retention in NPLC is typically determined by one or more of the following interactions: hydrogen bonding, dipole-dipole, charge transfer. If several solutes exhibit different polar interactions with a NPLC stationary phase, then a mixture of these solutes are amenable to separation by this technique. Typical stationary phases for NPLC include bare silica gel and silica modified with polar organic groups. Reversed phase liquid chromatography (RPLC) utilizes phases that are the 'reverse' of NPLC, that is, a polar mobile phase and a non-

Figure 1-1 Block Diagram for a Typical HPLC System

Liquid chomatograph

Mobile
phase
reservoir

Pump

Injection
valve

Column

Detector

Waste

Recorder

Data processing
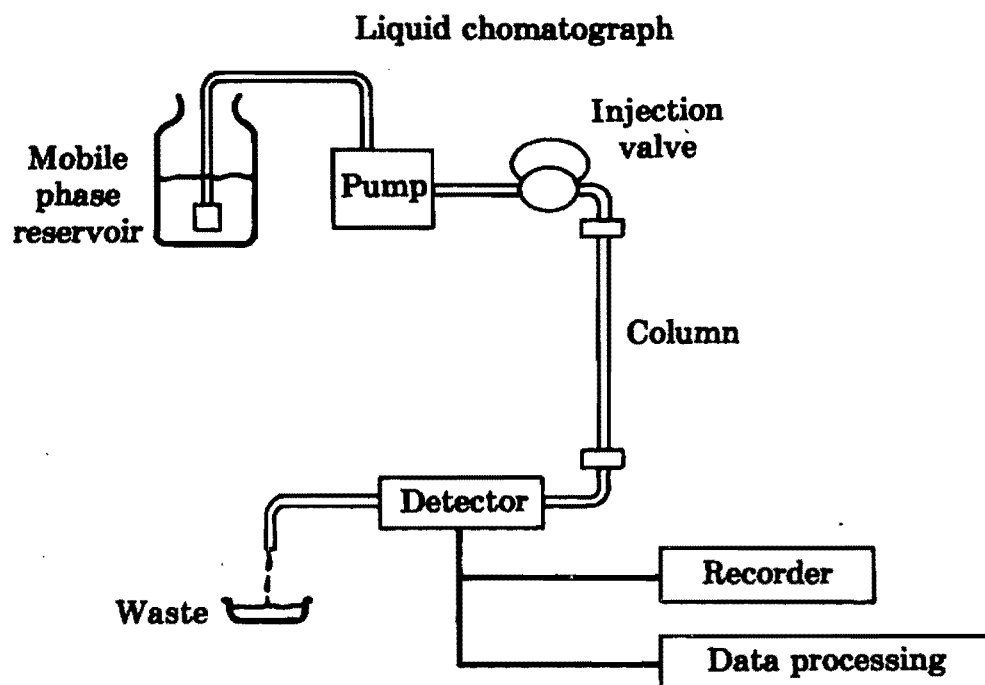
polar stationary phase are used [7]. The mobile phase used in RPLC is water modified with a polar solvent to foster hydrophobic interactions between the solute and the stationary phase. Two common hydrophobic stationary phases used for RPLC are silica modified with C-8 (RP-8) and C-18 (RP-18) hydrocarbon chains. Several solutes that possess different hydrophobic substituents can typically be separated by RPLC.

Retention and Selectivity in HPLC

Mechanisms

Depending on how an analyte interacts with the stationary phase, its retention may be described by either a partitioning or an adsorption process. Partitioning is a volume process that occurs when the stationary phase is thick enough to accommodate an analyte [8]. Thus, retention occurs by a distribution of analyte between the bulk mobile phase and bulk stationary phase. Some models for reversed phase chromatography attribute retention to a partitioning of the analyte between the hydro-organic mobile phase and the alkyl-silica bonded stationary phase, the latter phase likened to a layer of bulk liquid hydrocarbon on a silica surface [8-12]. However, this theory has been disputed in favor of pure adsorption or composite adsorption/partition mechanisms [13].

Adsorption is a process that occurs at a solid-liquid interface [8]. For HPLC, this type of retention process may exist for a liquid mobile phase and a porous, solid stationary phase that is impervious to the analyte [13]. In this case, retention occurs when an analyte in the mobile phase migrates to the solid phase and displaces adsorbed components of the mobile phase. Such a

4

displacement or competitive adsorption process dominates the retention in liquid chromatography utilizing polar stationary phases (i.e. NPLC) [13-15].

Analyte Equilibria

Retention of an analyte on a column can be related to the equilibrium distribution of the analyte in the mobile and stationary phases during the chromatographic process.

For a partition mechanism, the distribution of an analyte between the mobile and stationary phases is related to an equilibrium constant (K) for the ratio of the molar concentrations of analyte in the mobile $[A]_m$ and stationary phases $[A]_s$ [16]:

$$K = \frac{[A]_s}{[A]_m} \qquad\qquad [1\text{-}1]$$

The retention factor (k) of an analyte is can be measured from the retention volume V_r (or retention time t_r) of an analyte taken at the maximum of its chromatographic peak by the following:

$$k = \frac{(V_r - V_m)}{V_m} \qquad\qquad [1\text{-}3]$$

or

$$k = \frac{(t_r - t_m)}{t_m} \qquad\qquad [1\text{-}4]$$

where V_m is the volume of the mobile phase in the column or the 'dead volume' and t_m is the retention time of an unretained component that elutes in the dead volume of a chromatographic

run. Thus the retention factor can be calculated by the retention volumes (or times) from the peak maxima of the analyte and an unretained component. Figure 1-2 shows a chromatogram of a separation of two components with the retention time of each peak labeled.

The equivalence of expressions [1-3] and [1-4] arises from the relationship between the retention volume and mobile phase volumetric flow rate:

$$V = t_r \nu \qquad\qquad [1\text{-}5]$$

where: ν is the volumetric flow rate of the mobile phase.

For a partitioning mechanism, the retention factor is related to the equilibrium constant (K) by the following expression(s):

$$k = K\Phi \qquad\qquad [1\text{-}6]$$

where: $\Phi = [V_s]/[V_m]$ and V_s is the volume of the stationary phase in the column [17].

Combining equations [1-1] and [1-6] reveals the physical significance of the retention factor as the ratio of the molar amounts of analyte in the stationary phase (n_s) and mobile phase (n_m):

$$k = \frac{[A]_s [V_s]}{[A]_m [V_m]} = n_s / n_m \qquad\qquad [1\text{-}7]$$

Figure 1-2 Typical HPLC Chromatogram Showing the Separation of Two Components
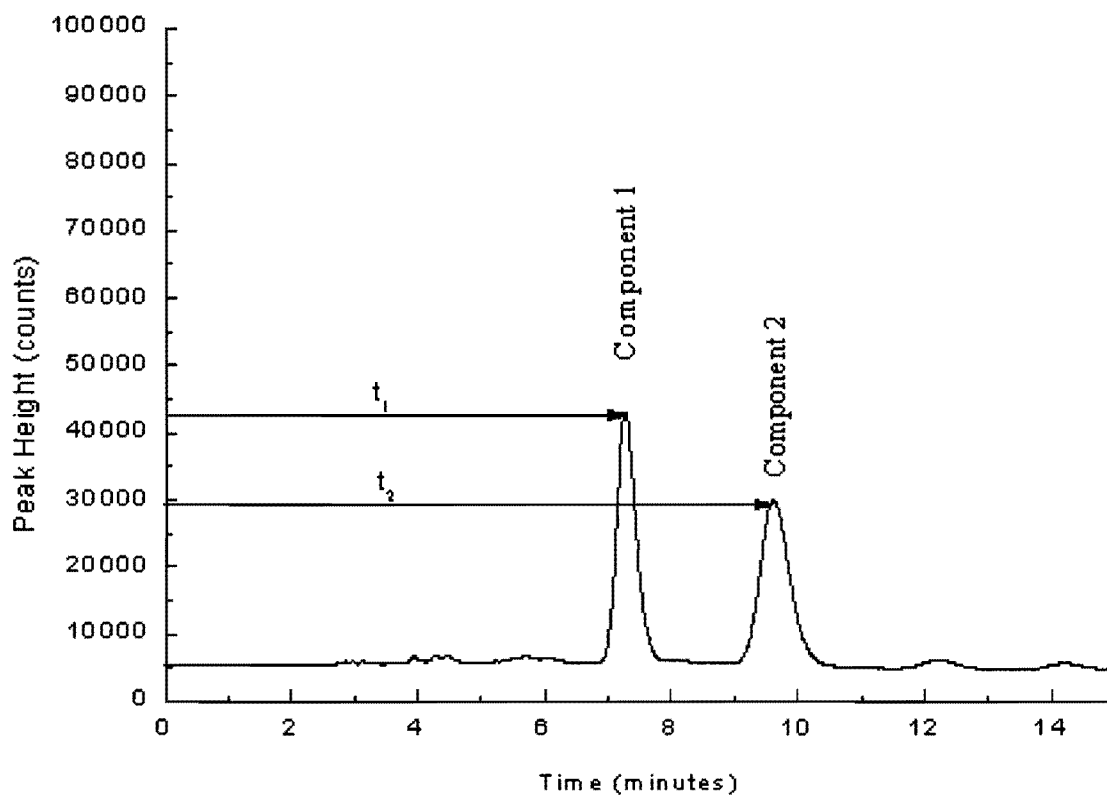
For adsorption processes, the phase ratio is more appropriately related to either the surface area (S) of the stationary phase [18-19] or the number of sites available to the analyte N_a on the stationary phases such that [20]:

$$k = K(S/ V_m) \qquad [1\text{-}8]$$

$$or$$

$$k = K(N_a / V_m) \qquad [1\text{-}9]$$

For equation 1-8, the equilibrium constant (K) is a Henry constant and for equation 1-9, K has units of M^{-1}.

Energetic Considerations

For both partitioning and adsorption processes, the distribution constant (K) for the analyte between the stationary and mobile phases is related to the thermodynamic parameters governing this distribution. Classical thermodynamics relates this equilibrium constant to the standard free energy change (ΔG^o) that the analyte undergoes as it transfers from the mobile phase to the stationary phase [3,16-17]:

$$\Delta G^o = -RT \ln K \qquad [1\text{-}10]$$

where: R is the gas constant, T is the absolute temperature, and

ΔG^o is the standard free energy for the transfer of the solute

from the mobile phase to the stationary phase.

The free energy can be expressed as:

$$\Delta G^{o} = \Delta H^{o} - T\Delta S^{o} \qquad [1\text{-}11]$$

Combining equations [1-2], [1-3], and [1-4] gives the following:

$$-RT \ln (k/\Phi) = \Delta H^{o} - T\Delta S^{o} \qquad [1\text{-}12]$$

which rearranged gives the van't Hoff equation:

$$\ln k = - (\Delta H^{o}/RT) + (\Delta S^{o}/R) + \ln \Phi \qquad [1\text{-}13]$$

Equation [1-6] predicts that a plot of ln k vs. 1/T will be a straight line with the slope of $-(\Delta H_{O}/R)$ and an intercept of $[(\Delta S_{O}/R) + \ln \Phi]$, providing that the thermodynamic parameters governing the separation (i.e. $-\Delta H^{o}$ and ΔS^{o}) do not change over the temperature range studied.

For separations utilizing a chiral stationary phase, the retention of each enantiomer of a chiral compound can be described by its own retention factor, k_1 and k_2, for the first and second eluted enantiomer. The ratio of these values is a measure of the selectivity (α) of the chiral phase for the two enantiomers, a large and small α indicating substantial and minimal enantioselectivity respectively:

$$\alpha = k_2 / k_1 \qquad [1\text{-}14]$$

9

From an energetic point of view, α can be related to the difference in the free energy of interaction of the two enantiomers in the chromatographic system:

$$\ln \alpha = -\Delta\Delta G^{o}/RT = -(\Delta\Delta H^{o}/RT) + (\Delta\Delta S^{o}/R) \qquad [1\text{-}15]$$

where: $\qquad\qquad \Delta(\Delta) G^{o} = \Delta G^{o}_{2} - \Delta G^{o}_{1}$

For an adsorption process, this difference in free energy takes into account the difference in free energy required for each enantiomer to desorb a competing mobile phase component from stationary phase. If the energy required to desorb the competitor is the same for both enantiomers, then the selectivity factor will be independent of the concentration of the mobile phase competitor. If the selectivity changes with mobile phase competitor concentration, this indicates that the energy to desorb the competitor is different at the adsorption sites available to each enantiomer. Thus, varying the mobile phase competitor concentration is useful in probing the nature of the sites on the stationary phase available to each enantiomer.

The chromatographic system does not only offer a means for separating a mixture of compounds, but it can also be used as a tool for investigating the magnitude of the thermodynamic forces driving the separation [3]. It is noteworthy that the above relationships are often too simplistic to calculate exact thermodynamic parameters [21], however, careful interpretation of the results of these calculations can provide an understanding of important thermodynamic *trends* associated with a chiral separation.

Separation of Enantiomers / Chiral Chromatography

Enantiomers are isomers whose molecules are chiral. A chiral molecule is defined as one that is not identical to its mirror image. Molecules that are superimposable on their mirror images are achiral.

The pioneering work of Pasteur marked the beginning of enantiomeric separations. He discovered that the spontaneous resolution of racemic ammonium sodium tartrate yielded two enantiomorphic crystals. Solutions of hand-picked crystals gave a levo or dextro rotation of polarized light. Because a difference in the optical rotation was observed in solution, he proposed that, like the two sets of crystals, the molecules were mirror images of each other. Furthermore, this discovery motivated Pasteur to study the influence of one asymmetric compound upon another and introduced the methodology of resolution via diastereomer formation. In his quest to understand the asymmetry and the specificity of biological systems, he proved that only the dextro isomer of a racemic tartrate was totally consumed by fermentation, while the levo remained intact. These three techniques: spontaneous resolution, diastereomeric separation, and differential enzymatic reactivity were, for more than a century, the only methods employed for enantiomeric purification [22].

Schlenk further contributed to the separation of enantiomers in 1952 with the introduction of urea inclusion compounds [23]. Urea forms inclusion compounds with a wide variety of variable straight aliphatic chain compounds. The long chain aliphatic molecules are included into hollow channels formed by the host molecule. The urea molecules form a right- or

left-handed screw along the channel, forming an enantiomorphous lattice, which includes enantiomers with different affinities. Trace amounts of chiral compound will induce the formation of only one of the chiral forms. This property of urea was utilized by Schlenk to resolve enantiomers such as chloro-octane with an enantiomeric yield of 95%.

Another approach was employed by Dickey [24] who produced silica gel in the presence of organic molecules. These molecules were later extracted, leaving an imprint. Such surfaces had a higher affinity for the imprinted molecule than other related compounds. Similarly, silica gel, can be produced in the presence of a chiral molecule leading to a surface with higher affinity for the imprinted enantiomer. For example, imprinting with (+)-N-methyl-3-methoxymorphinan produced a 30% enantiomeric enrichment of its racemate [25].

Introduction of chromatography produced a breakthrough for the field of chiral separations. It was understood that to achieve such separations, at least one of the phases (stationary or mobile) should have an asymmetry leading to a preferential complexation of one enantiomer. Complete separations were obtained using paper chromatography, while other asymmetric supports produced only partial or no resolution. In 1939, Henderson and Rule [26] demonstrated separation of d,l-p-phenylenediiminocamphor on d-lactose. In 1951, Kotake et al. [27] studied the influence of a chiral mobile phase on the resolution of a number of amino acids using paper chromatography and found that the separation was solely due to the cellulose stationary phase. The authors reported complete resolution of tyrosine-3-sulfonic acid and partial resolution of glutamic acid and tyrosine. Several other reports described chromatographic separation of other amino acids and their derivatives into their enantiomers using the same

12

support [28-31]. In 1952, Dangliesh [28], performing enantiomeric separation of phenylalanine derivatives, observed that 3,4-dihydroxyphenylalanine showed no resolution while closely related isomers could be separated. These results prompted Dangliesh to postulate that a necessary condition for chromatographic enantiomeric resolution is the existence of three- point simultaneous attachment between the resolvable amino acids and the cellulose surface. The 'three-point rule' is still widely recognized in the field of chiral separations today.

Currently, a host of chiral stationary phases are available including cyclodextrins [32], crown ethers [33], Pirkle phases [34], proteins [35], and cellulose derivatives [36]. The choice of a particular chiral phase is dictated by the nature of the enantiomeric compound to be separated.

The Importance of Chiral Separations

Over the past several years, the pharmaceutical industry has recognized the growing importance of developing optically pure drugs. In extreme cases, it has been shown that one enantiomer of a drug can have a beneficial effect while its optical antipode can be toxic. As a result, the industry has turned to techniques such as chiral resolution and assymetric syntheses to obtain the desired enantiomer of a drug. From a processing standpoint, this requires analytical techniques to control the chiral purity of the synthesis and the isolated drug. Chiral HPLC is commonly used for these types of applications.

The HPLC phases currently available for the analysis of chiral compounds are quite expensive and are often not stable under certain sampling conditions. These limitations often make it

difficult to analyze the chiral purity of in-process samples, which often contain a complex matrix of impurities and solvents that can destroy the typical chiral column. Furthermore, to separate a pair of enantiomers of interest, several chiral phases often need to be evaluated. Therefore, it would be desirable to have alternative chiral phases that are not only inexpensive and rugged over wider range of sampling conditions, but are also tailored to recognize a particular pair of enantiomers.

The research presented in this dissertation focuses on a relatively new class of selective phases known as molecular imprinted polymers (MIP's). For chiral chromatography, MIP's are prepared by imprinting an organic polymer with one enantiomer of a chiral compound and using the polymer as a stationary phase to separate a racemate of that compound. MIP's are an attractive alternative to traditional phases because they are both inexpensive to synthesize and extremely stable under most sampling conditions. Further, the selectivity of these phases for a pair of enantiomers is pre-determined, the imprinted enantiomer always elutes after its optical antipode. These advantages are prompting further studies of the technique in several laboratories in hope that MIP's can be exploited for commercial applications in the future. This dissertation reviews past MIP studies and applications and outlines the results of several experiments performed in our laboratory that probe the selectivity of two typical imprinted polymers. Our investigation utilizes these polymers as chiral stationary phases and exploits the chromatographic relationships developed above as a convenient tool to explore their selectivity. It is important to recognize, however, that these studies have been performed with a broader goal than preparing novel stationary phases for two compounds. Rather, it is hoped that the insight gained by these investigations will benefit the entire field of molecular imprinting.

Chapter 2.

Historical – Molecular Imprinting

Introduction

Interest in molecular imprinting, a technique for preparing adsorbents with sites selective for a particular molecule, is rapidly growing [37-38]. An imprinted polymer is formed by polymerizing a solution of monomers in the presence of a template molecule. Prior to the polymerization, a functional monomer is introduced to the reaction mixture that becomes associated with the template [39]. This monomer-template complex is then polymerized in the presence of a crosslinker to lock the orientation of the functional monomer and form a rigid polymer around the template. The template molecule is subsequently extracted from the polymer, leaving sites that are complementary in shape and functionality to the template. This process is schematically represented in Figure 2-1.

Molecular imprinting was first attempted by F.H Dickey in the 1950's [24,40] who precipitated silica gel in the presence of organic dyes. After removal of the dye, he found that the silica gel preferentially rebound its 'template'. Following this work, the first successful enantiomeric separation using imprinted gels was performed [25,41]. While the imprinting of silica gel appeared attractive, interest in the field dwindled because the selectivities of these gels, which were small to begin with, were easily lost [42]. The technique was revived in 1972 by G. Wulff et al. [43], who covalently imprinted glyceric acid derivatives into a crosslinked organic polymer. This technique was developed by G. Wulff [44-46] using the covalent approach and K. Mosbach et al. introduced the non-covalent approach to imprinting shortly thereafter. This pioneering work is the basis for most of the current research performed in molecular imprinting.

Figure 2-1 Scheme for Imprinting a Molecule
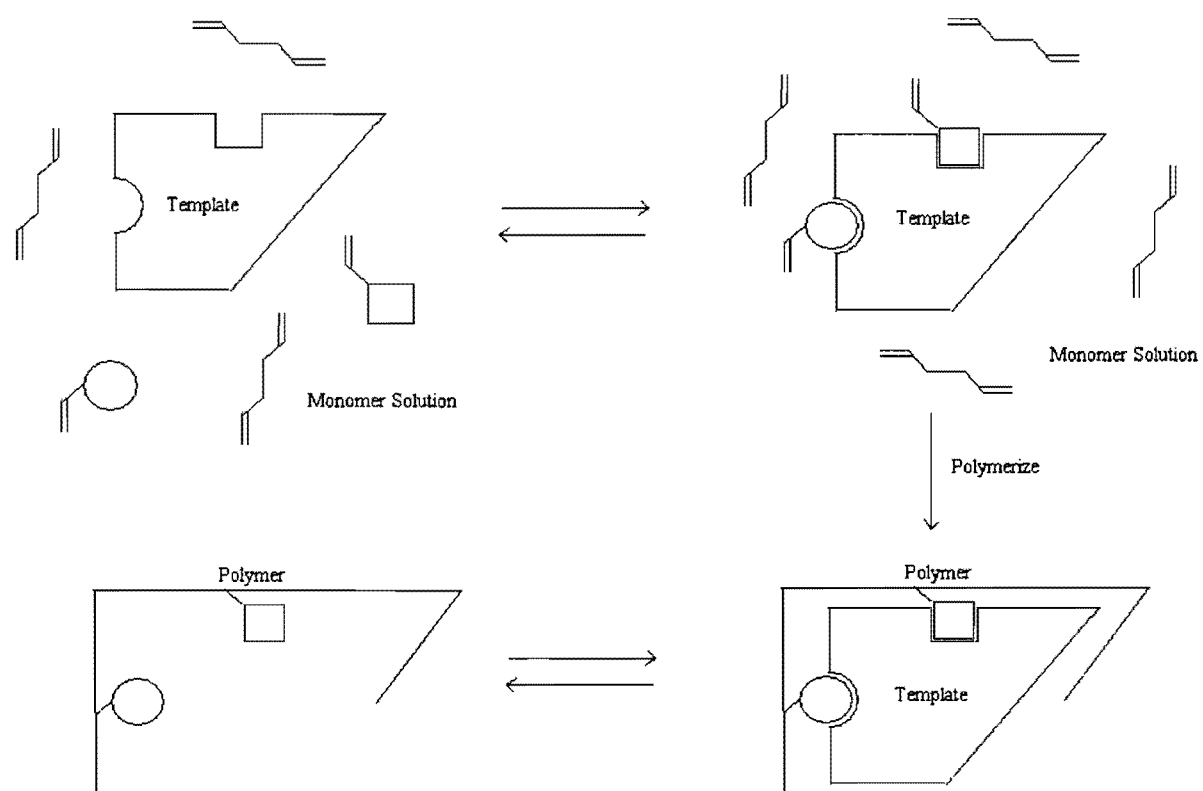
This chapter outlines the fundamental aspects of molecular imprinting and describes several scientific disciplines to which the technique has been applied. It concludes with a focus on the origins of selectivity of molecular imprinted polymers, the area of molecular imprinting that is explored in the remaining chapters of this dissertation.

Types of Molecular Imprinting

The key to synthesizing a successful imprinted polymer is achieving reaction conditions that favor the arrangement of functional monomer around the template during the polymerization. The method by which this monomer-template complex is maintained during the synthesis distinguishes the two major types of molecular imprinting that have been developed; covalent and non-covalent molecular imprinting.

Covalent molecular imprinting

In covalent molecular imprinting, the functional monomer is coupled to the template molecule by a reversible covalent bond during the polymerization [47-48]. This approach has been used to produce polymers selective for a host of compounds including glyceric acid derivatives [49-50], sugars [51-53], amino acid derivatives [54-55], ketones [56-58], and aldehydes[59].

One example of covalent molecular imprinting that has been extensively studied is the preparation of polymers selective for sugar derivatives [51-53]. The functional monomer 4-vinylphenylboronic acid *(1)* is used as the functional monomer because it undergoes a facile

esterification reaction [47] with cis hydroxyl groups of sugars and diols. The template-monomer

complex is polymerized with either a di-vinyl benzene *(2)* or ethylene glycol dimethacrylate *(3)*
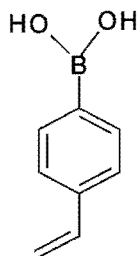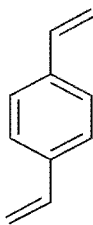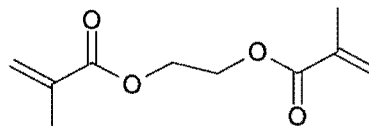
(1)   *(2)*   *(3)*

crosslinker to give a solid polymer. After removal of the template, sites are present in the

polymer that have an arrangement of boronic acid groups complementary to the sugar template.

An example of this process is presented in Figure 2-2. The resulting polymers were used in

either batch binding or chromatographic experiments and demonstrated selective binding of the

template in the presence of similar sugars. Similarly, ketones and aldehydes, have been

covalently imprinted by forming ketals [56-58] and Schiff bases [59] with the functional monomer.

Non-covalent molecular imprinting

The non-covalent approach to molecular imprinting utilizes functional monomers that

associate with the template through an intermolecular interaction such as hydrogen bonding or

ion-pairing [37]. Methacrylic acid *(4)* has been commonly used as a functional monomer in non-

covalent imprinting because it can undergo hydrogen bonding interactions with acid, ester,

(4)

18
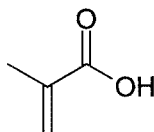
Figure 2-2 Covalent Imprinting of a Sugar Derivative [adapted from reference 47].
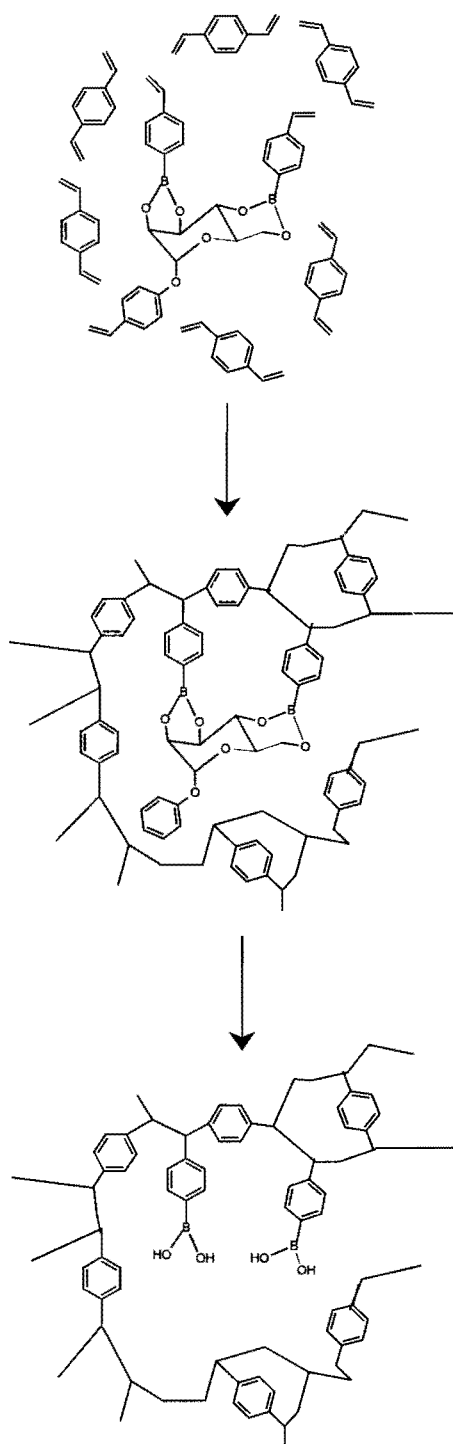
amide, and amine substituents [60-61]. The templates most commonly used for the study of non-covalent imprinting have been amino acid derivatives [60-65]. To prepare the imprinted polymer, the template is polymerized in the presence of methacrylic acid and crosslinker [48]. As the polymerization occurs, the monomers become locked into an orientation corresponding to the hydrogen bonding arrangement around the template. Subsequent removal of the template leaves a polymer with sites that have a shape and hydrogen bond selectivity for the template (Figure 2-3).

Applications of Molecular Imprinted Polymers

Prior to a discussion on the background of our research on the selectivity of molecular imprinted polymers, it is appropriate to first recognize the broad practical potential that molecular imprinting holds for a variety of areas. Such an understanding provides a strong justification for all of the current research focused on this technique. Thus, several recent applications of molecular imprinted polymers are outlined below.

Antibody Mimics / Sensors

Analytical techniques employing immobilized antibodies are often used to selectively bind and quantify a target compound in a complex sample. Traditional techniques such as the radioimmunoassay or Enzyme-linked immunosorbent assay (ELISA) indirectly measure the amount of the analyte-antibody complex formed [66]. More recently, immuno-sensors have been developed that directly measure the analyte concentration by monitoring either an electronic or spectroscopic change that occurs when a biomolecule (antibody, enzyme, etc.) modified surface binds a specific analyte [67]. Bioassays are advantageous because they exhibit

20

Figure 2-3 Non-Covalent Imprinting of an Amino Acid Derivative [adapted from reference 65]
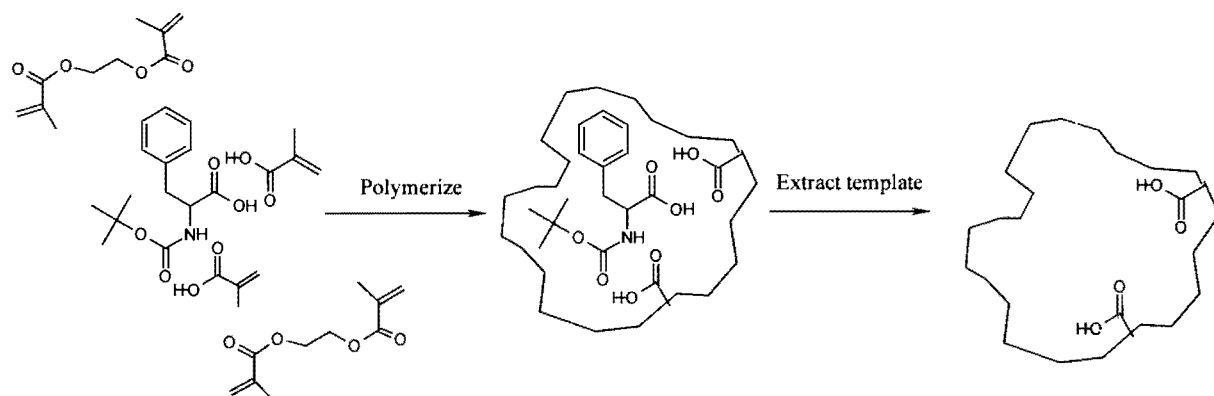
high specificity and sensitivity for their target compound. Unfortunately, the instability of most

biomolecular selectors in organic solvents and at extreme temperature or pH severely limits the

conditions under which this type of assay can be performed.

Molecular imprinted polymers are very stable and exhibit a binding specificity similar to

that of antibodies [68], making them ideal candidates to mimic antibodies in immuno-type assays.

In particular, MIP assays demonstrate excellent recognition in organic solvents, suggesting that

they may complement immunoassays, which must be performed in predominantly aqueous

media. As an example, MAA/EDMA imprinted polymers for theophylline and diazepam were

used as artificial receptors in a radioligand assay to quantify these drugs in human serum [69]. In

a manner similar to a traditional radioimmunoassay, the imprinted polymer was exposed to blood

extracts of the target drug spiked with standards of radio-labeled drug. After the competitive

binding of the analyte and radio-labeled analyte to the polymer reached an equilibrium, the

amount of unbound radiolabeled drug was determined by scintillation counting and related to the

concentration of drug in the sample. The linearity of the MIP-based assay was acceptable (μM

range) and the extent of cross-reactivity of the polymer with drugs of similar structure (a

measure of selectivity) was comparable to that of an antibody-based system.

Recently, a MIP radioligand assay was applied to the immuno-suppressive drug,

Cylosporin A, to determine the level of this drug in human serum [70]. The advantage of this

MIP-based system was that it could be used to directly analyze organic extracts of blood, unlike

the traditional immunoassay, which requires evaporation of the solvent and reconstitution of the

analyte in a buffer. Although it was observed that the assay could not differentiate between the

drug and very closely related metabolites, the MIP-based system appears to be a viable and convenient method for the determination of the total metabolite concentration of Cyclosporin A in serum.

Imprinted polymers have also been substituted for biomolecules in the design of several sensors using either electrochemical [71-73] or optical signal transducers [74]. For an electrochemical method, the MIP is immobilized on a conducting surface to achieve an intimate contact between the electrode and the MIP. The binding of an analyte to the MIP effects a measurable change in potential or current of the electrode and this response serves as the detection element of the sensor. Based on this premise, an MIP sensor was fabricated for morphine by immobilizing morphine imprinted polymer particles on the surface a platinum electrode [71]. To measure concentrations of morphine, the potential of the electrode was held above the oxidation potential of drug as it was exposed to a sample solution. After the circuit reached an equilibrium current, a known amount of an electro-inactive codeine analogue of morphine was spiked into the system to compete with morphine for imprinted sites on the electrode. The disturbance caused by the displacement of morphine by codeine resulted in a peak in the oxidation current that was related to the amount of morphine in the sample. The measurable concentration range and limit of detection of this MIP sensor was determined to be 0.1-10 μg/mL and 0.05 μg/mL. Importantly, it was demonstrated that the MIP sensor was stable at high temperature, extreme pH, and in organic solvents [71].

Several MIP optical sensors have been devised utilizing fluorescence detection. In one example, an enantioselective fiber-optic sensor was fabricated for a fluorescent compound,

dansyl-phenylalanine [74]. The vinylpyridine/MAA based polymer that had previously demonstrated optimum selectivity for Dns-l-Phe [75] was employed in this study. The MIP particles were immobilized between a nylon net and the quartz window of a fiber-optic device (Figure 2-4.) and the resulting MIP probe was exposed to acetonitrile solutions of each enantiomer of Dns-Phe. The probe was capable of distinguishing between the two enantiomers as evidenced by the significantly larger response generated by the imprint enantiomer at a particular concentration. The higher affinity of the immobilized polymer for the imprint enantiomer resulted in an enhanced concentration of this enantiomer at the probe tip and therefore a larger fluorescent response.

A novel monomer system was used by Turkewitsch et al.[76] to prepare a MIP based-fluorescence sensor for a non-fluorescent biomolecule, adenosine 3':5'-cylic monophosphate (cAMP) *(5)*. In this application, a fluorescent compound, trans-4-[p -(N,N Dimethylamino)styrylvinylbenzyl-pyridinium chloride *(6)* and 2-hydroxyethyl methacrylate

(5)   *(6)*   *(7)*

24
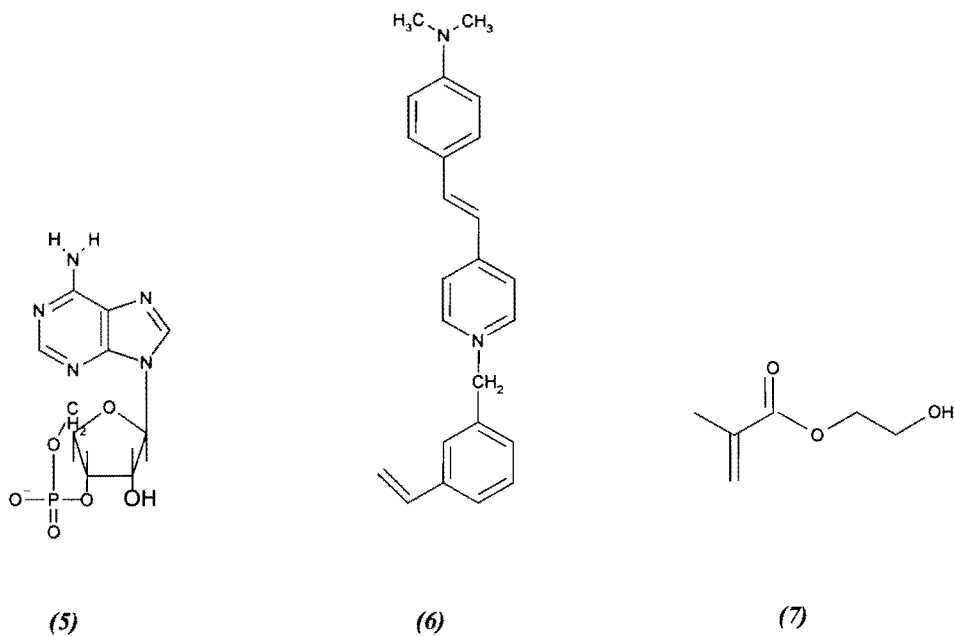
Figure 2-4. MIP-Based Optical Sensor for Dansyl-l-Phenylalanine [adapted from reference 75]
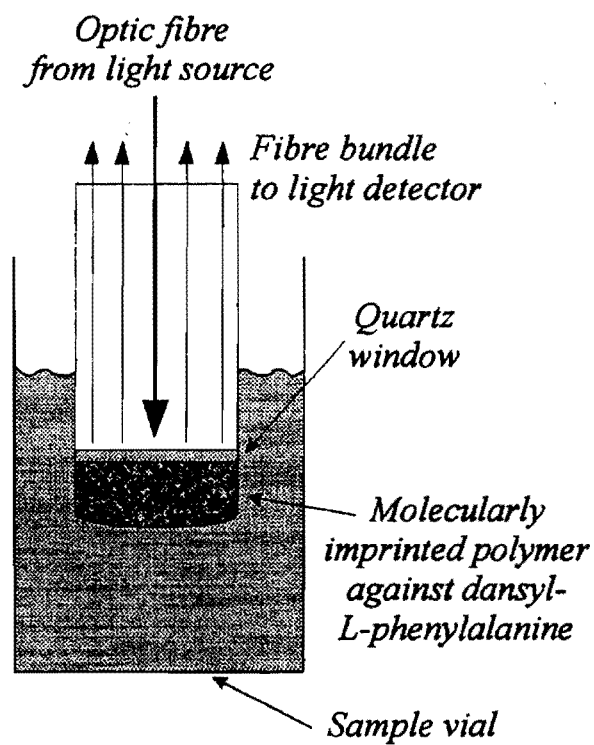
(HEMA) (7) were used as the functional monomers to form an imprint of cAMP. ('TRIM' refers to 2-ethyl-2-(hydroxymethyl)-1,3-propanediol trimethacrylate, a crosslinking monomer). The incorporated (6) residues resulted in a polymer that was it could be related to the amount of cAMP present. Because the MIP sensor did not respond to a structurally related compound, cGMP, and the non-imprinted reference polymer did not respond to either compound, the performance of this MIP sensor was likely a result of the selective binding of cAMP to the fluorescent imprinted sites on the polymer (Figure 2-5). This type of sensor configuration suggests that tailor-made fluorescent recognition devices based on MIP's may be achieved for a host of biological molecules irrespective of their inherent spectroscopic properties. MIP-based optical sensors for sialic acid [77-78], 9-ethyladenine [79], and chloramphenicol [80] have also recently been reported utilizing either fluorescence or visible detection.

Solid Phase Extraction

Quantitation of a target analyte in a sample often requires a preparation step that isolates the target compound from matrix interferences or concentrates the analyte to a level that can be accurately determined. Typically, the pre-concentrated sample is then isolated from remaining impurities and quantified in a second step using a chromatographic technique such as HPLC. Solid phase adsorbents used for the purpose of sample pre-treatment are chosen based on their ability to selectively retain or elute the analyte of interest. To date, imprinted polymers have been useful in preparing selective sorbents for several analytes. Table 2-1. lists several analytes that have been subjected to SPE using imprinted polymers.

Figure 2-5. Proposed Scheme for cAMP MIP Sensor [adapted from reference 76.]

Decreased Fluorescence

cAMP
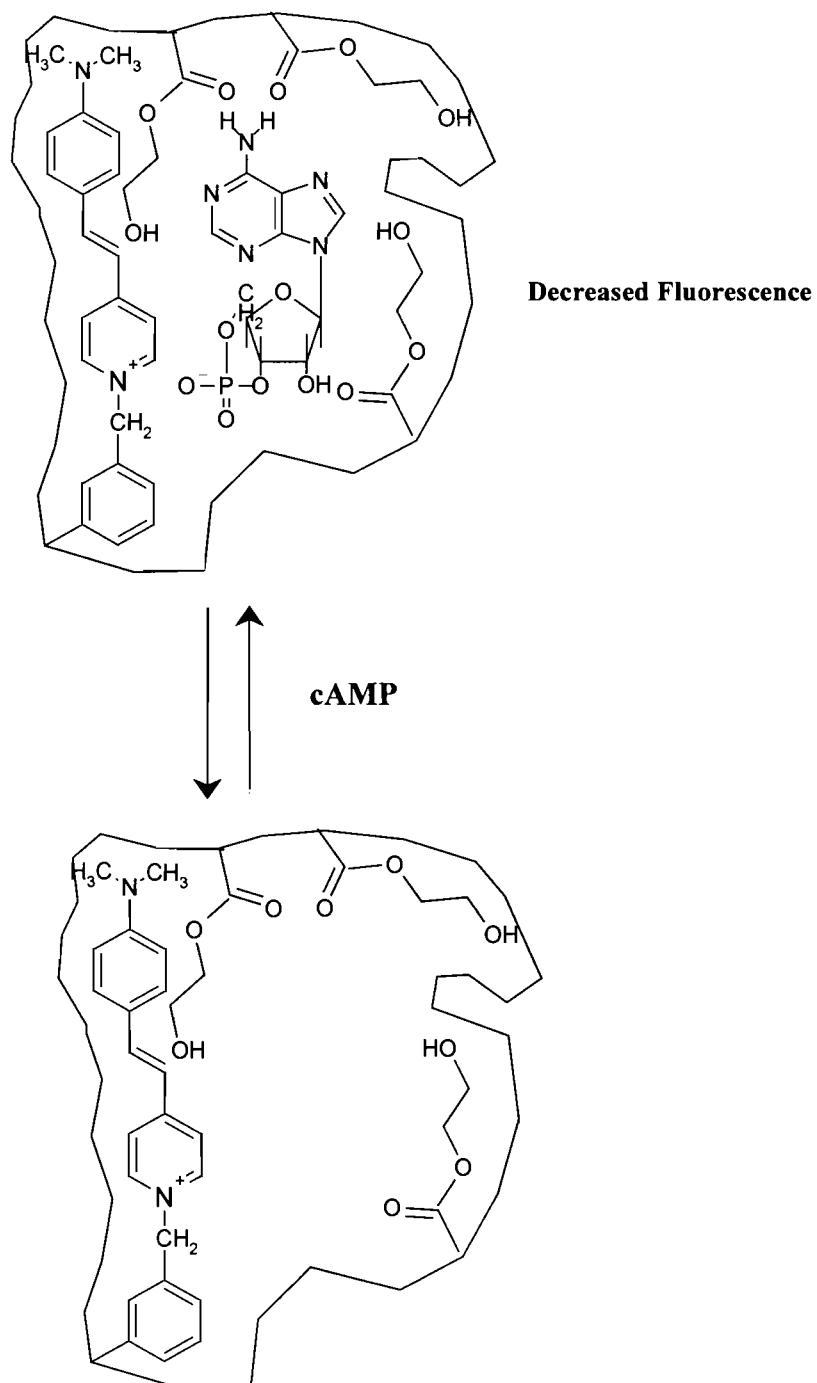
Table 2-1. Applications of MIP-Solid Phase Extractions

Compound	**Reference**
Pentamidine	[81]
Atrazine	[73, 82-86]
Aspartame Derivative	[87]
Sameridine	[88]
Theophylline	[89]
Nicotine	[90]

The utility of an imprinted polymer as a sample 'clean-up' medium is illustrated in a

report on the determination of a peticide, atrazine *(8)*, in beef liver [82].

$$Cl$$

(CH_3)_2CHNH \quad NHCH_2CH_3
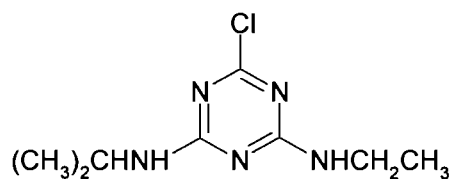
(8)

Crude chloroform extracts of beef liver were applied to a solid phase extraction device

employing an atrazine imprinted polymer as the sorbent. Careful optimization of the wash and

elution solvents applied to the extraction device resulted in significant removal of fats and lipids

from the sample and gave nearly quantitative recovery of atrazine. The eluted atrazine fraction

was then injected on a reversed-phase HPLC column. A comparison of typical HPLC

chromatograms of polymer purified and un-purified atrazine containing beef liver extracts are

presented in Figure 2-6. Because the major interfering peaks were eliminated, the accuracy and

precision of sub-ppm determinations of atrazine were significantly improved for the purified

(MISPE purified) samples.

In another application, a drug used to treat AIDS related pneumonia, pentamidine (PAM),

was imprinted and the resulting polymer was used to enrich and quantify the drug in samples of

urine [81]. The imprinted (PPAM) and reference polymers (PBAM) were prepared inside glass

tubes according to the procedure depicted in Figure 2-7. The reference polymer was prepared in

the presence of benzamidine (BAM) to achieve a similar monomer-template interaction during

Figure 2-6. HPLC Chromatograms of Beef Liver Extracts; 0.1 ppm spike of atrazine before

(A) and after (B) MISPE 'clean-up'. Arrow indicates atrazine peak [82].
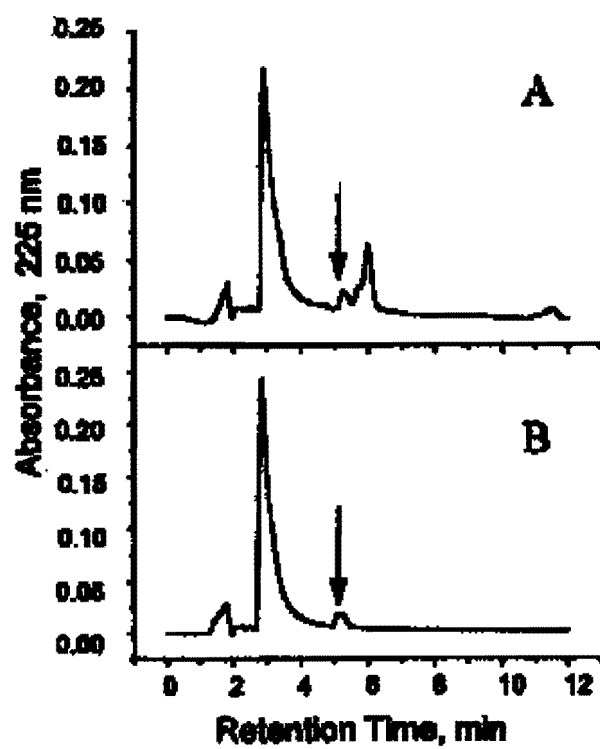
the polymerization and obtain a polymer with randomly distributed carboxyl groups. The retention and elution of PAM on each column was achieved by controlling the pH of the mobile phase, thereby controlling the electrostatic interaction between the protonated amidine of PAM and the carboxylate groups (Figure 2-7) on the polymer. In the procedure, a urine sample containing PAM was enriched by adjusting the sample to a pH at which PAM is retained (pH=5) and passing a fixed volume of sample through the column. The concentrated PAM was then eluted from the column at low pH (2-3) and determined directly by UV detection. For this method, the imprinted column enriched PAM at least 4 times greater than the reference column (Figure 2-8). Importantly, the authors noted that the highly selective polymer eliminated most of the interferences from the sample, thereby allowing for direct determination of PAM upon elution from the polymer. A secondary chromatographic or immunological step for the quantitation was therefore not necessary.

Recently, it has also been shown that the high selectivity of an imprinted polymer can be exploited to remove impurities from a reaction mixture. The desired product of the model reaction was an N-protected derivative of Aspartame, (α-L,L-ZAPM, **9**) [86]. A vinylpyridine/methacrylic acid polymer was imprinted with the β isomer of L,L-ZAPM *(10)*. The resulting MIP particles were used to extract a crude reaction sample of α-L,L-ZAPM, containing 59% α-L,L-ZAPM and 19% each of a β isomer (reaction impurity) and Z-L-aspartic acid (starting material, *11*). After five extractions of the reaction mixture with the imprinted polymer, the product purity increased from 59% to 96%. Further, the ability of the imprinted polymer to 'polish' the product was significantly better than a non-imprinted reference polymer,

31

Figure 2-7. Preparation of MIP Columns for PAM [81]
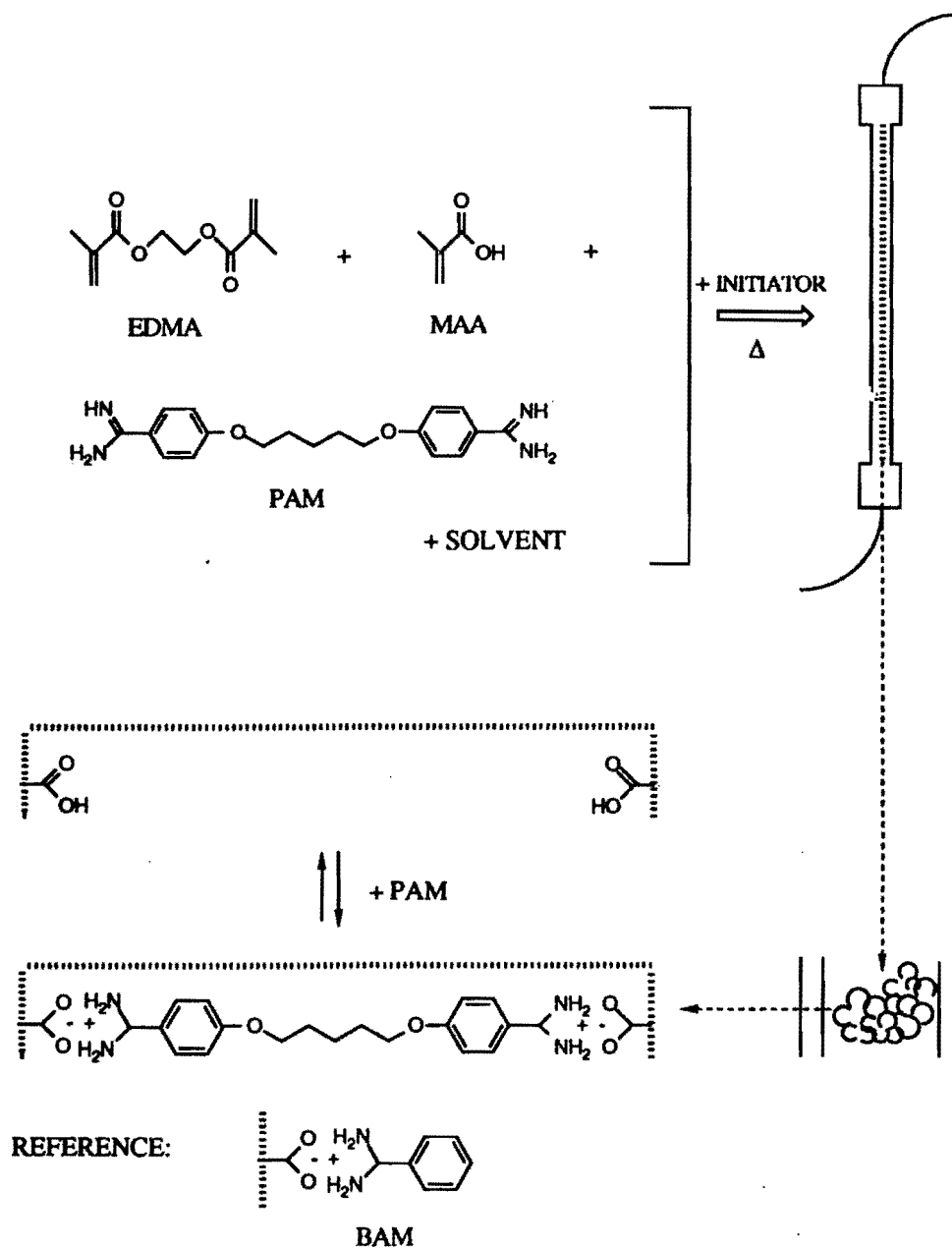
Figure 2-8. Desorption of PAM and BAM from PAM-MIP Column [81]

Desorption of PAM with a pH 2 mobile phase from PPAM (solid line) and PBAM

(dashed line). Flow rate: 0.1 mL/min. UV detection: 270 nm. Mobile phase:

acetonitrile/potassium phosphate buffer (0.05 M, 70/30 v/v).

1.0   0.5   0

Elution Volume

(9) *(10)* *(11)*
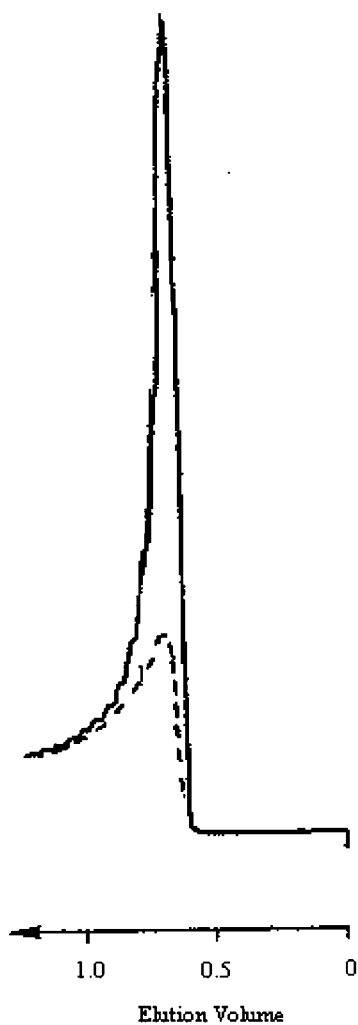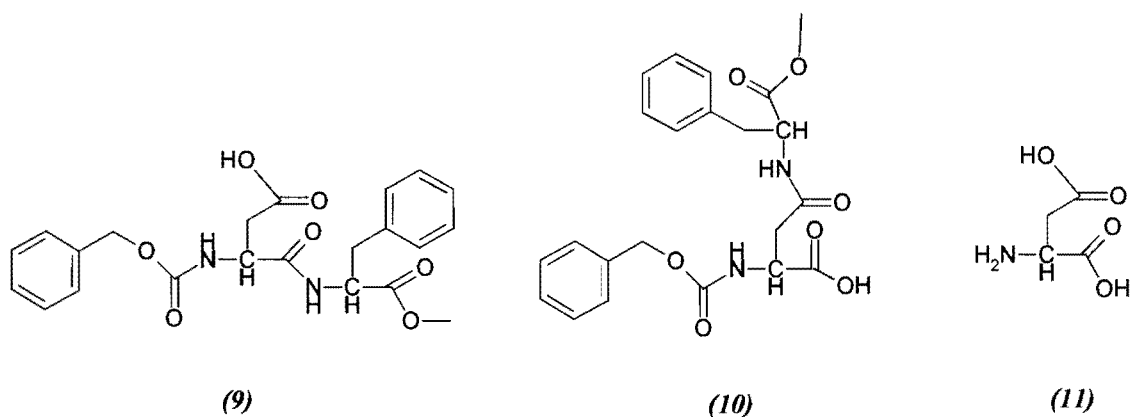
which only upgraded the purity of the crude α-L,L-ZAPM to 87%.

Enzyme Mimics / Catalysis

Enzymes catalyze reactions by providing a more energetically favorable pathway for the

reaction to occur as compared to the uncatalyzed system. The catalyst possesses sites that bind a

specific reaction substrate, such as the reactant or a transition state intermediate. Subsequent

interactions between the substrate and functional groups at the active site lower the energy of

conversion of the substrate to product. As a result, the rate of product formation is increased in

the presence of the catalyst. Molecular imprinting have been used to develop polymers

possessing catalytic binding sites [47,48,87-94]. Applying MIP technology to catalysis is

advantageous because the imprinted polymers are simple to produce, are stable [47] and can be

tailored to recognize almost any substrate. A molecular imprinted polymer facilitating the β-

elimination reaction of 4-fluoro-4-(p-nitrophenyl)-2-butanone *(12)* was synthesized using

methacrylic acid as the functional monomer [93]:

F O

-HF →

O

NO₂

NO₂

(12)
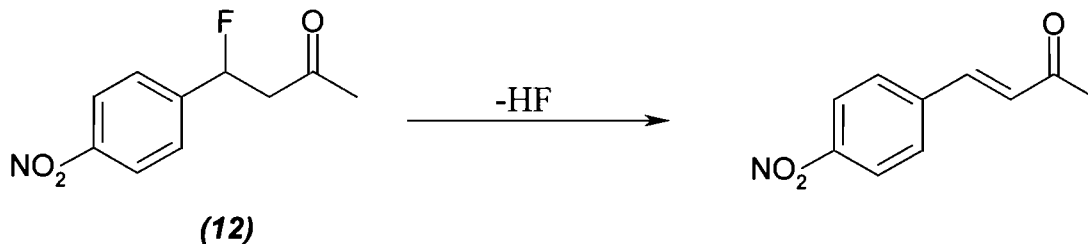
Several template molecules were evaluated, all of which were similar in structure to the substrate

and contained a complementary base (such as N-benzylisopropylamine) that directed the position

of the catalytic carboxyl group in the 'active site'. All imprinted polymers exhibited moderate

catalytic activity as demonstrated by an enhanced reaction rate relative to the control polymer.

The optimum incubation solvent was found to be acetonitrile containing 45mmol/L imidazole.

This medium facilitated the elimination reaction, presumably because it deprotonated the

carboxyl group of the 'active site' and minimized the non-specific interactions between the

polymer and substrate.

Imprinted polymers have been tailored to catalyze the hydrolysis of esters by imprinting a

transition state analogue of the substrate ester [89,94]. For the hydrolysis of p-nitrophenyl acetate

(13), Robinson and Mosbach [89] imprinted a phosphate analogue of p-nitrophenyl acetate *(14)*

achieve a polymer with catalytic sites complementary to the tetrahedral transition state of of the

substrate. Imidazole monomers were used in the synthesis because it is known that imidazole-

containing polymers catalyze the hydrolysis of active esters [95]. However, it was observed that

the imprinted polymer catalyzed the hydrolysis of *(13)* at a rate 60% greater than that of a blank

polymer prepared in the absence of *(14)*. Moreover, the rate of hydrolysis of *(13)* in the

(13)

(14)
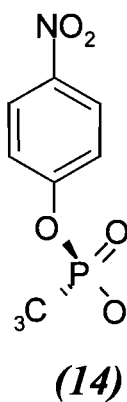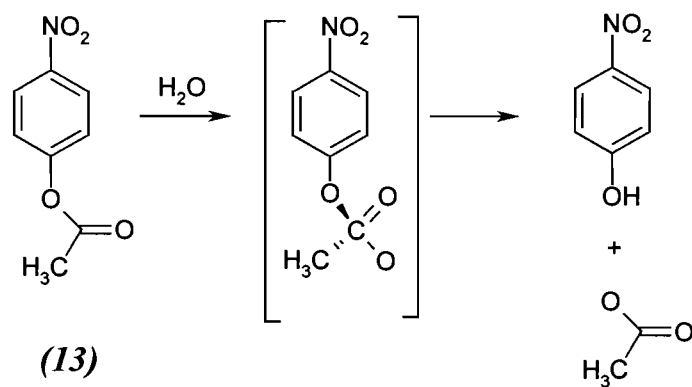
presence of the imprinted polymer was decreased when the template *(14)* was added to the reaction as an inhibitor. These observations suggested that cavities specific for the transition state analogue were formed during the imprinting step and binding of the substrate to these sites on the polymer facilitated the hydrolysis reaction.

Sellergren and Shea demonstrated that an imprinted polymer can be used to perform an enantioselective hydrolysis of a Boc-phenylalanine nitrophenylester [92]:

(15)
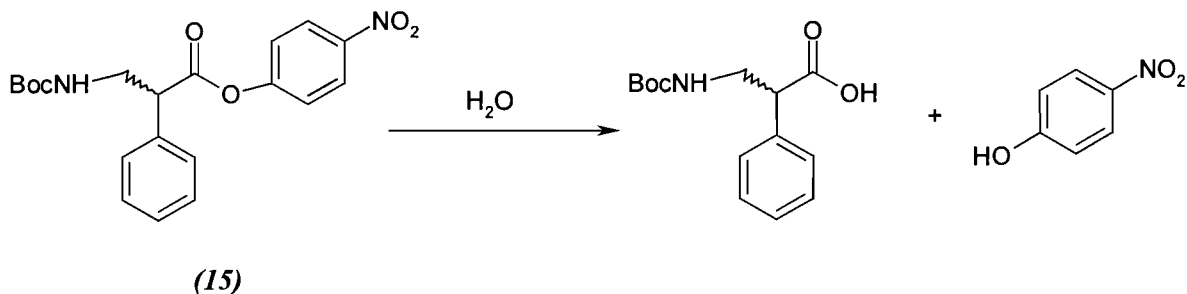
The chiral esterase site (Figure 2-9.) was formed by covalently imprinting *(16)* with a

MAA/EDMA polymer. Subsequent hydrolysis of the phosphate template afforded a polymer

(P1, Figure 2-17) that facilitated the hydrolysis of the D enantiomer of *(15)*. It was rationalized

that enantioselective binding and hydrolysis occurred due to the complementary arrangement of

the carboxylic acid and catalytic phenol-imidazole groups at the 'active' site. This was

supported by the observation that enantioselective activity was not observed for polymers

prepared with randomly distributed carboxyl groups and without the template molecule.

Reaction Directing / Equilibrium Shifting

Imprinted polymers have also been used for directing the stereochemistry of a reaction.

In one example, Bystrom et al. prepared a covalently imprinted polymer by crosslinking the

template *(17)* with divinyl benzene [91]. The template was subsequently removed from the

polymer by reducing the ester attachment with $LiAlH_4$, leaving an alcohol moiity near the 'C17'

portion of the imprint. The polymer was treated with additional $LiAlH_4$ to convert the hydroxyl

group to an active hydride, $-CH_3OAlH_3^{-1}$ after which it was used to selectively reduce *(18)* at the

C17 position.

(17)   *(18)*
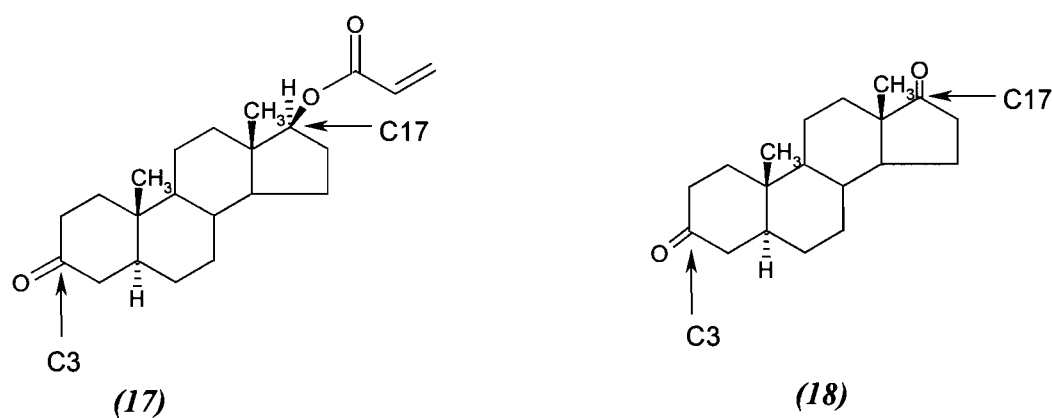
Figure 2-9. Formation of Molecular Imprinted Catalytic Sites for Hydrolysis of *(15)*.

[adapted from reference 92.]

38
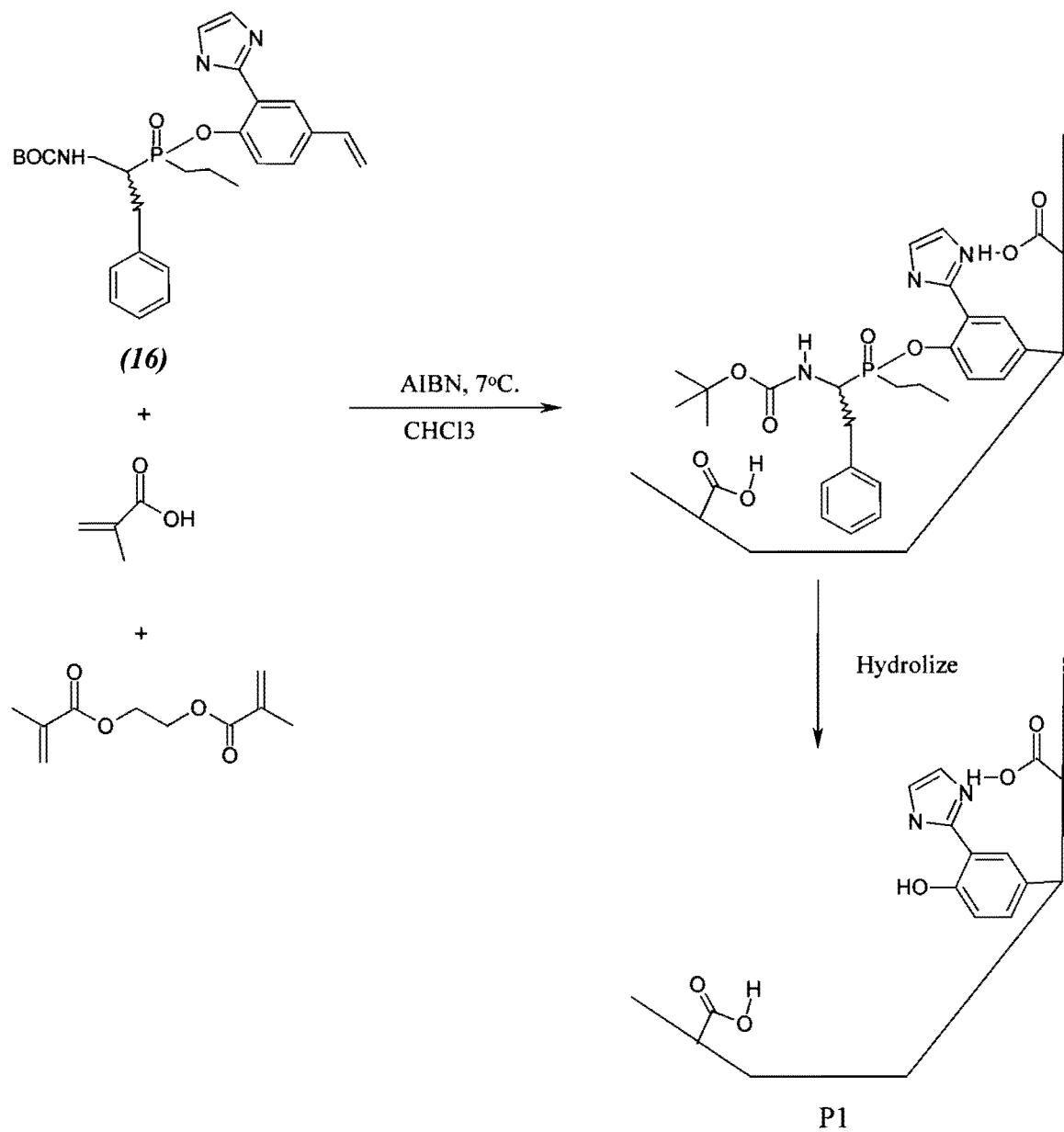
This contrasted the preferred reduction at position 3 that occurred in the absence of polymer. These observations suggested that the template *(17)* had created imprinted sites selective for *(18)* containing a hydride function close to the 17-carbonyl of the steroid. proximity to the hydride donor.

Imprinted polymers have also been used to shift the equilibrium of a reaction toward product by 'trapping' the product as it is formed. This was demonstrated by Ye and Ramstrom, for the synthesis of Z-α-Aspatame [86]. The reaction yield of Z-α-Aspartame was markedly increased (63%) when the reaction was performed in the presence of a polymer imprinted with the product as compared to the 'free' reaction (15%) performed in the absence of polymer.

Stationary Phases for Chromatography

The use of imprinted polymer particles as stationary phases in HPLC has been the most common application for molecular imprinting [51,54, 96-101]. For chiral separations, perhaps the greatest advantage of MIP's as chiral stationary phases is that the elution order of the enantiomers is predetermined. That is, the imprint enantiomer always elutes after the other enantiomer. Figure 2-21 shows the separation of racemic Boc-phenylalanine anilide using a MIP stationary phase imprinted with the L-enantiomer [65]. As suggested by the broad peaks, the efficiency of MIP columns are poor, especially for the imprint enantiomer. Aside from the physical irregularities of the MIP particles used to prepare the column, it has been proposed that the broad peaks are due to slow mass transfer of the analyte at the imprinted sites [96,101]. This is likely the case for small sample sizes. However, when large sample sizes are used, the capacity

Figure 2-10. Chromatogram Showing the Separation of Racemic Boc-Phenylalanine using a

MIP Column Prepared with the L-enantiomer. [adapted from reference 65.]

elution volume (ml)
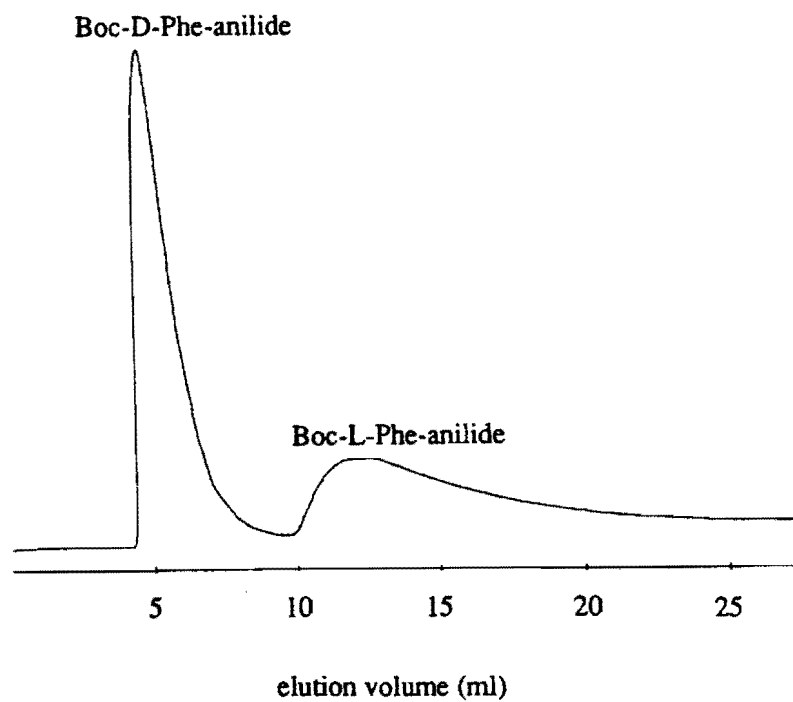
of the imprinted sites, which is typically small [102], is exceeded, making sample overload (i.e. a non-linear adsorption isotherm) the primary cause of band broadening and peak tailing [100].

Factors Influencing Selectivity

To prepare a molecular imprinted polymer by the non-covalent approach, the template molecule, functional monomer, and crosslinker are dissolved in a suitable solvent. A free radical initiator is added to the system and the solution is polymerized via either thermal or photolytic initiation. The template molecule is subsequently removed leaving sites in the polymer with a functional group arrangement and shape complementary to the original template. The polymer can then be used to selectively rebind the template itself, or analogs similar in structure to the template. The relative contribution of the shape and functional group arrangement of the imprint to the observed selectivity has been a subject of several studies [55,57,65,96,104-105]. It appears that both shape and functional group arrangement can play a dominant role depending on the type of template used.

Functional Group Arrangement vs. Shape Selectivity

For the covalent imprinting of sugars it has been shown that, one, two, or three functional groups per imprinted cavity give rise to enantioselectivity [103]. This indicates that the 'three-point' rule must be satisfied by a steric or 'shape' interaction for cases of only one or two functional groups per cavity. Interestingly, for these systems, it was found that 2-point binding, in general, gives the best selectivity [103]. It has been suggested that covalent three-point

rebinding processes may be too sterically demanding [103] or the kinetics of this process is too

slow to observe maximum selectivity. As a result, it is possible that a combination two-point

binding/steric interaction at the imprinted site is more favorable for selectivity. Nevertheless,

systematic changes in the structure of the rebinding sugar has shown that those with the same

stereochemical arrangement of hydroxyl groups to the original template are most strongly

rebound to the polymer [104-105]. As a result, it was concluded that the functional group the

complementary arrangement of functional groups at the imprinted site is the primary factor

determining selectivity while shape is less important.

For non-covalent molecular imprinting, it may be expected that the rebinding process is

more kinetically favorable as compared to a covalent process. As a result, it is possible that

more points of interaction at the imprinted site will yield better selectivity. This premise has

been demonstrated for the imprintation of one enantiomer of several phenylalanine derivatives

that differed in the number of hydrogen bonding groups that could interact with methacrylic acid

during the polymerization (Figure 2-11) [106]. It was postulated that templates with a greater

number of hydrogen bonding groups could direct more methacrylic acid units to the imprinted

site, leading to a site with greater selectivity. Changes were also made in the rigidity of the

template, assuming that a greater steric rigidity would also lead to sites with better selectivity.

The selectivity of the resulting polymers for the enantiomers of each template is given in Figure

2-11 alongside each structure. Changing the ester substituent to a more rigid amide, able to

undergo stronger hydrogen bonds with methacrylic acid improved the selectivity of the resulting

Figure 2-11. Imprinting of Several Similar Amino Acid Derivatives – Arrows indicate Points of

Interaction with Methacrylic Acid. [adapted from reference 106.]

α = 1.3

α = 2.0

α = 3.7

α = 1.8

α = 5.7
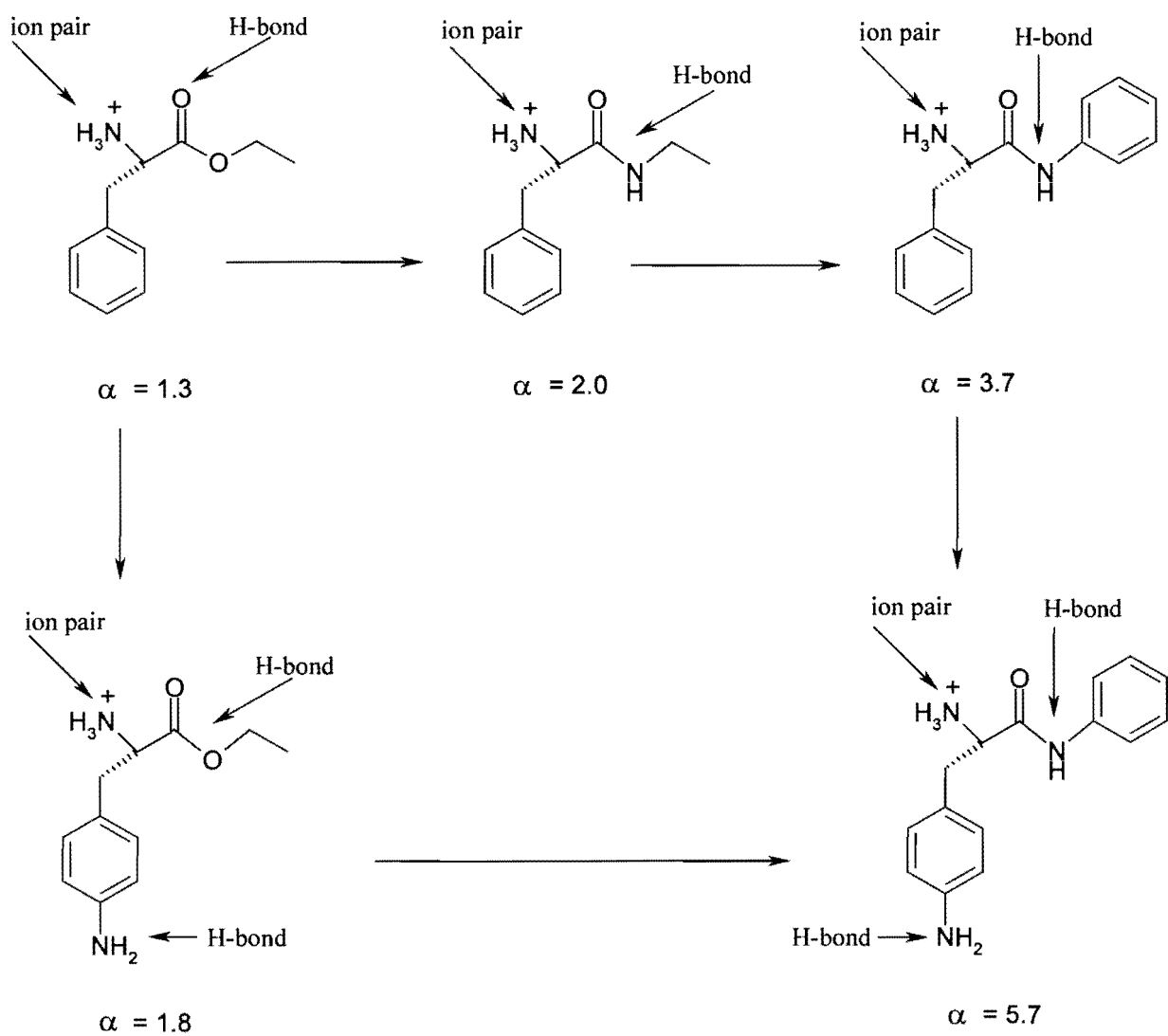
polymer from 1.3 to 2.0. Further, a change in the alkyl substituent to a more rigid and bulky phenyl group further increased the enantioselectivity of the resulting polymer (3.7). On the other hand, placement of an amino group on the phenyl side-chain of the original phenylalanine ester upgraded the selectivity from 1.3 to 1.8. Finally, a combination of the aromatic amide and amino group on the side chain increased the selectivity of the polymer to approximately four times that of the original polymer (1.3 to 5.7). This study clearly demonstrated that the interactive sites are only partially responsible for enantioselectivity. The steric bulk of the template molecule also determines the selectivity of the resulting polymers. In an extension of this study [55], it was observed that an additional amide or pyridinyl group on phenylalanine anilide also improved the selectivity of the resulting polymers (see below), the effect being substantial in the latter case.
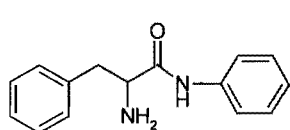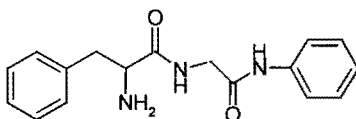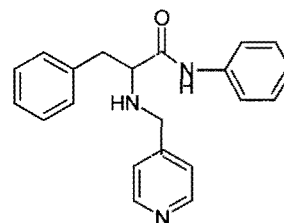
$\alpha = 4.1$ $\alpha = 5.1$ $\alpha = 8.4$

It was hypothesized that the pyidinyl group imparts extra rigidity to the template and provides a strong hydrogen bonding interaction with methacrylic acid during the polymerization, leading to a polymer with more defined recognition sites.

Rebinding experiments comparing the selectivity of imprinted polymer phases for the template and sets of enantiomers that differed from the template only by the shape of their substituents have also been performed in an attempt to isolate the contribution of shape to

selectivity. Such studies have revealed some conflicting results. In one study [65], the N-protecting group of the amino acid derivative was varied from the original imprint. In general, it was noted that the original template gave the best selectivity on its own imprinted polymer. Also, when the side chain of the amino acid derivative was varied, a similar trend was observed. For example, the enantioselectivity of a polymer prepared for a single enantiomer of *(19)* demonstrated better enantioselectivity for racemic *(19)* than a racemate of *(20)*. Based on this observation, the authors concluded that imprinted site for *(19)* should be able to accommodate the sterically smaller *(20)*, yet the better selectivity of the polymer for *(19)*, its own imprint, must be due to a stabilizing 'fit' of the side chain into the imprinted site.
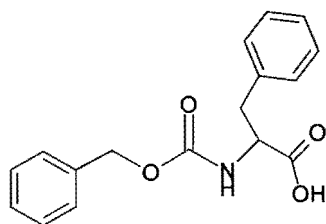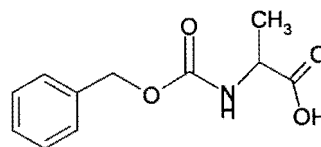
(19)   *(20)*

In this study, however, it was not clear if the interactions between the rebinding analyte and the imprint were also altered by the significant changes made in the shapes of the molecules.

In another report, the effect changing the amide substituent on the selectivity of MIP's prepared for amino acid derivatives was explored [55]. In one instance, an opposite trend was observed to that of the above report. For an imprint prepared for one enantiomer of *(21)*, the selectivity factor of the polymer for a racemate of *(21)* was 3.8, while a significantly better

selectivity factor (4.8) was observed for the enantiomers of a non-imprinted compound that possessed a less sterically hindered amide substituent *(22)*.
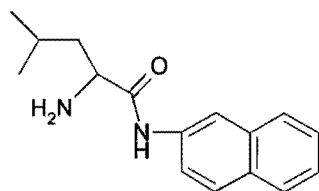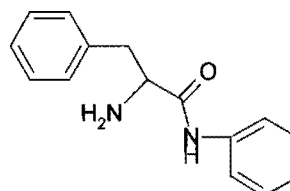
(21)   *(22)*

In this case, it appeared that *(22)* had better access to the imprinted site than the actual imprint and a tight steric fit of the molecule was not as important to the selectivity. We rationalized that this discrepancy may be due to relatively slow mass transfer kinetics of the imprint enantiomer with the phase. Since the retention of the enantiomers on this MIP column was assumed to be controlled by thermodynamics, a possible kinetic contribution may have been ignored.

One of the goals of the first study presented in this dissertation was to address two concerns alluded to above. First, to study the selectivity of an imprinted polymer, it is necessary evaluate the kinetics of mass transfer at the imprinted site to ensure that such thermodynamic phenomena are properly assessed. Also, a thorough study of the mechanism of rebinding of an amino acid template to its MIP is desirable to elucidate the contributions of both shape and functional group arrangement on the template to the selectivity of the imprinted site.

In other studies, further evidence suggesting that rigid, multi-functional templates give rise to highly selective polymers was indirectly demonstrated by the marked enantioselectivity

factors achieved for polymers imprinted with N-Ac-L-Phe-L-Trp-OMe [107] (*23*, α = 17.8) and

cinchonidine [108] (*24*, α = 31):
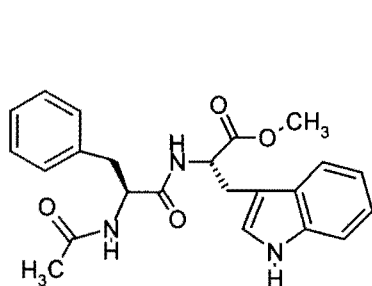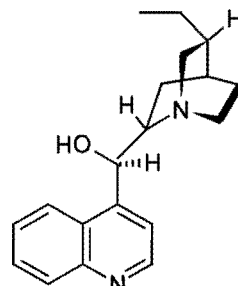
(23)   *(24)*

The relatively large selectivity factors observed for these molecules suggested that MIP

technology may be particularly useful for preparing selective adsorbents for sophisticated

molecules such as pharmaceutical drugs. Since MIP's may become an important tool for

analyzing drug levels in serum and urine, the goal of the second part of the research presented

within this dissertation was to provide a rational procedure for imprinting a sophisticated drug

compound such that the extent of the selectivity of the imprint could be predicted prior to

performing the polymerization.

The selectivity of MIP's are also dependent on the polymerization conditions. The most

important of these, polymerization temperature, polymerization solvent, and nature of the

functional monomer are described below.

47

Effect of Polymerization Temperature

Elevated temperatures and thermal initiators were initially used for molecular

imprinting [109]. O'Shannessy et al. attempted to increase the imprinting efficiency by preparing

an MIP at low temperature (0^0C) using ultraviolet initiation [63]. The template and functional

monomer used in the study were the l-enantiomer of phenylalanine anilide and methacrylic acid,

respectively. As hypothesized in earlier studies, initial NMR studies confirmed the presence of a

hydrogen bonded complex of methacrylic acid and phenylalanine anilide in the pre-polymer

solution [109]. The polymer prepared at 0°C showed a significantly better selectivity ($\alpha = 2.28$)

for a racemate of phenylalanine anilide than a similar polymer prepared at 60°C ($\alpha = 1.57$), when

both polymers were used as HPLC stationary phases. Other studies have also shown that

imprinted polymers formed at sub-ambient temperatures exhibit larger selectivity factors [39]. It

is believed that lower temperatures shift the monomer-template equilibrium toward the hydrogen

bonded complex, since the unfavorable entropy change associated with this process contributes

less to the total free energy change at lower temperatures [39]. As a result, more defined

recognition sites are 'stamped' into the polymer, leading to enhanced selectivity.

Effect of Polymerization Solvent

The nature of the solvent used for the polymerization also has a dramatic effect on the

selectivity of the resulting polymers. This was demonstrated by preparing several imprinted

polymers for phenylalanine anilide using solvents of varying hydrogen bonding capacity [110].

When solvents with relatively low hydrogen bonding capacity (CH_2Cl_2, CH_3Cl, benzene) were

used, the resulting polymers exhibited higher selectivity than those prepared in polar, hydrogen

bonding solvents (acetonitrile, dimethylformamide, isopropanol). It has been argued that polar

solvents, such as alcohols, compete with the functional monomer for interaction with the print molecule. In these solvents, the hydrogen bonded functional monomer-template complex is disrupted thereby producing polymers with reduced selectivity [111]. The same studies [110] also indicated that the porosity and surface area (as determined by nitrogen adsorption/desorption) of the polymers strongly depend on the solvent used prepare the polymer. For instance, polymers prepared in acetonitrile were macroporous with surface areas of approximately 250 m^2/g, while those prepared in chlorinated solvents (i.e., methylene chloride and chloroform) were essentially non-porous possessing very small surface areas (<10 m^2/g). However, the latter polymers demonstrated significant swelling in their solvent (approximately 2:1 v/v), suggesting that adsorbates probably have access to larger surface areas than is suggested by the measured porosity and surface area, which are obtained using dry polymer.

Effect of Functional Monomer

The nature and concentration of the functional monomer may be manipulated to enhance the formation of the monomer-template complex, thereby maximizing the selectivity of the resulting imprinted polymers. For instance, while methacrylic acid is a versatile hydrogen bonding monomer, vinyl-pyridine *(25)* has shown to be a better functional monomer for imprinting molecules possessing a carboxyl group [75]. For example, a dansyl-L-phenylalanine polymer imprinted using 2-vinylpyridine exhibited larger enantioselectivity (2.20) than a similar polymer imprinted using methacrylic acid ($\alpha = 1.49$). Furthermore, when both monomers were used simultaneously, the resulting polymers demonstrated even better selectivity ($\alpha = 3.15$). To explain these results, the author proposed that there is a concerted interaction of both functional monomers with the imprint molecule in the pre-polymer solution [75]. Namely, vinyl-pyridine
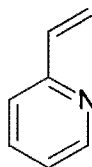
(25)

interacts strongly with the carboxyl group of dansyl-phenylalanine, while methacrylic acid

interacts more strongly with the sulfonamide and amino groups of the template (Figure 2-12).

Thus, using the two functional monomers maximizes the number and strength of the hydrogen

bonding interactions between monomer and template during the polymerization. In the same

study, it was also observed that methacrylic acid provided better selectivity for templates that

lacked a carboxyl group (e.g., Ac-l-Trp-OEt) [75], since this monomer is expected to hydrogen

bond with ester and amide functional groups better than vinyl-pyridine.

In other studies, it was observed that the tri-fluoromethyl analogue of methacrylic acid

provided polymers with better selectivity than those prepared using methacrylic acid for the print

molecules nicotine and triazine [112-113]. To explain these results, enhanced acidity of the tri-

fluoro monomer resulting in stronger interactions with the basic print molecules during the

polymerization was suggested [113]. However, it has recently been noted that methacrylic acid

provides polymers with better selectivity than tri-fluoromethacrylic acid for some templates [90],

suggesting that a hypothesis relating polymer selectivity to the strength of the acid-base

50

Figure 2-12. Proposed Imprinting Scheme for Dansyl-Phenylalanine using Two Functional

Monomers [adapted from reference 75.]
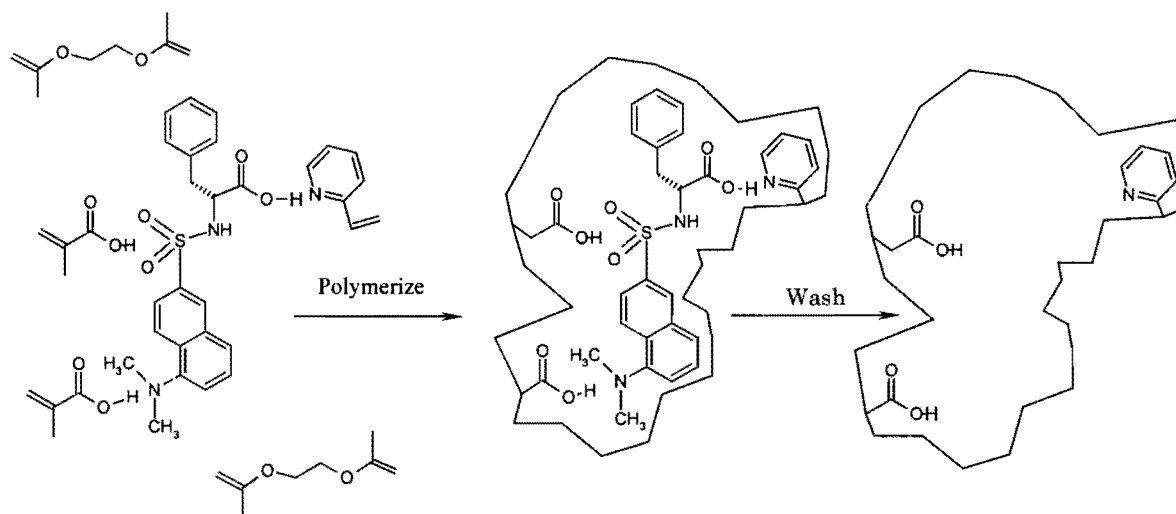
interactions occurring during the polymerization may be too simplistic or the strength of the hydrogen bonds between methacrylic acid and the template during the polymerization were unexpectedly stronger case than those between the template and the tri-fluoro monomer [90]. Since the strength of the hydrogen bonds between the monomers and the template in the pre-polymer solution were not investigated in these studies, no conclusion can be made about this premise.

The discrepancies observed in the selectivity of tri-fluoromethacrylic acid imprinted polymers and the recent observation that acrylamide *(26)* yielded imprinted polymers with better selectivity than methacrylic acid for some amino acid derivatives [37] suggest that the strength of
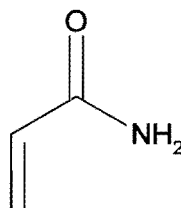
(26)

the hydrogen bonds between the template and the monomer in the pre-polymer solution must be empirically assessed before predications on the selectivity of the polymers are made.

In the study using acrylamide as the functional monomer, the authors argued that the superior selectivity for this monomer was due to stronger hydrogen bond formation with the template in the polar polymerization solvent [37]. This is not necessarily expected. Based on the substantially lower acidity of acrylamide relative to methacrylic acid, it may be argued that the

latter monomer will more effectively donate hydrogen bonds. Furthermore, several hydrogen bonding studies and quantum mechanical calculations performed on simple amide and acid systems (such as formamide, n-methylformamide, formic acid, and acetic acid) do not unambiguously reveal a definite order of strength for amide-amide, acid-acid, and acid-amide hydrogen bonds [114-118]. It can be concluded, however, that all of the above hydrogen bonds in their dimeric forms (two H-bonds between each functional group) are strong hydrogen bonds with a dimerization energy of >10 kcal/mol.

Based on the argument presented above, we rationalized that the strength of hydrogen bonds between different monomers and the template in the pre-polymer solution cannot be predicted without empirically evaluating their strength. This is not only because of the ambiguities observed for the strength of amide and acid hydrogen bonds, but also because the steric nature of the template may also determine the number and strength of the hydrogen bonds formed with a monomer in the pre-polymerization solution.

Thus, in our design of a MIP for a drug molecule, the strength and number of the hydrogen bonding interactions are more clearly defined in the pre-polymer solution by using an independent technique, IR spectroscopy. As such, it is believed that better conclusions are drawn about the strength of these hydrogen bonds and the selectivity of the resulting polymers.

Summary

A variety of applications utilizing imprinted polymers are becoming available alongside a growing research effort focused on characterizing the fundamental processes underlying the

selectivity of these phases. The goal of the remaining chapters of this dissertation is to attempt to address several fundamental aspects of molecular imprinting that are still not thoroughly understood.

Chapter 3.

Mechanistic Aspects of Chiral Discrimination
on a Molecular Imprinted Polymer Phase

Summary

The goal of the first part of this dissertation was to describe the interactions, both selective and non-selective, governing the rebinding of a simple template to its imprinted polymer. To achieve this goal, an imprinted polymer for dansyl-L-phenylalanine was used as a HPLC stationary phase. The chromatographic parameters manipulated in this study included temperature and the structure of the analyte. The temperature studies revealed that the mass transfer of the imprinted enantiomer with the polymer was sluggish at low temperatures, leading to a non-equilibrium migration down the column. Conversely, retention of the non-imprinted enantiomer was controlled by a thermodynamic equilibrium over the entire temperature range of the study. Variation of the structure of the analyte indicated a single leading interaction between both enantiomers of dansyl-phenylalanine and the polymer phase; a hydrogen bonding interaction between the carboxylic acid group of dansyl-phenylalanine and pyridinyl sites on the polymer. Secondary processes contributing to enantioselectivity were also deduced; a hydrogen bonding interaction occurring between the imprinted (L) enantiomer and carboxyl sites on the polymer and a precise steric fit of the amino acid side chain into the imprinted sites. Studies varying the mobile phase hydrogen bond competitor agree with the results obtained by the structural studies.

Introduction

The polymer used for this study has previously been used as a biomimetic sensor to selectively bind Dns-L-Phe from its optical antipode [74]. For this polymer, both methacrylic acid and 2-vinylpyridine were used as the functional monomers. It was shown that better enantioselectivity was obtained for this difunctional polymer as compared to similar polymers prepared using only one of the two functional monomers [75]. It was assumed that the acid group of Dns-Phe hydrogen bonds with vinyl pyridine and the dimethylamino and sulfonamide groups of Dns-Phe hydrogen bond with methacrylic acid during the polymerization [75]. Presumably, the hydrogen bonding monomers become locked into their hydrogen bonding positions after polymerization, leaving sites in the polymer that are complementary to Dns-L-Phe.

The Dns-L-Phe imprinted polymer incorporating both acid and pyridine groups was chosen as a model for our investigations because little attention has been given to the study of MIP's using multiple functional monomers. We believe that the use of multiple functional monomers for molecular imprinting will be important in further expanding this technique to more sophisticated molecules, such as pharmaceutical drugs. In this paper, we explore the types of interactions, selective and non-selective, occurring between this polymer and its imprint molecule, Dns-Phe, in an attempt to provide further insight into the mechanism of selectivity on this difunctional imprinted polymer phase.

Experimental

Instrumentation

The HPLC system consisted of a Spectra-Physics (Piscataway, N.J., USA) SP-8700 pump and a Waters (Medford, MA., USA) 715 ULTRA WISP autosampler. The column temperature was controlled by a Neslab RTE-110 (Newington, NH, USA) recirculating water / ethylene glycol bath. An Applied Biosystems (Foster City, CA, USA) 908 Fluorescence Detector (Excitation = 305 nm, Detection < 375 nm.) and a 757 absorbance detector set at 250 nm was used. The chromatographic data analysis was performed using P.E. Nelson (Cupertino, CA, USA) Access*Chrom software. The statistical analysis of the data were done using Origin software (Microcal, Northampton, Ma, USA). The FTIR spectrometer was a Nicolet (Madison, WI) and the particle size analysis was done by image analysis (Leica RMRD) with Qwin software (Cambridge, UK).

Reagents

The monomers ethylene glycol dimethacrylate (EDMA), methacrylic acid (MAA), and 2-vinyl-pyridine were obtained from Aldrich (Milwaukee, WI). Both enantiomers of dansyl-phenylalanine (Dns-Phe), dansyl-leucine (Dns-Leu), dansyl-alanine (Dns-Ala) and dansyl-valine (Dns-Val) were obtained from Sigma (St. Louis, Mo.). The AIBN initiator was obtained from Pfaltz and Bauer (Waterbury, CT.).

Synthesis of Dansyl-phenylalanine Methyl Ester

Each enantiomer of dansyl-phenylalanine methyl ester (Dns-Phe-Me-ester) was prepared by dissolving 300 mg (1.4 mmol) of either L-or D- phenylalanine methylester hydochloride

(Aldrich) in 100 mL of 70/30 v/v water/acetonitrile in a 500mL roundbottom flask. To this solution was added 100 mL of 3 equivalents (4.2 mmol) of sodium bicarbonate in water. As the solution was mixed with an overhead stirrer, 1.1 equivalents (1.5 mmol) of dansyl-chloride (Aldrich), in 50 mL of acetonitrile was slowly added (by syringe over 30 minutes in 10 x 5 mL increments) to the phenylalanine solution. The reaction conversion was monitored by RPLC; the product peak area versus the total area of the product and phenylalanine peaks was > 90% after the 30 minute addition period. The reaction was then stirred overnight giving >95% conversion to product. The solution was extracted with 250mL of toluene. The toluene layer was evaporated to dryness to afford the product as a yellow oil.

Synthesis of Napthyl-Sulfonyl-Phenylalanine

Each enantiomer of napthyl-sulfonyl-phenylalanine (Napth-Phe) was prepared in a similar manner to that of dansyl-phenylalanine methyl ester using L- and D-phenylalanine as the substrate and 1-naphthylsulfonic acid as the derivatizing agent. After the overnight age, the pH of the reaction solution was adjusted to 2.5 with formic acid and the product was extracted into toluene. The toluene layer was evaporated to dryness to afford the product as an oil.

Polymer and Column Preparation

The imprinted polymer was prepared by combining EDMA (65.5mmol), MAA (13.09mmol), 2-vinyl-pyridine (13.08mmol), dansyl-L-phenylalanine (1.64 mmol), AIBN initiator (100mg), and 20mL of dry acetonitrile (60ug/mL water by Karl Fischer titration) in a 200mL pyrex bottle. The solution was purged with nitrogen for 5 min. The bottle was capped tightly and placed in an oven at 55°C for 36 hours. The resulting solid polymer was removed

from the bottle and ground with a mortar and pestle and washed with 2 liters of 10% acetic acid in acetonitrile. The polymer particles were sized by passing them through 38 and 25μm sieves. Approximately 1 gram of the 25-38μm sized particles was slurry packed (in 10% acetic acid in acetonitrile) into an HPLC column (15cm x 0.46cm) at ~ 80mL/min using a Waters Preparative HPLC pump (Medford, MA., USA). The remaining particles were washed with methanol, dried under vacuum, and characterized by Diffuse-Reflectance IR spectroscopy: $3300cm^{-1}$ (O-H), $1742cm^{-1}$ (ester), $1636cm^{-1}$ (vinyl), $1569cm^{-1}$ (pyridine), $1550 cm^{-1}$ (pyridine). The mean particle size was determined to be 33μm by a MicroTrak particle size analyzer.

The imprinted polymer column was connected to the HPLC system and equilibrated with 4% acetic acid in acetonitrile until the system was equilibrated. Each time the mobile phase composition or temperature was adjusted, the column was re-equilibrated at the new conditions for at least 60 min. The samples were prepared by dissolving 5 mg of each Dns-Phe enantiomer in 100mL acetonitrile. A 5 μl volume of the sample was injected onto the column. Injections of acetone were used to estimate the void time (t_o) of the column. For convenience, the retention factor of each was calculated from the peak maximum instead of the first moment. For cases of peak tailing, (i.e., for the imprint enantiomer) this method actually underestimates the retention factor. However, for these studies, only the trend in the retention factor of each enantiomer is desired over the different chromatographic conditions, so using the peak maximum is justified.

For the structural variation studies, the samples were prepared in a similar manner with the exception that each enantiomer was dissolved and injected separately.

Results and Discussion

Typical Chromatograms

The mobile phase used to separate racemic Dns-Phe on the imprinted polymer column was acetonitrile modified with varying amounts of glacial acetic acid. Figure 3-1. shows the effect of increasing acetic acid concentration at a constant temperature (60°C). The second eluting broad peak is the imprinted (Dns-L-Phe) enantiomer. The broadness of this peak indicates that it undergoes a slower mass transfer with the polymer relative to the non-imprinted (D) enantiomer [119]. As the concentration of the acetic acid is increased from 4-8%, mass transfer kinetics increase and the peaks sharpen. At the same time, this increase in acetic acid concentration results in a decrease in enantioselectivity (from $\alpha=4.4$ down to $\alpha=2.7$). Figure 3-2. shows the effect of increasing temperature at a constant acetic acid concentration. There is a significant increase in resolution with temperature as a result of faster mass transfer kinetics.

Influence of Sample Size

Prior to the selectivity studies, it was necessary to evaluate the capacity of the imprinted polymer column for each Dns-Phe enantiomer. It has been shown that imprinted polymers have a limited capacity [120]. Figure 3-3. gives a plot of retention factor (k) for each enantiomer versus the logarithm of the weight of Dns-Phe injected. For the imprinted (L) enantiomer, the retention factor (k) is approximately constant for sample loads between ~30 to 300 ng, after which there is a smooth decrease in k with further increases in sample size. This behavior indicates that, for sample sizes above 300 ng, the binding of this enantiomer becomes non-linear [121] as the capacity of the sites available to this enantiomer is approached. On the other hand, k remains essentially

Figure 3-1. Chromatograms of Racemic Dansyl-phenylalanine.

a.) mobile phase: 4% acetic acid in acetonitrile; b.) mobile phase: 6% acetic acid in acetonitrile; c.) mobile phase: 8% acetic acid in acetonitrile; column temperature: 60°C; flowrate: 0.5mL/min; sample size: 300 ng each enantiomer; detection: fluorescence- excitation λ=305 nm, detection λ < 375 nm.

Figure 3-2. Chromatograms of Racemic Dansyl-phenylalanine.

a.) column temperature: 40°C; b.) column temperature: 60°C; c.) column

temperature: 80°C; mobile phase: 8% acetic acid in acetonitrile; flowrate:

0.5mL/min; sample size: 300 ng each enantiomer; detection: fluorescence-

excitation λ=305 nm, detection λ < 375 nm.
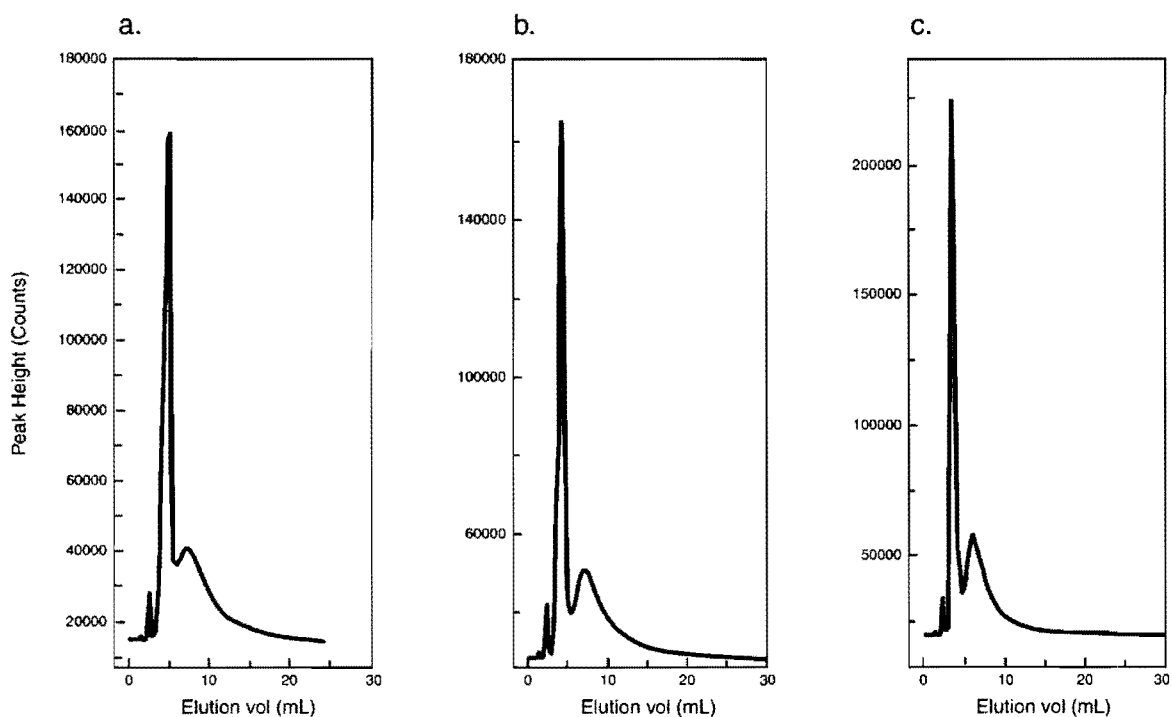
Figure 3-3. Effect of Sample Load on k for Each Dansyl-phenylalanine Enantiomer.

Mobile phase: 4% acetic acid in acetonitrile; flowrate: 0.5mL/min; sample size: 300

ng each enantiomer; column temperature: 60°C; detection: fluorescence- excitation

λ=305 nm, detection λ < 375 nm.
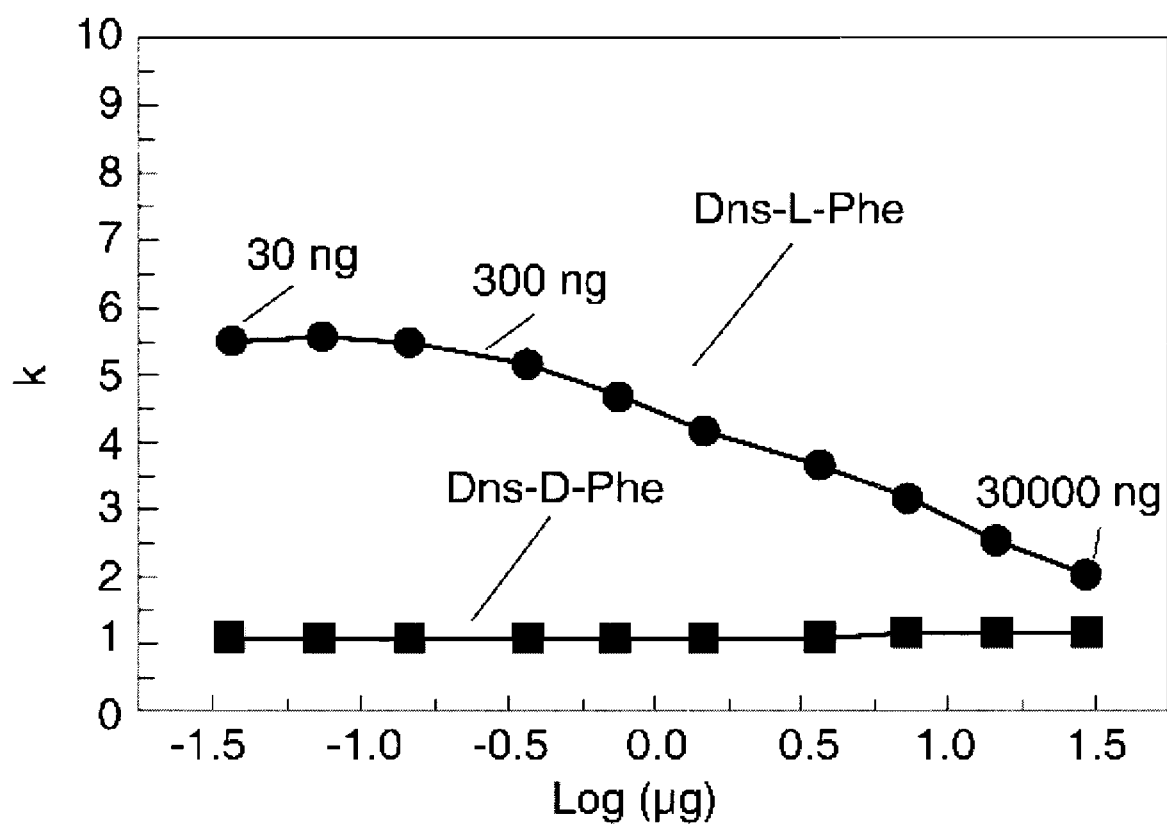
constant for the non-imprinted (D) enantiomer over the same loading range. These results

suggest that there are two distinct types of binding sites on the polymer. There are a limited

number of imprinted sites that bind the imprint enantiomer and there are also non-specific sites

that occupy the bulk of the polymer. Apparently, it is at the bulk non-selective sites where the

non-imprinted enantiomer interacts because overloading of this enantiomer is not observed. For

further experiments, a sample size of 300 ng of each enantiomer was used to ensure that

overloading effects did not impact the results.

Influence of Temperature

The retention factor (k) can be related to the change in enthalpy (ΔH^o) and entropy (ΔS^o)

of an analyte when moves from the mobile phase to stationary phase in a chromatographic

system by the van't Hoff equation:

$$\ln k = - (\Delta H^o/RT) + (\Delta S^o/R) + \ln \Phi \qquad \text{[3-1]}$$

where: Φ is the phase ratio and T is the absolute temperature. See Chapter 1. for a discussion on

van't Hoff plots.

van't Hoff plots in k were constructed for each Dns-Phe enantiomer at 3 different acetic acid

concentrations (4,6,8% in acetonitrile) between 25°C and 90°C. The retention factors (k) were

calculated from the peak maxima of each enantiomer. Initially, an assumption was made that the

peak maximum was a point of equilibrium between each Dns-Phe enantiomer and the polymer

phase [119]. A typical plot at 6% acetic acid is given in Figure 3-4. For the non-imprinted (D)

enantiomer, the plot is a straight line with a positive slope, indicating a favorable enthalpy change (-1.9Kcal/mol) when this enantiomer interacts with the stationary phase. On the other hand, a distinct curvature was observed in the van't Hoff plot for the imprinted enantiomer. At higher temperatures (60°C to 90°C), the plot was linear with a positive slope, but leveled off below 60°C with a slope approaching zero.

Prior to interpretation of the van't Hoff plots, it was necessary to test the assumption that an equilibrium exists at the peak maximum of each enantiomer. As shown in Figures 3-1 and 3-2, the band profile for the imprinted (L) enantiomer shows strong tailing, which suggests that there may be a kinetic contribution to the retention of this enantiomer [120]. It has been shown that slow adsorption/desorption kinetics can lead to a non-equilibrium migration of an analyte down a chromatographic column [121-122]. For a peak to be at equilibrium, the apparent retention factor (k) should be independent of the mobile phase flow rate. Thus, van't Hoff plots were reconstructed at a range of flow rates varying between 0.1 mL/min and 1.5 mL/min. An overlay of these plots is presented in Figure 3-5. For Dns-D-Phe, k is essentially independent of flow rate over the temperature range studied. Indeed, equilibrium is achieved for this peak and it is therefore reasonable to use the slope of this plot to determine $\Delta H°$. However, at lower temperatures, a dramatic difference is seen in the apparent k (k_{app}) for Dns-L-Phe at each flow rate, with a larger k_{app} observed at lower flow rates. As the temperature is increased, the change in k_{app} with flow rate is reduced and at higher temperatures (80°C-90°C), the retention factor becomes essentially independent of flow rate. The source of non-linearity in the van't Hoff plot for the Dns-L-Phe was therefore attributed to a strong kinetic contribution to its apparent

Figure 3-4. Typical Van't Hoff Plot for Dansyl-phenylalanine Enantiomers:

Mobile phase: 6% acetic acid in acetonitrile; flowrate: 0.5mL/min; sample size: 300

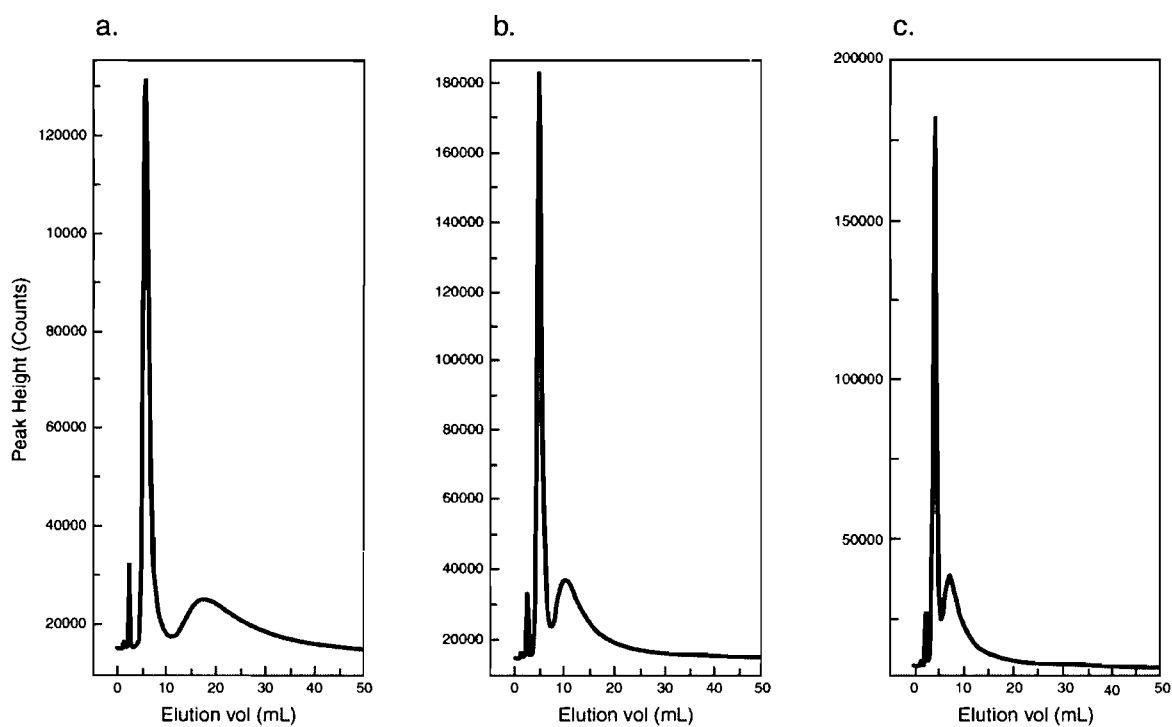ng each enantiomer; detection: fluorescence- excitiation $\lambda=305$ nm, detection $\lambda <$
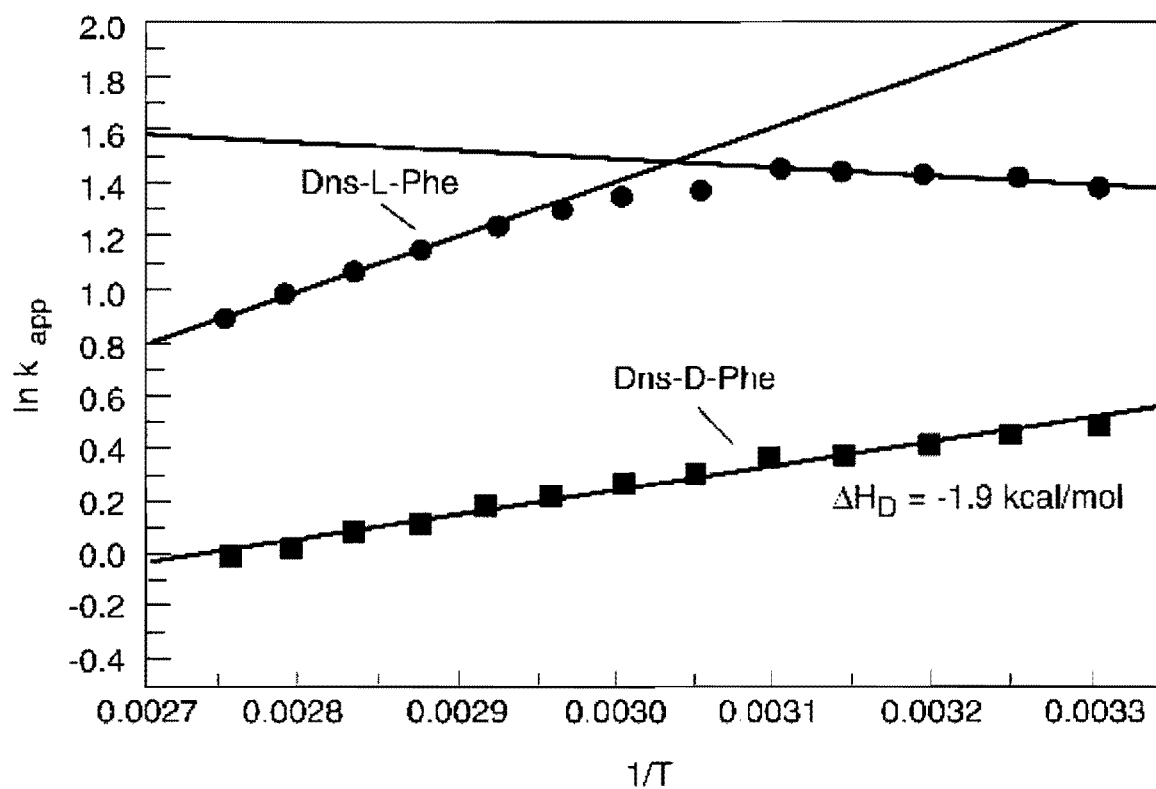
375 nm.

Figure 3-5. Van't Hoff Plots for Dansyl-phenylalanine Enantiomers at Different Flow Rates.

Mobile phase: 6% acetic acid in acetonitrile; sample size: 300 ng each enantiomer;

detection: fluorescence- excitation λ=305 nm, detection λ < 375 nm.
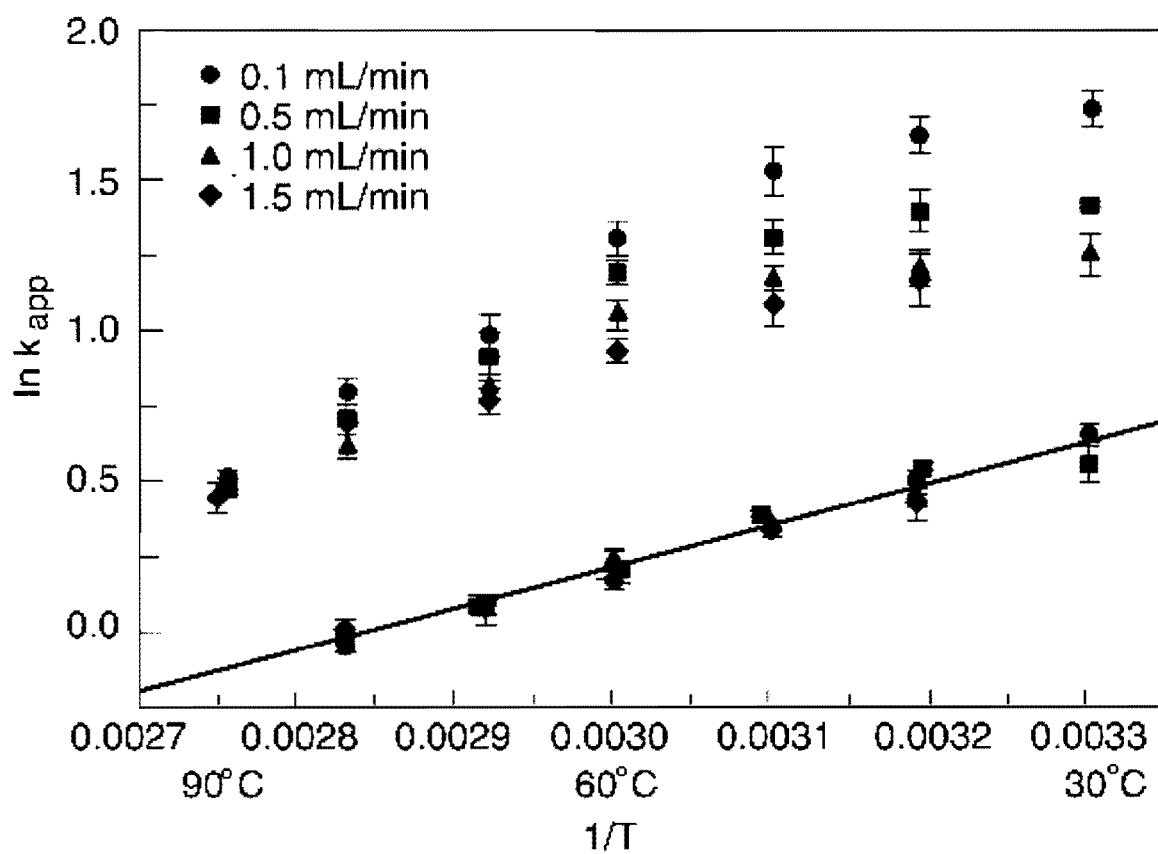
retention factor at low temperature. It is only at high temperatures (80°C-90°C), that the mass transfer of this enantiomer is rapid enough to achieve equilibrium and thermodynamic treatments become valid. For the structural studies presented below, the experiments were performed at elevated temperatures (90°C) to ensure that comparison of thermodynamic parameters such as selectivity (α) and $\Delta\Delta G^o$ are reasonable.

Influence of Structure

The processes underlying recognition on this Dns-L-Phe MIP was investigated by performing chromatographic experiments using the imprint molecule and several structurally related compounds. In an initial study, our goal was to characterize the role interactions at the carboxylic acid and dimethylamino groups of Dns-Phe play in the separation process. This experiment was performed by synthesizing two amino acid derivatives that each prevented potential interaction at one of these groups. Enantiomers of Dansyl-phenylalanine methyl ester (Dns-Phe-Me-ester) were synthesized to assess the importance of interaction between the carboxylic acid group and the polymer. Alternatively, each enantiomer of Napthyl-sulfonyl-phenylalanine (Napth-Phe) was synthesized to probe the importance of interaction at the dimethylamino group. The capacity factors and selectivity factors for Dns-Phe and these derivatives are listed in Table 3-1 below the structures of each compound. The results in Table 3-1. indicate that blocking the carboxyl group on the amino acid causes each enantiomer of Dns-Phe-Me-ester to travel through the column unretained. Apparently, interaction between this group and the polymer is the leading interaction providing retention of the enantiomers. It was hypothesized that this interaction occurs primarily between the carboxyl group of Dns-Phe and

.Table 3-1. Effect of Varying the Functionality of the Amino Acid Derivative. Mobile phase: 6% acetic acid in acetonitrile; flowrate: 0.5mL/min; sample size: 300 ng each enantiomer; column temperature: $90^{\circ}C$; detection: fluorescence- excitation $\lambda=305$ nm, detection $\lambda < 375$ nm.
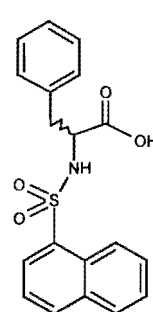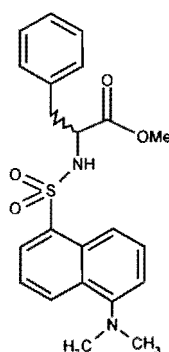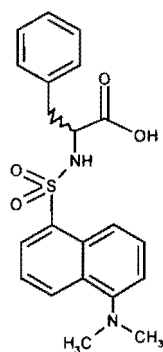
	Dns-Phe	Dns-Phe-Me-ester	Napth-Phe
k D-enantiomer	1.0	0.0	1.1
Δ H (kcal/mol)	-1.8	0.0	-1.9
k L-enantiomer	2.2	0.0	1.7
α	2.2	- -	1.5

pyridinyl groups on the polymer. Two experiments were performed to confirm this hypothesis.

First, a similar MIP was prepared for Dns-L-Phe omitting the pyridinyl monomer in the

synthesis. For a column prepared with this polymer, no retention was observed for both

enantiomers of Dns-Phe under the same mobile phase conditions. This eliminated the possibility

of a leading interaction existing between Dns-Phe and acid sites on the polymer. Further,

Diffuse Reflectance IR experiments were performed on the original polymer. A comparison was

made between the IR spectrum of dry polymer and a spectrum of polymer doped with acetic

acid. The spectrum for the polymer doped with acetic acid showed a distinct shift for one of the

pyridinyl ring stretch bands (from $1590cm^{-1}$ to $1600cm^{-1}$) as compared to the dry polymer. This

observation is consistent with the hypothesis that pyridinyl groups incorporated into the polymer

are accessible for hydrogen bonding with a carboxylic acid group. Further analysis of Table 3-1.

reveals that the D-enantiomers of Dns-Phe and Napth-Phe have approximately the same retention

factor (k) and enthalpy (ΔH°) of interaction with the polymer (as determined by van't Hoff

plots). However, the retention factor for the L-enantiomer of Napth-Phe is reduced by 20%

relative to that of Dns-L-Phe. As a result, a 30% decrease is observed in the enantioselectivity

(α) for Napth-Phe.
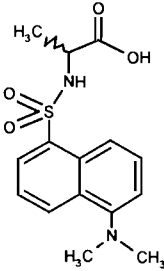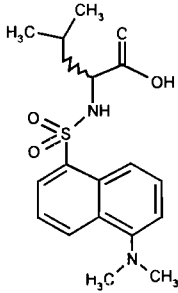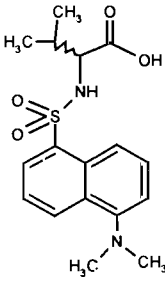
The above results suggest that the carboxyl group of the amino acid participates in a

leading interaction with pyridinyl groups on the polymer to retain the enantiomers, while the role

of the dimethylamino group is to provide for a secondary cooperative interaction with acid sites

on the polymer. This dimethylamino interaction occurs solely at the imprinted sites to stabilize

the inclusion of the imprinted enantiomer and is unimportant to non-selective binding to the

polymer. This hypothesis is further supported by the mobile phase modifier studies presented below.

In a second study, our goal was to assess the importance molecular shape on the selectivity of this polymer phase. To perform this experiment, the side chain of the amino acid by using the compounds Dns-Ala, Dns-Leu, and Dns-Val. Changing the side chain of the amino acid does not alter the potential points of interaction with the polymer, but does change the steric bulk of the molecule. The retention factors and selectivity factors for Dns-Phe and these derivatives are listed in Table 3-2. below the structures of each compound.

As shown in Table 3-2., the L-enantiomers of each derivative are selectively retained over their D-antipodes, suggesting that the L-enantiomers have access to the imprinted sites. It is also important to note here that the apparent van't Hoff plots for the L-enantiomers (not shown) of these amino acids showed a curvature similar to Dns-L-Phe while plots of the D-enantiomers were straight lines. This observation suggests that slow kinetics also contribute to the retention of the L-enantiomers of these compounds. While there is selectivity for these enantiomers, the selectivity factors are lower than that of Dns-Phe. This is consistent with the results of Kempe and Mosbach [62], who noted a decrease in enantioselectivity when injecting the enantiomers of Z-alanine on a Z-phenylalanine polymer imprinted using methacrylic acid as the functional monomer. Such a loss in selectivity can be due to an improper fit of the side chain into the imprinted cavities. While the side chain may not interact with the polymer, a tight fit at the imprinted sites can be a secondary process that enhances the hydrogen bonding interactions at the imprinted sites.

Table 3-2. Effect of Varying the Sterics of the Side Chain of the Amino Acid. Mobile phase: 6% acetic acid in acetonitrile; flowrate: 0.5mL/min; sample size: 300 ng each enantiomer; column temperature: 90°C; detection: fluorescence- excitation λ=305 nm, detection λ < 375 nm.

	Dns-Ala	Dns-Leu	Dns-Val
k D-enantiomer	0.8	0.5	0.5
k L-enantiomer	1.0	0.6	0.7
α	1.3	1.2	1.4

The difference in the free energy of binding of the two enantiomers ($\Delta\Delta G^o$) to the polymer phase can be deduced from the selectivity factors by the following equation:

$$\Delta\Delta G^o = -RT\ln\alpha \qquad [3\text{-}2]$$

The $\Delta\Delta G^o$ for each amino acid derivative was calculated using eqn. [3-2] and the results are presented in Table 3-3. By comparing the $\Delta\Delta G^o$ of Dns-Phe and the Napth-Phe, it is seen that approximately half of the enantioselective energy is lost when the dimethylamino group is removed from the molecule. This is consistent with the loss of one of two hydrogen bonds (that are similar in energy) at the imprinted sites. For the derivatives with different side chains, a reduction in $\Delta\Delta G^o$ of similar magnitude is also observed. Regardless of whether the side chain is less sterically hindered (Dns-Ala) or more sterically hindered (Dns-Leu) than Dns-Phe (as determined by the bulk around the β carbon), enantioselectivity is reduced to a similar extent. This further supports the premise that a tight steric fit of the side chain enhances the stability of the hydrogen bonding interactions occurring at the imprinted sites.

Influence of Mobile Phase Competitor

To further investigate the interactions responsible for enantioselectivity, the concentration of the mobile phase competitor was varied. For these studies, a temperature of 60°C and flow rate of 0.5 ml/min were used. Under these conditions, it was assumed that retention of the imprinted enantiomer is dominated by thermodynamics. This assumption is reasonable based on

73

Table 3-3. $\Delta\Delta G°$ for the Enantiomers of Different Amino Acid Derivatives. Mobile phase: 6% acetic acid in acetonitrile; flowrate: 0.5mL/min; sample size: 300 ng each enantiomer; column temperature: 90°C; detection: fluorescence- excitation λ=305 nm, detection λ < 375 nm.

	α	$\Delta\Delta G°$
Dns-Phe	2.2	-570 cal/mol
Napth-Phe	1.5	-292 cal/mol
Dns-Ala	1.3	-190 cal/mol
Dns-Le	1.2	-130 cal/mol
Dns-Val	1.4	-240 cal/mol

the relatively small difference observed in k at 0.5 ml/min (k=3.3) and 0.1 ml/min (k=3.7) at 60°C.

Initially, the molarity of acetic acid in acetonitrile was varied from 0.1M - 1M. Figures 3-6a. and 3-6b. give plots of k and α respectively for Dns-Phe and Napth-Phe. For both enantiomers of each derivative, k decreases with increasing acetic acid concentration. This decrease is expected because retention of the analyte is determined by hydrogen bonding between the carboxyl group of the amino acid and pyridinyl groups on the polymer. By increasing the acetic acid concentration in the mobile phase, the strong hydrogen bonding interactions between the analyte and polymer are diminished as acetic acid competes more effectively for these sites on the polymer. In addition, these data further support the conclusion that non-specific interactions occurring between each derivative and the polymer are identical, as the retention factors for the D-enantiomers of each derivative are similar over the entire acetic acid concentration range.

The nature of the enantioselective interactions occurring between the analyte and polymer are further clarified by looking at the dependence of the selectivity factor (α) for each derivative with increasing acetic acid concentration. For Dns-Phe, Figure 6b. shows an initial decrease in α with increasing acetic acid concentration between 0.1M-0.7M, after which α levels off with further increases in acetic acid. For Napth-Phe, a relatively weak dependence of α is seen with changing acetic acid concentration. It is possible to explain this behavior by considering the enhanced solvation of the analyte and polymer by increasing the acetic acid concentration. From the structural studies presented above, it was proposed that a secondary

Figure 3-6a. Effect of Mobile Phase Acetic Acid Concentration on the k of the Dns-Phe and

Napth-Phe Enantiomers. flowrate: 0.5mL/min; sample size: 300 ng each

enantiomer; column temperature: $60^{\circ}C$; detection: fluorescence- excitation $\lambda=305$
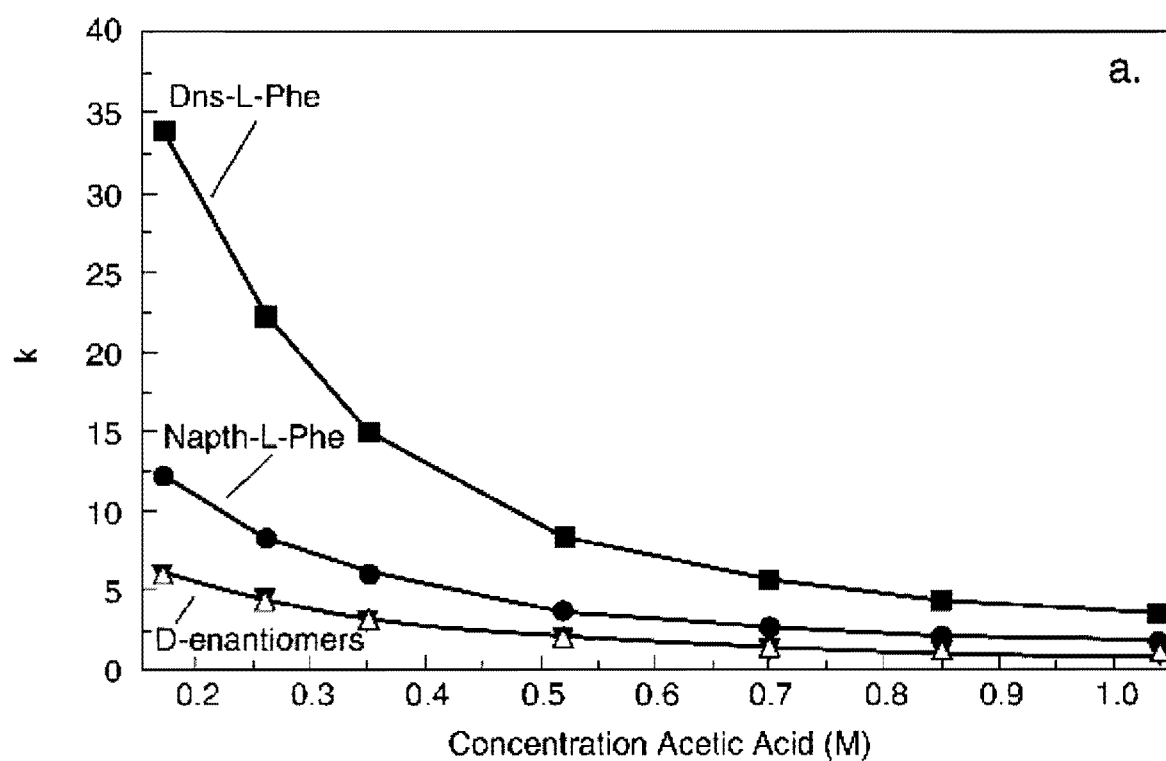
nm, detection $\lambda < 375$ nm.

Figure 3-6b. Effect of Mobile Phase Acetic Acid Concentration on α of Dns-Phe and Napth-Phe. flowrate: 0.5mL/min; sample size: 300 ng each enantiomer; column temperature: 60°C; detection: fluorescence- excitation λ=305 nm, detection λ < 375 nm.
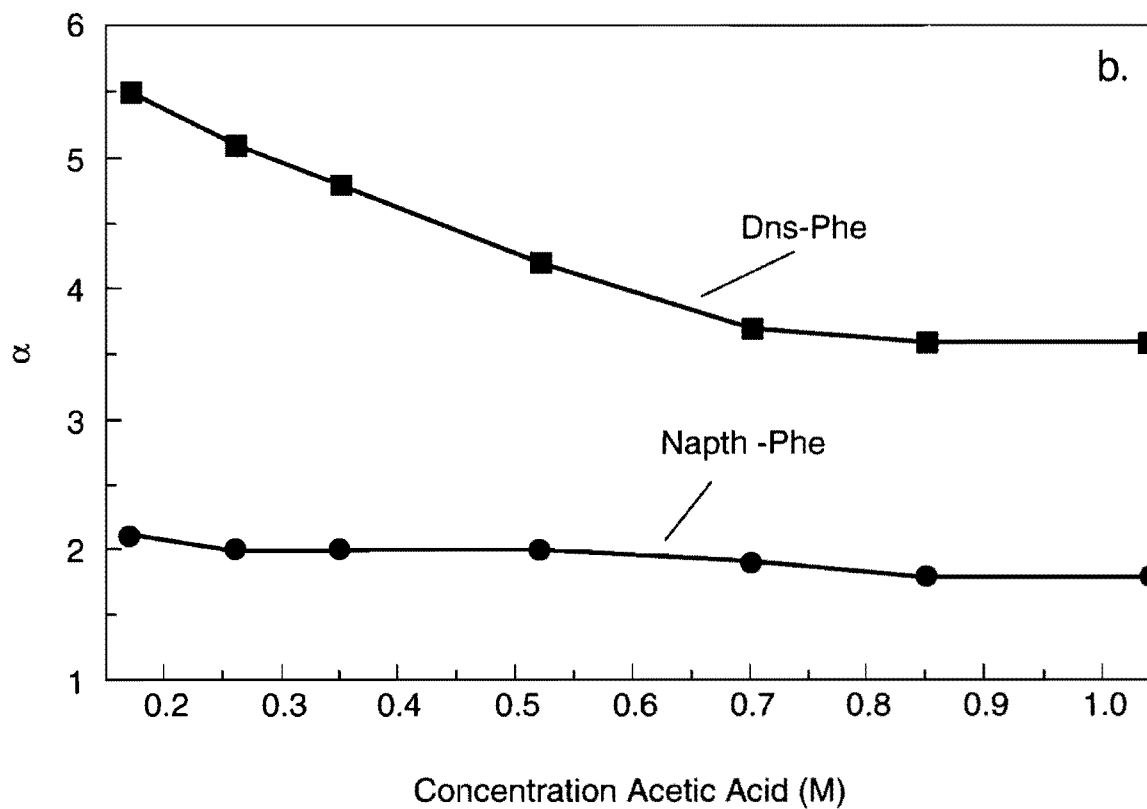
interaction occurs between the dimethylamino group of Dns-L-Phe and carboxyl groups on the polymer that contributes to enantioselectivity. By increasing the acetic acid concentration, Dns-Phe and the polymer become more solvated with acetic acid. As a result, the enantioselective interaction between the dimethylamino group and the polymer is reduced, as it becomes more difficult for this group to lose acetic acid to interact with the polymer. As a result, a significant decrease in the selectivity is observed. For the Napth-Phe, this enantioselective interaction cannot occur and while the retention factor decreases with increasing acetic acid, the enantioselectivity remains essentially unchanged. It is important to note the selectivity factor for the enantiomers of Dns-Phe appear to level off at higher acetic acid concentration rather than approach that of the Napth-Phe. An explanation of this behavior is not straightforward, but may indicate that interaction between the dimethylamino group and the polymer cannot be completely suppressed or there is also a significant contribution of the shape of the dimethylamino group to the enantioselectivity.

In a second study, the retention and selectivity of Dns-Phe was studied using a mixture of pyridine and acetic acid as the mobile phase modifier. The total modifier concentration was held constant at 0.52M while the individual amounts of pyridine and acetic acid were varied from 0-0.52M. Figures 7a. and 7b.give plots of k and α respectively for the enantiomers of Dns-Phe. Introduction of pyridine to the system results in strong hydrogen bonding between pyridine and the carboxyl groups on the amino acid and carboxyl sites on the polymer. These interactions reduce the retention factor of each enantiomer relative to the system with the same concentration of acetic acid in the absence of pyridine (Figure 6a.). As pyridine is replaced by acetic acid, the retention factor of each enantiomer is initially reduced. Apparently, the competition between

Figure 7a. Effect of Mobile Phase Pyridine/Acetic Acid Concentration on the k of the Dns-Phe

Enantiomers. flowrate: 0.5mL/min; sample size: 300 ng each enantiomer; column

temperature: 60°C; detection: fluorescence- excitation λ=305 nm, detection λ < 375

nm.
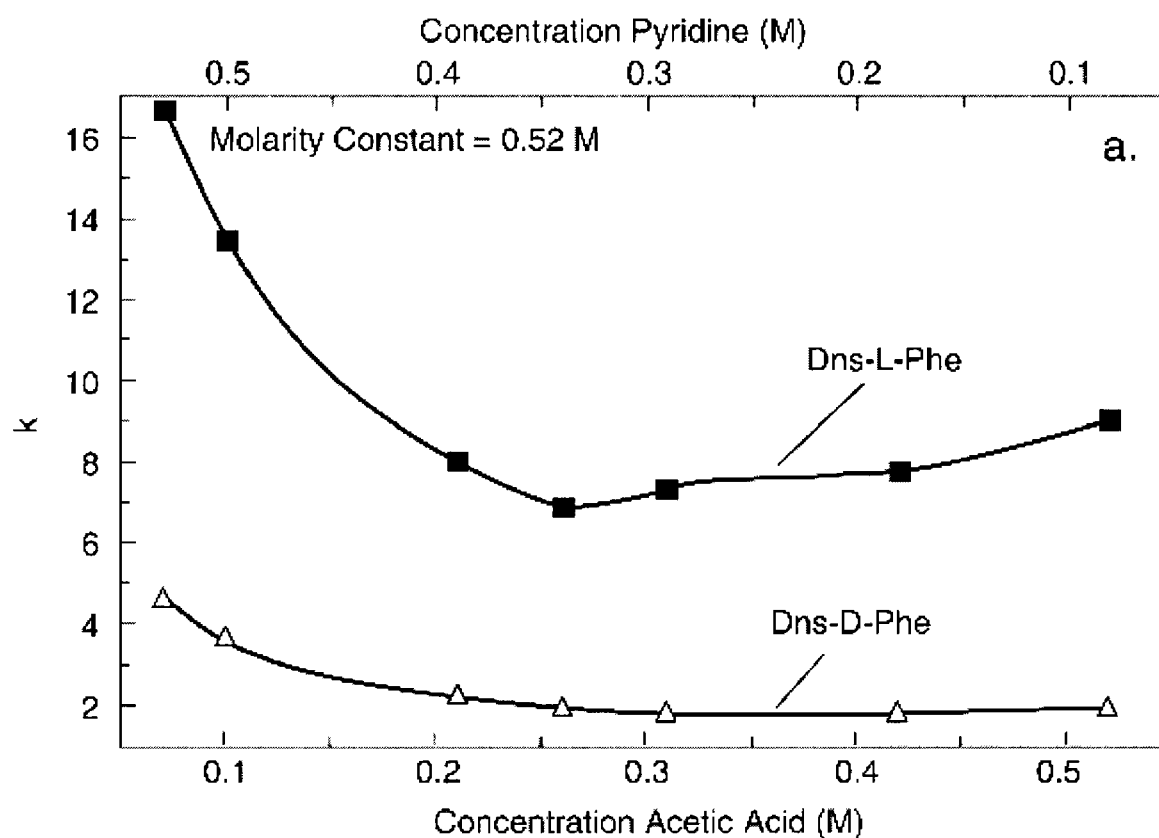
Figure 7b. Effect of Mobile Phase Pyridine/Acetic Acid Concentration on α of the Dns-Phe

Enantiomers. flowrate: 0.5mL/min; sample size: 300 ng each enantiomer; column

temperature: 60°C; detection: fluorescence- excitation λ=305 nm, detection λ < 375

nm.
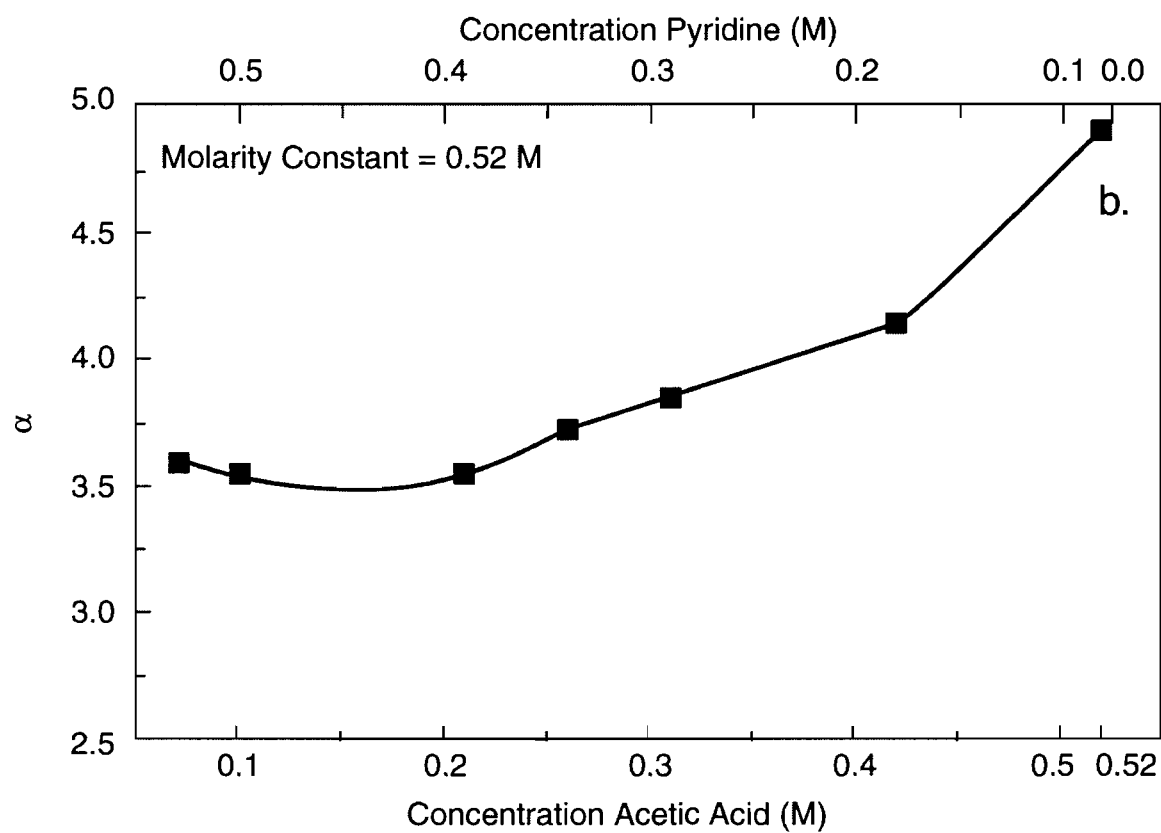
acetic acid and Dns-Phe for pyridinyl sites on the polymer is more effective in eluting the analyte than solvation of Dns-Phe by pyridine in the mobile phase. This is supported by the fact that when the acetic acid concentration was reduced to 0M (0.52M pyridine), neither enantiomer eluted.

Figure 7a. also shows that when the concentrations of acetic acid and pyridine in the mobile phase become approximately equal (~0.26M) and pyridine is no longer in excess, the retention factor of Dns-L-Phe reaches a minimum while that of Dns-D-Phe levels off. This behavior can be explained by the differences in solvation pyridine and acetic acid exhibit in the system. At high pyridine/low acetic acid concentration, the retention factor of each enantiomer is relatively large because there is little acetic acid to compete with the analytes for the pyridinyl sites on the polymer. As pyridine is replaced by acetic acid, the retention factors drop as acetic acid begins to compete for these sites on the polymer. At the same time, the hydrogen bonding between the pyridine and carboxyl sites on the polymer is reduced, fostering the secondary enantioselective interaction between the dimethylamino group of the imprinted enantiomer (Dns-L-Phe) and the carboxyl sites on the polymer. As a result, a minimum is observed in the retention factor for Dns-L-Phe as this secondary interaction becomes more pronounced. Based on this argument, it is expected that the enantioselectivity for Dns-Phe will increase as pyridine is replaced by acetic acid. Indeed, this is the case, as shown in Figure 7b., which gives a plot of the selectivity factor of Dns-Phe for this study.

Conclusions

Chromatographic experiments performed on a polymer imprinted with Dns-L-Phe using carboxyl and pyridine functional monomers indicated that the adsorption/desorption kinetics at the imprinted sites are slow. Structural studies indicated that the leading interaction is between the carboxyl group of Dns-Phe and the pyridinyl sites on the polymer. Further, interaction between the dimethylamino group of Dns-Phe and the polymer occurs only at the imprinted sites and is unimportant to non-selective binding on the polymer. From these data, we propose that chiral recognition on this polymer is a cooperative process. There must first be a leading interaction between the carboxyl group of Dns-Phe and the pyridinyl groups on the polymers to retain the enantiomers. This is followed by secondary stabilizing processes that contribute to enantioselectivity; interaction at the dimethylamino group and correct steric fit of the amino acid side chain into the imprinted cavities. We believe that this fundamental study further contributes to the understanding of the mechanism of chiral separations on imprinted polymer phases, in particular, one in which multiple functional groups were used to enhance the enantioselectivity.

Chapter 4

Insight into the Origins of Selectivity of Polymer

Imprinted with a HIV Protease Inhibitor

Summary

The goal of the second part of this dissertation was to systematically investigate the types of template-monomer hydrogen bonding interactions necessary to achieve a successful imprint of a molecule. To achieve this goal, several CRIXIVAN™ molecular imprinted polymers (MIP's) were prepared using several alternate functional monomers, each differing in their ability to hydrogen bond with the drug during the polymerization. The relative strength of these interactions was assessed by Infrared (IR) spectroscopy. For the IR studies, 'functional surrogates' of CRIXIVAN™ were used because the spectrum of the parent molecule was too complicated to observe band shifts due to hydrogen bonding. The relative selectivity of the MIP's for CRIXIVAN™ and its enantiomer correlated well with the relative hydrogen bonding propensities of the functional monomers used to prepare the polymers. The two weak hydrogen bonding monomers, vinyl pyridine and acrylamide, resulted in polymers with minimal ($\alpha = 1.1$) and moderate ($\alpha = 1.6$) selectivity while the strong H-bonding monomer, methacrylic acid (MAA), resulted in a highly selective polymer ($\alpha \geq 14$). A control polymer prepared using a monomer not expected to hydrogen with CRIXIVAN™ (MeACRYL) failed to demonstrate selectivity ($\alpha = 1.0$). To further explore the origins of the selectivity of the MAA polymer, binding studies were performed on solutions of MAA and CRIXIVAN™ using IR spectroscopy. Scatchard plots of these data indicated distinct 'strong' and 'weak' binding regions

corresponding to MAA concentrations for which different hydrogen bonding groups on the template drive the formation of the template-monomer complex. Furthermore, the relative selectivity of several MIP's prepared using different MAA concentrations was correlated to the type of MAA-CRIXIVAN™ complex present in the pre-polymer solution. These experiments demonstrate the possibility of using IR spectroscopy as a tool to explore the origins of selectivity of an imprinted polymer.

Introduction

The most common interaction between the template and functional monomer in the formation of MIP's has been hydrogen bonding. The formation of a hydrogen bond can be regarded as a preliminary step in a Bronsted-Lowry acid-base reaction that leads to a dipolar reaction product $R-X^{-}\cdots H-Y^{+}-R$', where X and Y are atoms of higher electronegativity than hydrogen (e.g. C, N, P, O, S, F, Cl, Br, I). Both inter- and intramolecular hydrogen bonding is possible when X and Y belong to the same molecule. The most important electron pair donors (hydrogen bond acceptors) are the oxygen atoms in alcohols, ethers and carbonyl compounds as well as nitrogen atoms in amines and N-heterocycles. Hydroxy-, amino-, carboxyl and amide groups are the most important donor groups. Strong hydrogen bonds are formed by $O-H\cdots O$, $O-H\cdots N$ and $N-H\cdots O$ pairs, weaker ones occur between $N-H\cdots N$ and the weakest are between groups such as $Cl_3C-H\cdots O$ and $Cl_3C-H\cdots N$. The strength of a hydrogen bond is roughly ten times weaker than a covalent bond and about ten times stronger than the nonspecific intermolecular interaction forces [123]. Hydrogen bonds are characterized by the following structural and spectroscopic features [124]: (1) The distance between the neighboring atoms involved in the

84

hydrogen bond are much smaller than the sum of their van-der-Waals radii. (2) The X-H bond length is increased and the IR stretching mode is shifted toward lower frequencies. (3) The dipolarity of the X-H bond increases upon hydrogen bond formation, leading to a larger dipole moment of the complex than expected from vectorial addition of its dipolar components R-X-H and Y-R'. (4) Due to the reduced electron density at protons involved in hydrogen bonding, they are deshielded, resulting in substantial downfield shifts of their ^{1}H-NMR. (5) In hetero-molecular hydrogen bonds, a shift of the Bronsted-Lowry acid/base equilibrium occurs toward the dissociation of the complex with increasing solvent polarity.

Hydrogen bonding is a major source of interaction between the template and the functional monomers. Thus, probing these interactions prior to the polymerization may lead to further insight into the selectivity of the imprinted polymer. Limited work has been done in this area. Thus far, spectroscopic studies such as ^{1}H NMR [109] and UV difference spectroscopy [125] have been used to assess interactions between the template and monomers.

CRIXIVAN™ is a drug used for the treatment of HIV (human immunodeficiency virus), the virus responsible for AIDS (acquired immune deficiency syndrome). The molecule (Figure 4-1.) has 5 chiral centers and several potential H-bonding groups, located at the hydroxyl, amides, piperazine, and pyridine sites. Thus, preparation of an imprinted polymer for CRIXIVAN™ for use as a separation support appeared to be an attractive study.

Figure 4-1. CRIXIVAN™ Molecule
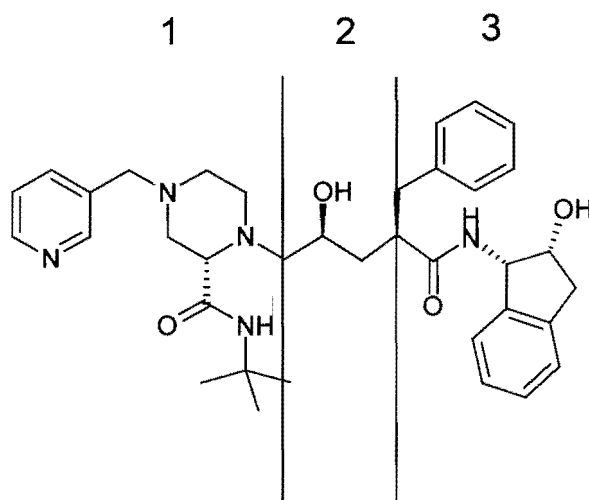
The goals of this study were to probe the types of monomer-template hydrogen bonding interactions necessary to achieve a successful imprint of CRIXIVAN™ and to thoroughly characterize those which yielded polymers with the best selectivity. To achieve this goal, attenuated total reflection IR spectroscopy (ATR-IR) was used to assess the hydrogen bonding interactions occurring between several alternative functional monomers and fragments of CRIXIVAN™ in solutions similar to those of the polymerization mixtures. The strength and number of these interactions were then compared to the selectivity of the imprints prepared with each monomer.

Experimental

Reagents

Methacrylic acid (MAA), 4-vinyl-pyridine (4-VP), acrylamide (ACRYL), methylacrylate (MeACRYL), ethylene glycol dimethacrylate (EDMA), pyridine, N,N Dimethylpiperazine, *t*-butylacetamide, and 2-butanol were obtained from Aldrich (Milwaukee, WI). CRIXIVAN™, its enantiomer, its diastereomers, and hydroxyamide were synthesized and characterized by Merck and Company's Process Research Department (Rahway, NJ). All solvents, chloroform, acetonitrile, acetic acid, and water were obtained from Fischer (Raritan, NJ) and were HPLC grade. AIBN was obtained from Pfaltz and Bauer (Waterbury, CT).

Instrumentation

The HPLC system consisted of a Beckmann System Gold pump and a Waters (Medford, MA) 715 ULTRA WISP autosampler. The column temperature was controlled by a Neslab

RTE-110 (Newington, NH) recirculating water / ethylene glycol bath. An Applied Biosystems

(Foster City, CA) 757 absorbance detector set 260 nm was used. The chromatographic data

analysis was performed using P.E. Nelson (Cupertino, CA) Turbo*Chrom software. The

statistical analysis of the data were done using Origin software (Microcal, Northampton, Ma).

The IR spectra were collected using a Nicolet IR spectrometer equipped with a diffuse

reflectance apparatus or attenuated total reflectance (ATR) apparatus. All IR spectra were

collected at room temperature (approximately $22\,^{\circ}C$ +/- $2\,^{\circ}C$).

Polymer Preparation and Characterization

Four polymers were evaluated, each prepared with a different hydrogen bonding

functional monomer (see Figure 4-2): methacrylic acid (MAA), 4-vinyl-pyridine (4-VP),

acrylamide (ACRYL), and methylacrylate (MeACRYL). The polymers were prepared by

combining EDMA (35 mmol), functional monomer (6.1mmol), CRIXIVAN™ (0.87mmol),

AIBN initiator (50mg), and 10mL of dry chloroform (KF=60μg/mL) in a 25 ml glass vial. The

solutions were purged with nitrogen for 5 min and each bottle was capped tightly and placed

under a UV lamp (466 nm) at ~$16^{0}C$ (+/- $2^{\circ}C$) for 10 hours. The resulting solid polymers were

ground with a mortar and pestle and washed with 1 liter of 10% acetic acid in acetonitrile

followed by 1 liter of acetonitrile. Quantitation of the washes indicated > 90% incorporation of

each monomer into its respective polymer. A portion of each batch of polymer was washed with

methanol, dried, and characterized by Diffuse-Reflectance IR spectroscopy. MAA polymer:

$3300cm^{-1}$ (O-H), $1742cm^{-1}$ (ester C-O); 4-VP polymer: $1569cm^{-1}$ (pyridine), $1550\ cm^{-1}$

(pyridine). $1742cm^{-1}$ (ester C-O); ACRYL polymer: $3300cm^{-1}$ (N-H), $1650cm^{-1}$ (amide C-O),

$1742cm^{-1}$ (ester C-O); MeACRYL polymer: $1742cm^{-1}$ (ester C-O).

Figure 4-2.   Structure of Monomers used for Synthesis of Different Polymers
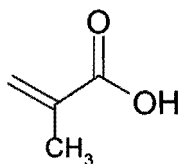
Methacrylic acid (MAA)
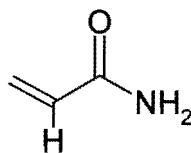
Acrylamide (ACRYL)
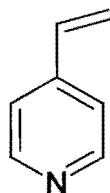
4-vinyl pyridine (4-VP)
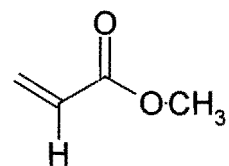
Methyl acrylate (MeACRYL)

Column and Sample Preparation

The polymer particles were passed through 38 and 25μm sieves and approximately

1 gram of the 25-38μm sized particles were suspended in acetonitrile and packed into a 10 x 0.46

cm. HPLC columns. These columns were attached to the HPLC system and washed with 10%

acetic acid prior to equilibration with mobile phase. The samples were prepared by dissolving

CRIXIVAN™, its enantiomer, or diastereomer in chloroform (0.5-1.0 mg/ml). A 7-50μl volume

sample (~4-50μg) was injected onto the column, the exact amount depending on the experiment.

To evaluate the selectivity of each polymer, separate samples of CRIXIVAN™, CRIXIVAN™

diastereomer, or CRIXIVAN™ enantiomer were injected. For chromatograms showing

resolution between two isomers, both components were injected simultaneously.

ATR-Infrared Spectroscopic Studies

Comparison of Different Functional Monomers

ATR-IR spectroscopy was used to evaluate hydrogen bonding between each functional

monomer and the template in the polymerization solution. In order to study the interaction at

each functional group, CRIXIVAN™ was replaced with several representative fragments (Figure

4-3.), each mimicking a potential hydrogen bonding group of the parent molecule. Each

fragment was separately dissolved in chloroform with MAA, ACRYL, or pyridine (representing

4-VP) to achieve a concentration of 0.1M of each component and the resulting solutions were

analyzed by ATR-IR spectroscopy. These spectra were compared to spectra of each individual

fragment to identify band shifts indicative of hydrogen bonding and to determine the relative

strength of the intermolecular hydrogen bonds formed with each fragment. This method

provided well-resolved IR bands for all of the functional groups in question.

Figure 4-3 Representative Fragments of CRIXIVAN™
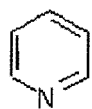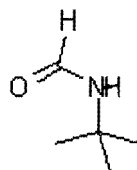
pyridine   n-t-butylformamide   2-butanol
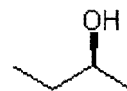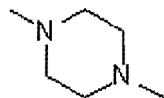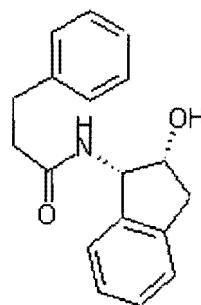
n,n dimethylpiperazine   hydroxyamide

Binding Studies of Methacrylic Acid with CRIXIVAN™

Throughout the study, it was found that the intensity of the carbonyl stretch of MAA

(1635 cm^{-1}) decreased in the presence of CRIXIVAN™. This behavior was used as basis for

measuring the hydrogen bonding interactions occurring between these two species. The intensity

of the carbonyl stretch was measured for several chloroform solutions of CRIXIVAN™ (0.1M)

containing increasing amounts of MAA (0-21 mole equivalents). A calibration curve of peak

intensities for solutions of 'free' MAA was used to calculated the effective decrease of the MAA

band due to hydrogen bonding with CRIXIVAN™, [MAA 'Crixivan Bound']:

$$q/V = [MAA_{\text{'added'}}] - (I_{\text{sample}} / Rf) \qquad [4\text{-}1]$$

$$C = [MAA_{\text{'added'}}] - [MAA_{\text{'Crixivan Bound'}}] \qquad [4\text{-}2]$$

where:

q	= effective amount of MAA 'bound' to CRIXIVAN™.
V	= the volume of the solution.
[MAA 'added']	= total concentration MAA added to the solution.
I sample	= intensity of 1690cm^{-1} peak of MAA in sample.
Rf	= slope of calibration curve for intensity $_{1690cm\text{-}1}$ for solutions of MAA without CRIXIVAN™.
C	= concentration of 'free' MAA remaining after q moles become bound.

Binding Equilibria

For this study, MAA can be considered a ligand that binds to multiple hydrogen bonding sites on CRIXIVAN™. In general, if each site on a substrate possessing *n* sites demonstrates the same equilibrium constant for the binding of a ligand, the sites are considered identical and independent. In this case, the overall equilibrium is governed by the following relationship that considers the statistical aspect of the binding events [126]:

$$q = \frac{bnC}{1 + bC} \qquad [4\text{-}3]$$

where q and C are as described above and,

b = the equilibrium constant for the binding process.

n = the number of binding sites on the substrate available to bind the ligand.

Equation [4-3] can be rearranged into an expression known as the Scatchard plot:

$$q/C = -bq + bn \qquad [4\text{-}4]$$

For a substrate with identical and independent binding sites, a Scatchard plot is linear with a slope of -b and an abscissa intercept of *n*.

If the binding sites on the substrate are not identical and/or independent, then the Scatchard plot for the binding process will be curved. When the sites are not identical, the

93

equilibrium constant (b) between the ligand and each site is different. In such a case, the Scatchard plot is curved concave upwards. The sites are considered non-independent when the binding of a ligand at one site, alters the binding constant of a second ligand at a neighboring site, producing a continuous variation in the equilibrium constant (b). If b increases with increasing saturation, the process exhibits 'positive cooperativity' and is characterized by a concave downwards curved Scatchard plot. If b decreases with increasing saturation, a 'negative cooperative' process is operating that is characterized by a concave upwards Scatchard plot [126].

Using the data obtained from equations [4-1] and [4-2] above, a binding isotherm (q versus C) and Scatchard plot were constructed for various concentrations of MAA in the presence of a constant concentration of CRIXIVAN™ (0.1M).

Results and Discussion

ATR-IR Studies – Comparison of the Hydrogen Bonding Propensities of Different Monomers

Infrared spectroscopy is a convenient tool for identifying and quantifying hydrogen bonding interactions. The most prominent effects of hydrogen bonding on a peak in the vibrational spectrum are shifts in the maximum frequency and/or a broadening and change in intensity of the band at that frequency [114].

The imprint molecule of this study possesses multiple potential hydrogen bonding groups, suggesting that it would be an ideal template for molecular imprinting. It was unclear, however, as to the types of hydrogen bonding interactions that would lead to a successful imprint

94

of this functionally diverse molecule. To address this question, several functional monomers (Figure 4-2) were explored to imprint CRIXIVAN™, each differing in their ability to hydrogen bond with the template during the polymerization.

As shown in Figure 4-1, we have arbitrarily divided CRIXIVAN™ into three portions for discussion. Portion 1 of the molecule contains pyridinyl and piperazine groups capable of undergoing hydrogen bond accepting interactions with monomers and a *t*-butylamide group that may participate in both donating and accepting interactions. Portions 2 and 3 of the molecule possess hydroxy and hydroxyamide groups respectively, that may undergo both hydrogen bond accepting and donating interactions with the monomers. Our initial IR studies used representative fragments of CRIXIVAN™ (Figure 4-3) to separately assess the ability of each of these fragments to hydrogen bond with the functional monomers.

Piperazine/Pyridine Groups

For the IR studies, the piperazine and pyridine groups on CRIXIVAN™ were substituted with the fragments, dimethylpiperazine and pyridine respectively. The IR spectrum of an amine contains a band in the 2700-2800cm^{-1} region that is associated with the nitrogen lone pair that disappears when the amine becomes protonated [127]. Therefore, it was postulated that the corresponding amine band of dimethylpiperazine would be perturbed when it hydrogen bonds with the donor monomers, MAA and ACRYL. Similarly, for pyridine, two of the C=C ring stretches (1585 cm^{-1} and 1600 cm^{-1} [127]) were expected to be sensitive to hydrogen bonding between the ring nitrogen and the donor monomers. The pyridine monomer was not considered in either case because it is not capable of hydrogen bonding with either acceptor group.

Comparisons of the IR spectra of dimethylpiperazine and pyridine alone and in the presence of each monomer are presented in Figures 4-4 through 4-7. As shown, only the MAA monomer affected a significant change in the bands of interest, suggesting that it hydrogen bonds to the piperazine and pyridinyl groups of CRIXIVAN™ to a greater extent than ACRYL. This result is not surprising considering that the MAA carboxylic proton is more acidic than the amide proton of ACRYL.

Hydroxyamide/*t*-butylamide Groups

An amide can donate or accept hydrogen bonds through its carbonyl oxygen and amide proton respectively:

$$C=O\cdots\cdots Donor \quad or \quad N\text{-}H\cdots\cdots Acceptor$$
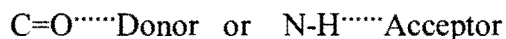
The IR peak corresponding to the C-N stretch ($\sim1510\text{cm}^{-1}$) of an amide responds to hydrogen bonding interactions by undergoing a shift to higher frequencies [127]. This criterion was used to investigate the possibility of hydrogen bonding between each functional monomer and the hydroxyamide and *t*-butylamide groups of CRIXIVAN™. Thus, IR studies were performed on solutions of MAA, ACRYL, or PYR in the presence of either, hydroxyamide or *t*-butylformamide. These spectra were then compared to the corresponding spectra of solutions of hydroxyamide or *t*-butylformamide without monomer to identify perturbations in the C-N stretch due to hydrogen bonding.

Figure 4-4. Effect of MAA on Piperazine Infrared Stretch at 2800cm^{-1}: Solvent: chloroform; concentration: 0.1M; Resolution: 1 cm^{-1}; Scans: 200x.

Figure 4-5. Effect of ACRYL on Piperazine Infrared Stretch at 2800cm^{-1}: Solvent: chloroform; concentration: 0.1M; Resolution: 1 cm^{-1}; Scans: 200x.
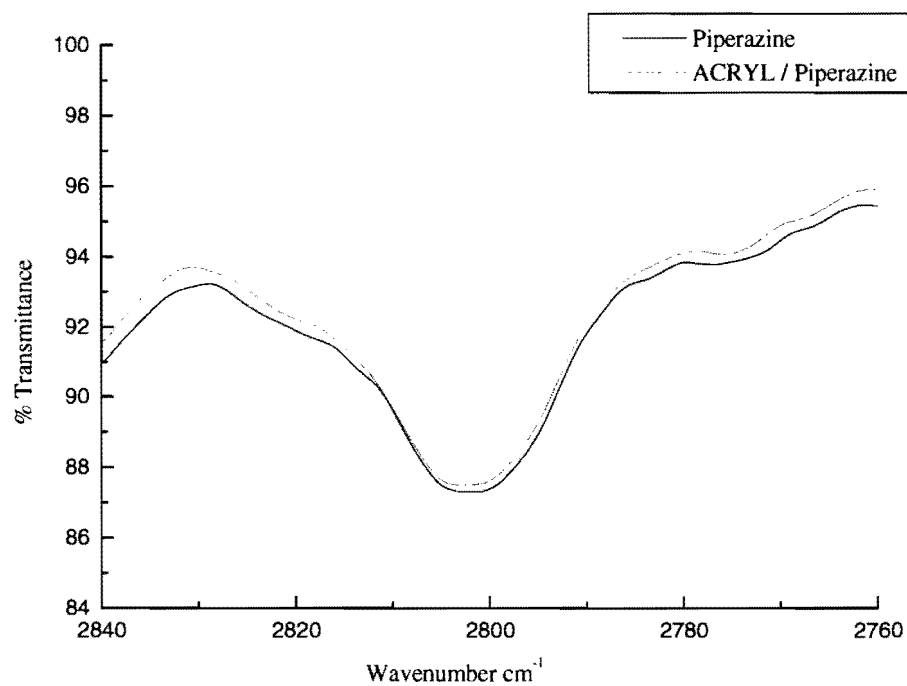
Figure 4-6. Effect of MAA on Pyridine Infrared Stretches at 1585 and 1600cm^{-1}: Solvent: chloroform; concentration: 0.1M; Resolution: 1 cm^{-1}; Scans: 200x.
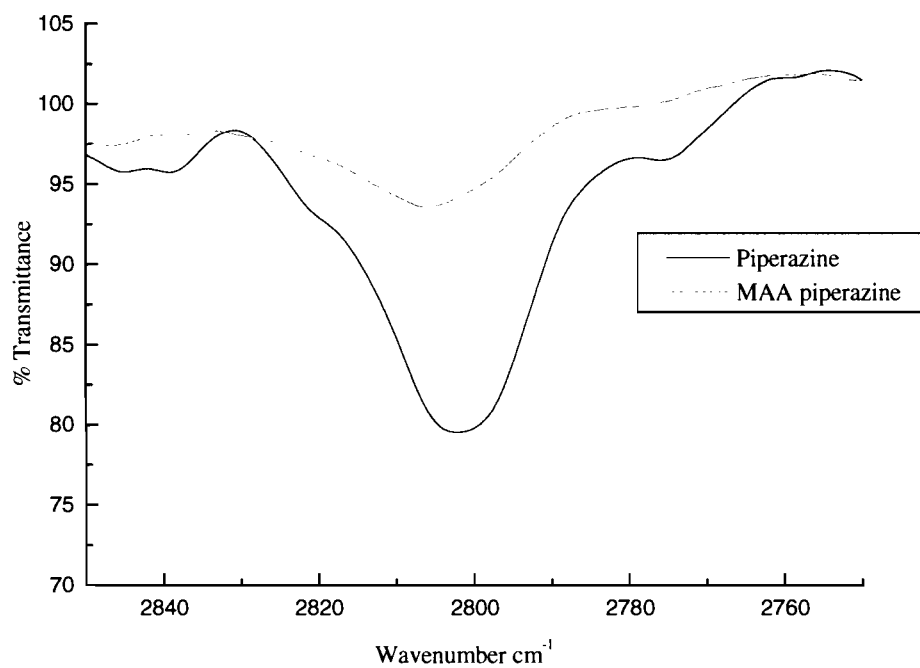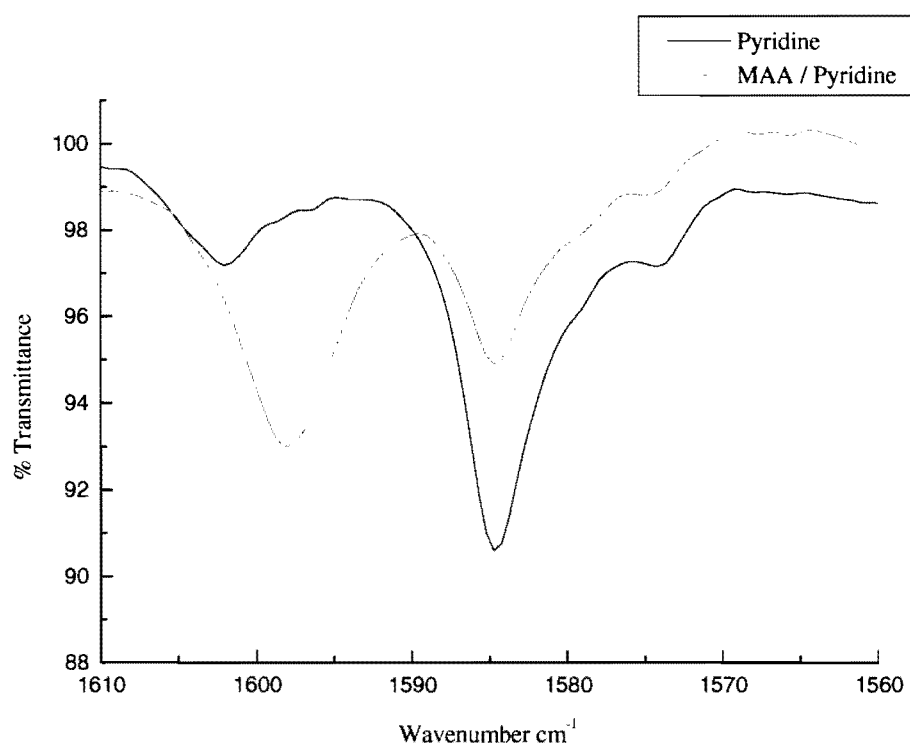
Figure 4-7. Effect of ACRYL on Pyridine Infrared Stretch at 1585 and 1600cm^{-1}: Solvent:

chloroform; concentration: 0.1M; Resolution: 1 cm^{-1}; Scans: 200x.
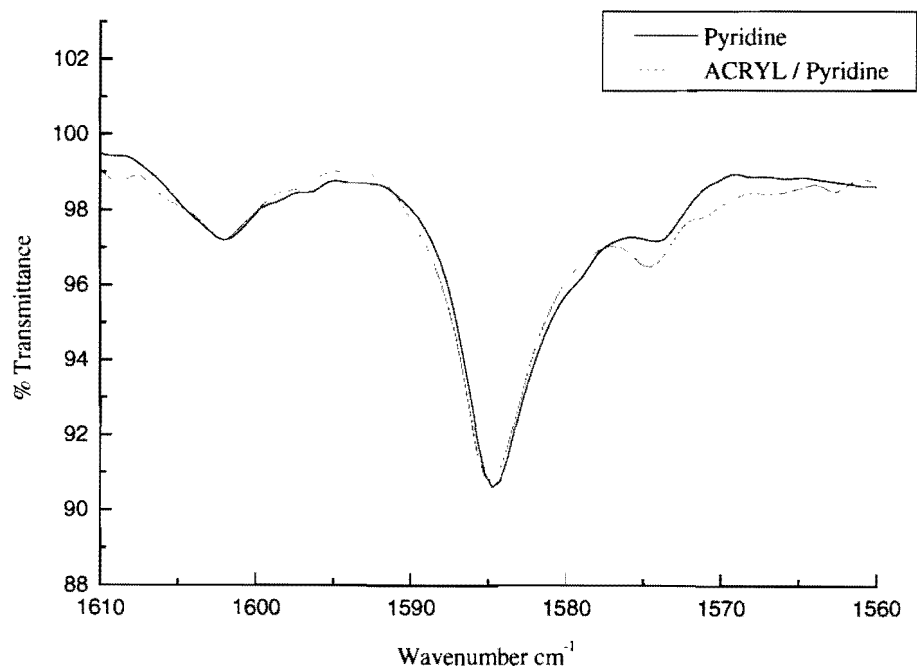
Portions of the IR spectra of hydroxyamide alone and in the presence of each monomer are presented in Figure 4-8. For hydroxyamide, a shift in the C-N peak (1509 cm^{-1}) of 3 cm^{-1} and 1 cm^{-1} respectively occurred in the presence of MAA and ACRYL , while no observable perturbation occurred in the presence of PYR . It was also possible that the O-H group of the hydroxyamide hydrogen bonds with each monomer. However, because no perturbations were observed for the hydroxyamide the O-H stretch (~3570 cm^{-1}), it was assumed that this interaction was relatively small. A similar hydrogen bonding behavior was observed for the amide group of t-butylformamide. Thus, it was concluded that the hydrogen bonding strength between the corresponding amide groups on CRIXIVAN™ and the monomers likely follow the order MAA>ACRYL>PYR.

Hydroxyl Group

To assess the hydrogen bonding behavior of the center hydroxyl group of CRIXIVAN™, 2-butanol was used as a functional mimic. The O-H stretch of an alcohol shifts to a lower frequency when this group forms a hydrogen bond [127]. Accordingly, the corresponding shift for 2-butanol (~3615 cm^{-1}) was used to observe the hydrogen bonding with each monomer. Indeed, spectra of solutions of 2-butanol showed a red shift in the O-H band in the presence of each monomer. The band shifts were 2.5 cm^{-1} for MAA, 1.5 cm^{-1} for PYR, and < 1 cm^{-1} for ACRYL, suggesting that each monomer forms hydrogen bonds with the hydroxyl group of CRIXIVAN™ and the order of the strength of these bonds is MAA>PYR>ACRYL. The spectra for this study are given in Figure 4-9.

Figure 4-8. Effect of Monomers on Hydroxylamide C-N Infrared Stretch at 1509cm^{-1}: Solvent: chloroform; concentration: 0.1M; Resolution: 1 cm^{-1}; Scans: 200x.
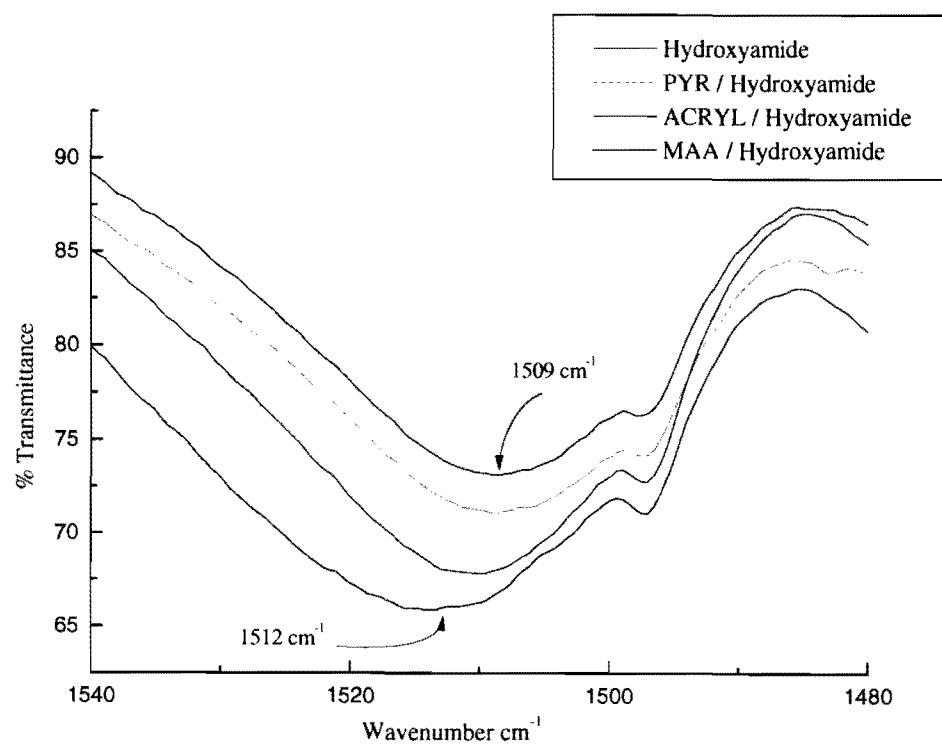
Figure 4-9. Effect of Monomers on 2-butanol O-H Infrared Stretch at ~3614 cm^{-1}: Solvent: chloroform; concentration: 0.1M; Resolution: 1 cm^{-1}; Scans: 200x.
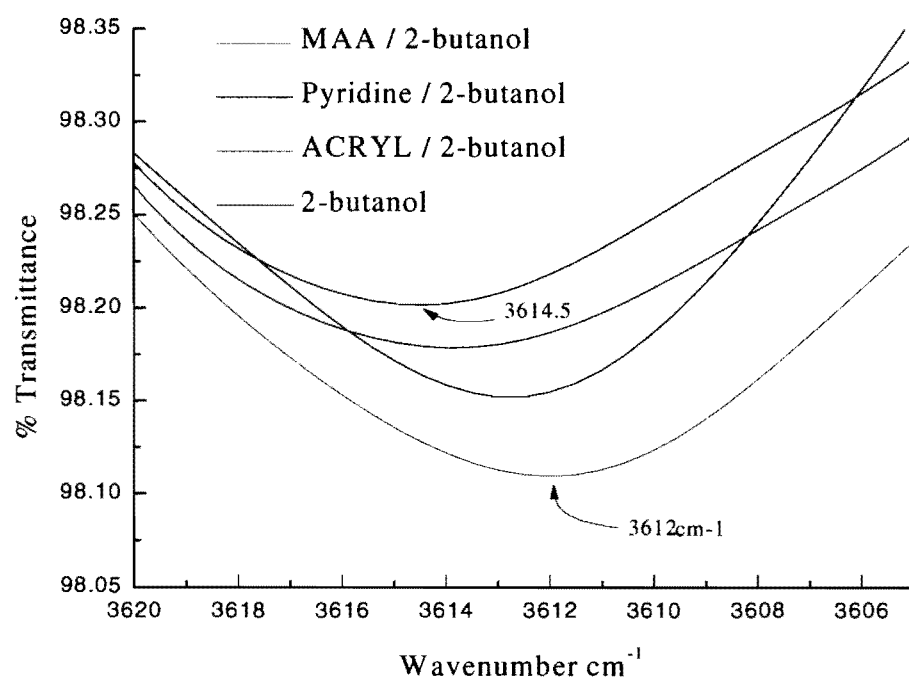
To test the hypothesis that polymer selectivity is directly related to the strength of the hydrogen bonds formed between the template and the functional monomer during the polymer formation, several MIP's were prepared for CRIXIVAN™ using each functional monomer evaluated above. Assuming that the CRIXIVAN™ fragments adequately mimicked the hydrogen bonding behavior of their representative portions of CRIXIVAN™, it was predicted that the MAA imprinted polymer would demonstrate significantly better selectivity than the other two polymers. However, because both ACRYL and pyridine demonstrated comparably weaker hydrogen bonding by IR, it was difficult to predict the order of selectivity of their corresponding polymers.

Chromatographic Analyses of the Polymers

MIP's for CRIXIVAN™ were prepared using the three functional monomers investigated in the ATR-IR studies. In addition, a control polymer was synthesized in the absence of functional monomer. For this polymer, methyl acrylate (MeACRYL) was added in the same proportion as the functional monomers to obtain a polymer with the same crosslinking percentage. However, since MeACRYL is similar in functionality to the crosslinker EDMA (both are esters), it was not expected that this monomer would preferentially hydrgoen bond with CRIXIVAN™ during the polymerization.

Selectivity of MAA MIP

The selectivity of the MAA polymer was evaluated by injecting each enantiomer of CRIXIVAN™ on a column prepared with this polymer as the stationary phase. To elute the enantiomers, acetic acid was a necessary component of the chloroform mobile phase.

Apparently, the interactions between each enantiomer and the polymer are very strong and acetic acid is required as a hydrogen bond competitor to weaken these interactions and hasten the elution of the enantiomers. The retention factors (k) and the selectivity factor (α) for the enantiomers using this mobile phase are given in Table 4-1. A typical chromatogram is given in Figure 4-10. Substantial selectivity (α =14.5) was observed for CRIXIVAN™ and its enantiomer, indicating that a successful imprint was achieved with MAA

Selectivity of ACRYL, 4-VP, and MeACRYL MIP's

In contrast to the MAA polymer, it was observed the ACRYL, 4-VP, MeACRYL polymers did not retain the enantiomers (k's = 0) using unmodified chloroform as the mobile phase. This is a result of the relatively weak hydrogen bonding interactions occurring between the enantiomers and these phases as compared to the MAA polymer. Because these polymers were prepared in chloroform, this observation initially suggested that the hydrogen bonding interactions between the monomers and CRIXIVAN™ during polymer formation were probably too weak to establish an imprint. Nevertheless, it was necessary to retain the enantiomers on these phases to prove the presence or absence of selectivity. After careful optimization of the mobile phase conditions, it was determined that the CRIXIVAN™ enantiomers could be retained on these polymers using 55/45 heptane/chloroform as the mobile phase. Presumably, this relatively non-polar mobile phase fosters hydrogen bonding between CRIXIVAN™ and each polymer.

Table 4-2. compares the retention factors and selectivity of CRIXIVAN™ on the ACRYL, 4-VP, MeACRYL, and MAA polymers using the 55/45 heptane/chloroform mobile

Table 4-1. Retention Factors (k) and Selectivity Factor α for CRIXIVAN^{TM} Enantiomers on
Methacrylic Acid Polymer. Mobile phase: 2% acetic acid in chloroform; flowrate: 1.0
mL/min; sample size: 50µg each enantiomer; column Temperature: 30°C; detection:
260nm.

	k non-imprinted	k imprinted	α
MAA Polymer	1.0	14.5	14.5

Figure 4-10. Typical Chromatogram for the Separation of the CRIXIVAN™ Enantiomers on the

MAA Column. Mobile phase: 5% acetic acid in chloroform; flowrate: 1.0

mL/min; sample size: 50μg each enantiomer; column Temperature: 80°C;

detection: 260nm.
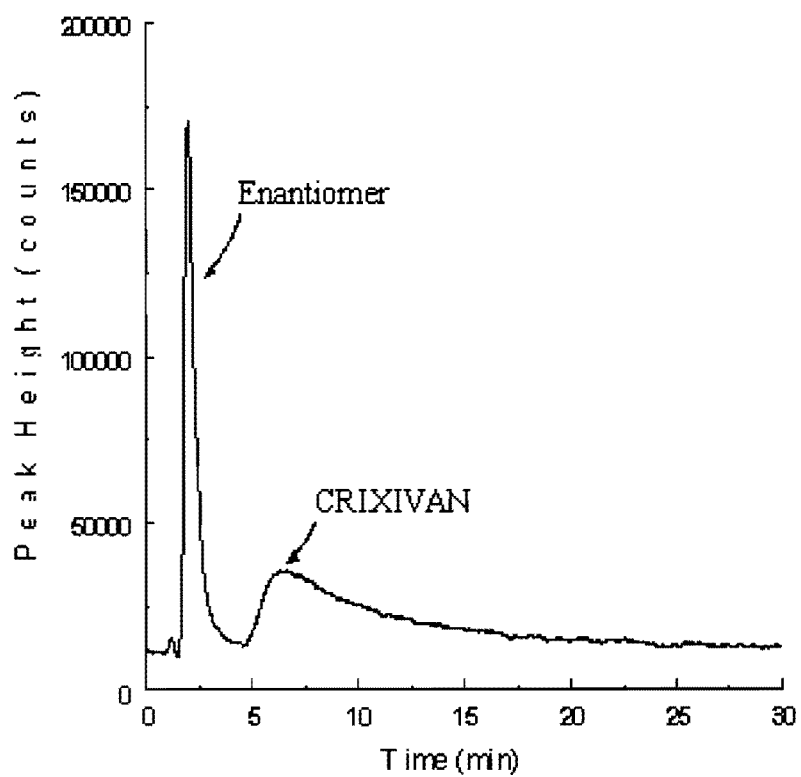
Table 4-2. Retention Factors (k) and Selectivity Factor α for CRIXIVAN™ Enantiomers on

Various Polymers. Mobile phase: 55/45 heptane/chloroform*; flowrate: 1.0 mL/min;

sample size: 4μg each enantiomer; column Temperature: 30°C; detection: 260nm.

	k non-imprinted	k imprinted	α
ACRYL	4.6	7.3	1.6
4-VP	1.5	1.6	1.1
MeACRYL	0.8	0.8	1.0
MAA (w/ 5% acetic acid)	*4.6*	*27.8*	*6.0*

* Except for the MAA column, for which acetic acid was added to the mobile phase.

phase. Once again, for the MAA polymer, it was necessary to add acetic acid to the mobile

phase to elute the enantiomers. The ACRYL and 4-VP polymers demonstrated modest

selectivity (1.6 and 1.1 respectively), indicating that imprints of CRIXIVAN™ can be formed

with fairly weak interactions. This may be a result of the cumulative effect of the multiple weak

interactions occurring between these monomers and the several functional groups on

CRIXIVAN™. While none of these interactions are strong, several moles of monomer can

interact with CRIXIVAN™ during the polymerization and cooperatively 'trap' some of the

structural features of the template into the polymer.

The IR experiments suggested that the ACRYL and 4-VP monomers would hydrogen

bond to a similar extent with the amide and hydroxyl groups of CRIXIVAN™, but only the

former monomer could undergo weak interactions with the piperazine and pyridinyl groups.

Thus, it was rationalized that these additional interactions led to sites in the ACRYL polymer

that were more defined than those of the 4-VP polymer, an idea that is supported by the greater

selectivity factor observed for the former polymer (Table 4-2).

The above explanation is further supported by the fact that the polymer prepared with

MeACRYL showed no selectivity (Table 4-2). This polymer was considered a suitable control

for our experiments because hydrogen bonding between this monomer and CRIXIVAN™ was

not expected to be favored in the pre-polymer solution. As a result, this monomer could not

orient itself around CRIXIVAN™ during the polymerization. If selectivity had been observed

for this polymer, this would have suggested that an imprint could result by simple

'entanglement' of CRIXIVAN™ within the backbone of the growing polymer. This is not the

case, suggesting that an arrangement of hydrogen bonding monomers around CRIXIVAN™

during the polymerization is necessary to achieve a successful imprint.

Comparing the retention factors of CRIXIVAN™ for each of the polymers (Table 4-2)

suggests that the backbone of the polymer does not significantly contribute to non-specific

retention of the CRIXIVAN™ enantiomers. This is evidenced by the very small retention factors

observed for the enantiomers on the MeACRYL polymer under the non-polar mobile phase

conditions. Thus, retention of CRIXIVAN™ on the imprinted polymers can be attributed to the

hydrogen bonding interactions with MAA, ACRYL, or 4-VP moieties. This observation is

noteworthy, as the performance of MIP's under non-polar solvent conditions has not previously

been studied and may be important for the future development of the technique. A typical

chromatogram for the ACRYL polymer is given in Figure 4-11.

While it appeared that the MAA polymer was more selective than the other polymers,

comparing the selectivity of these polymers using different mobile phases was not entirely

justified, as the effect of acetic acid and heptane on the selectivity of the polymers was not clear.

As a result, efforts were put forth to identify the effect of acetic acid and heptane on the MAA

separation, so the selectivity factor for this column could be compared to those of the other MIP

columns. To achieve this, the effect of acetic acid on the retention and selectivity of the

enantiomers on the MAA polymer was compared using both 55/45 heptane/chloroform (Figure

4-12) and chloroform (Figure 4-13). In both cases, increasing the acetic acid concentration

causes a decrease in both the retention and selectivity factors of the enantiomers. This behavior

Figure 4-11. Typical Chromatogram for the Separation of the CRIXIVAN™ Enantiomers on the

ACRYL Column. Mobile phase: 55/45 heptane/chloroform; flowrate: 1.0 mL/min;

sample size: 4μg each enantiomer; column Temperature: 30°C; detection: 260nm.

Figure 4-12. Effect of Acetic Acid on the Retention Factors (k) and Selectivity Factor (α) for the

CRIXIVAN™ Enantiomers. Mobile phase: 55/45 heptane/chloroform; flowrate:

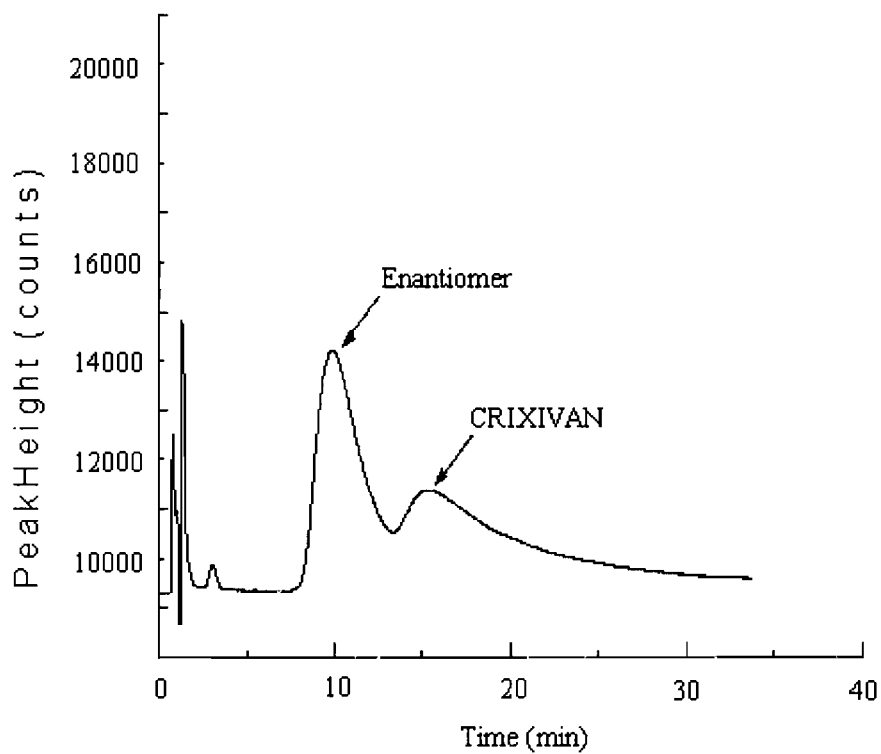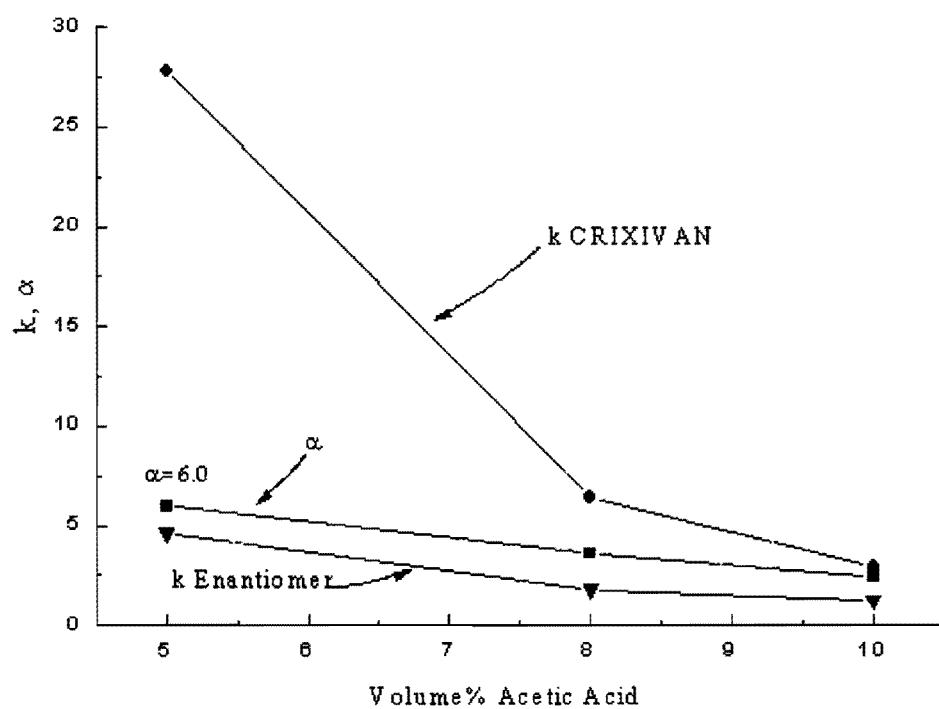1.0 mL/min; sample size: 50μg each enantiomer; column Temperature: 30°C;

detection: 260nm.

Figure 4-13. Effect of Acetic Acid on the Retention Factors (k) and Selectivity Factor (α) for the

CRIXIVAN™ Enantiomers. Mobile phase: Chloroform; flowrate: 1.0 mL/min;

sample size: 50μg each enantiomer; column Temperature: 30°C; detection: 260nm.
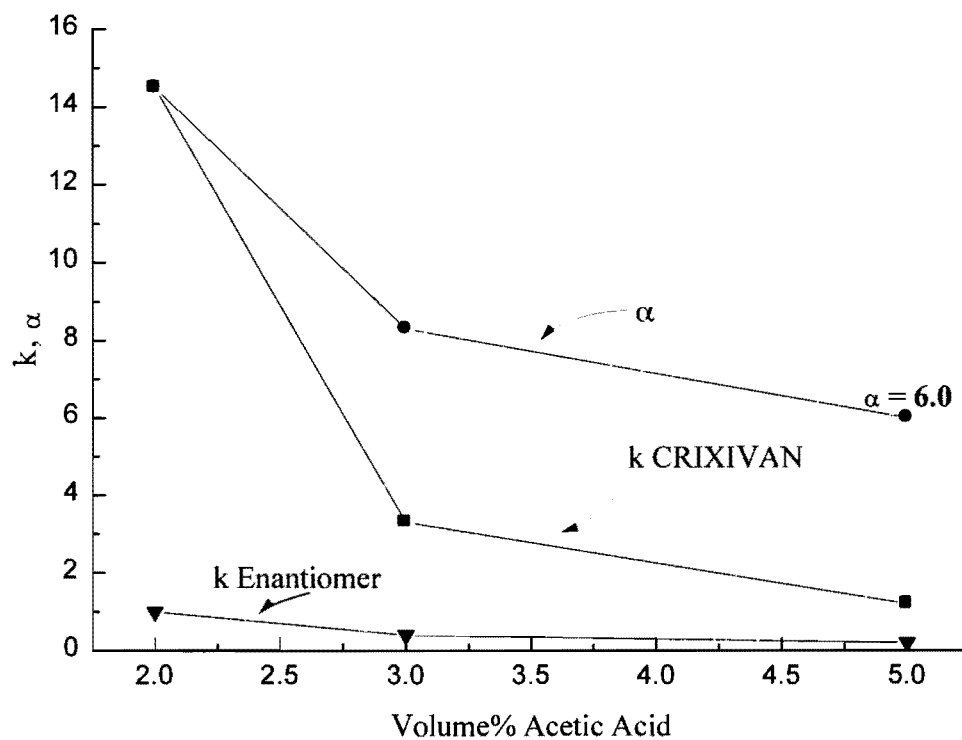
suggests that removal of acetic acid from either mobile phase (if possible) would only amplify the greater selectivity observed for the MAA polymer. Further, comparison of the retention and selectivity factors at 5% v/v acetic acid in each graph shows that non-selective retention of the enantiomers increases in the presence of heptane, but the selectivity factor (6.0) remains unchanged. These observations suggest that the MAA polymer is indeed substantially more selective than the other polymers, regardless of the mobile phase used.

Infrared Spectroscopy Studies of CRIXIVAN^{TM} / Methacrylic Acid Solutions.

As described above, IR spectroscopy can be used to observe hydrogen bonding interactions occurring between each functional monomer and CRIXIVAN^{TM} in the pre-polymer solution. The relative strength of these hydrogen bonds as observed by IR correlated with the order of selectivity of the corresponding polymers. Namely, the monomer (MAA) that formed the strongest hydrogen bonds with the surrogate portions of CRIXIVAN^{TM} gave an imprint with the best selectivity. For these experiments, to better assess the hydrogen bonding interactions occurring at each functional group of CRIXIVAN^{TM}, fragments of the parent molecule were used to separately observe these interactions. This approach, while a significant simplification of the actual system, was considered reasonable for the qualitative observations made above. However, a more rigorous analysis using CRIXIVAN^{TM} was also required to account for the possible cooperative effects associated with the binding of multiple functional monomers to this multi-functional template. This rationale prompted the second set of IR experiments described below.

To obtain quantitative information about hydrogen bonding in the pre-polymer solution, several CRIXIVAN^{TM}-MAA solutions were examined by IR spectroscopy. We felt that a clear

114

understanding of the position of the CRIXIVAN™–MAA equilibrium as a function of monomer concentration could be useful in determining the number of equivalents of monomer necessary to maximize the hydrogen bonding interactions with the template. For these studies, methacrylic acid was chosen as the model functional monomer because it had provided polymers with the best selectivity and its characteristic carbonyl stretch ($\sim$1695 cm^{-1}) is well resolved from the multiple bands of CRIXIVAN™. Figure 4-14. shows the carbonyl stretches for a 0.1M chloroform solution of methacrylic acid (1735cm^{-1}, 1695cm^{-1}). The spectra were taken under conditions that reasonably mimicked the actual polymerization solution*. The major (1695cm^{-1}) and minor stretches (1730 cm^{-1}) in Figure 4-14 arise from dimeric and monomeric methacrylic acid species respectively [127], each frequency being characteristic of the energy of the carbonyl stretch for that form of MAA:

'Free' (solvated)   'H-Bond Dimer'

C=O 1735 cm^{-1} C=O 1695 cm^{-1}
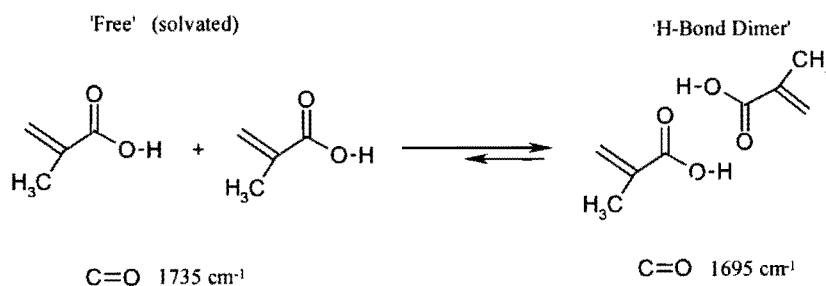
* EDMA was omitted because it interfered with the spectra. While EDMA likely complicates the hydrogen bonding equilibrium, we believe that the *trends* observed by IR for the MAA- CRIXIVAN™ hydrogen bonding are still valid because EDMA is a relatively weak H-bonding component of the solution.

115

Figure 4-14. Infrared Spectra of the Carbonyl Stretches for MAA Solvent: chloroform; concentration: 0.1M; Resolution: 1 cm^{-1}; Scans: 200x.
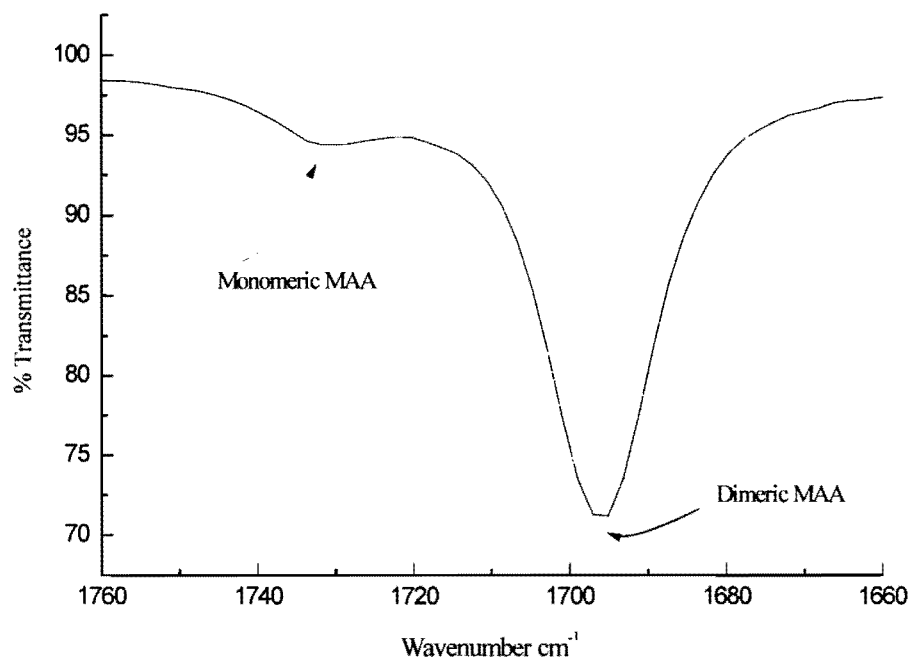
Comparison of the intensities of each peak suggested that the dimeric form predominates, as

expected for concentrated acids (>0.01M) in non-polar media [127]. When a portion

of the MAA forms hydrogen bonds with CRIXIVAN^{TM}, the above equilibrium will shift away

from the dimer:
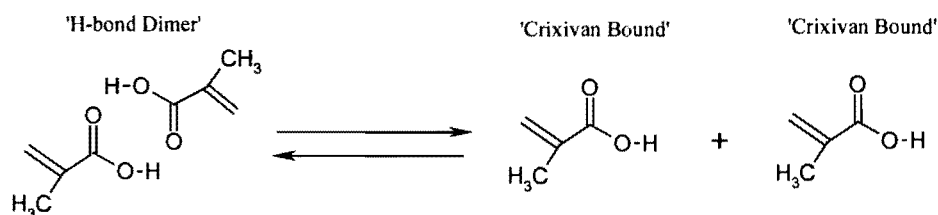
Along with this perturbation, it was hypothesized that the peak intensity at 1695cm^{-1} would

decrease as the carbonyl stretching energy for some of the MAA shifted to a value

characteristic of CRIXIVAN^{TM}-bound MAA. Figure 4-15 compares the 1695cm^{-1} region of the

IR spectra of 0.1M chloroform solutions of methacrylic acid alone and in the presence of 1

equivalent of CRIXIVAN^{TM}. Indeed, a decrease in the peak intensity (and peak area) is

observed for MAA in the presence of CRIXIVAN^{TM}.

The multi-functional nature of CRIXIVAN^{TM} suggests that the hydrogen bonding

stoichiometry between MAA and CRIXIVAN^{TM} may be greater than unity, depending on the

MAA concentration present in the pre-polymer solution. Viewing this equilibrium as a step

association, each addition of MAA to CRIXIVAN^{TM} is characterized by a separate equilibrium

constant (b) and the shape of the binding isotherm for this process depends on the relative values

of b for each step. A binding isotherm for this process was generated by monitoring the intensity

Figure 4-15. Infrared Spectra of the Carbonyl Stretch for MAA: 0.4M MAA alone (a);

MAA/Crixivan (b). Solvent: chloroform; concentration: 0.1M CRIXIVAN^{TM},

0.4M methacrylic acid; Resolution: 1 cm^{-1}; Scans: 200x.
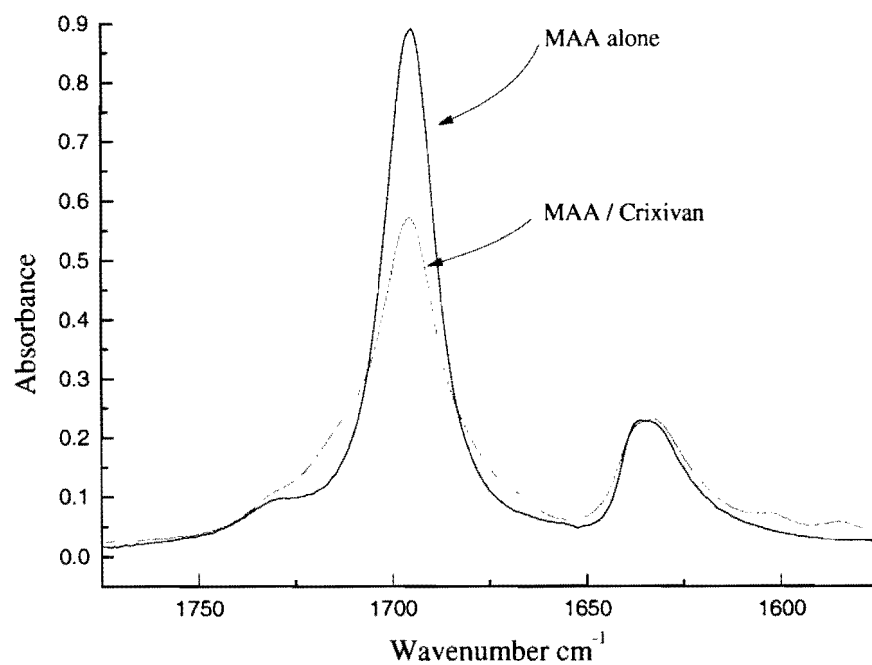
of the 1695 cm^{-1} stretch over a MAA concentration corresponding to ~0.5 – 20 mole equivalents of the CRIXIVAN^{TM} in solution. These intensities were compared to a calibration curve prepared for MAA solutions without CRIXIVAN^{TM} to calculate an 'effective loss' of the methacrylic acid dimer due to hydrogen bonding with CRIXIVAN^{TM}. From these data, a binding isotherm (q vs. C) representing the solution binding of MAA to CRIXIVAN^{TM} was constructed (see eqn. 4-3.). The calibration curve and binding isotherm are presented in Figures 4-16 and 4-17 respectively.

As shown in Figure 4-17, the binding of MAA to CRIXIVAN^{TM} extends beyond a 20-fold molar excess of this monomer, confirming that several moles of MAA associate with each mole of CRIXIVAN^{TM} in the pre-polymer solution.

To further probe the nature of this hydrogen bonded complex, the binding data were cast into the form of a Scatchard plot (see Figure 4-18). As shown, the Scatchard plot is non-linear, concave upward, indicating a 'negative cooperative' binding process. That is, the binding affinity of MAA decreases as successive moles of monomer bind to CRIXIVAN^{TM}. This observation was not surprising, since it was already shown that the MAA monomer binds to the several 'functional surrogates' of CRIXIVAN^{TM} to different extents, a trend that was also expected for corresponding functional groups on CRIXIVAN^{TM}. The IR data supports this premise as shown in Figure 4-19 which compares the perturbation of the MAA carbonyl stretch in the presence of the strongest, dimethylpiperazine, and weakest, 2-butanol, hydrogen bonding

Figure 4-16 Calibration Curve of the Infrared Carboxyl Intensities. Solvent: chloroform;

Resolution: 1 cm^{-1}; Scans: 200x.
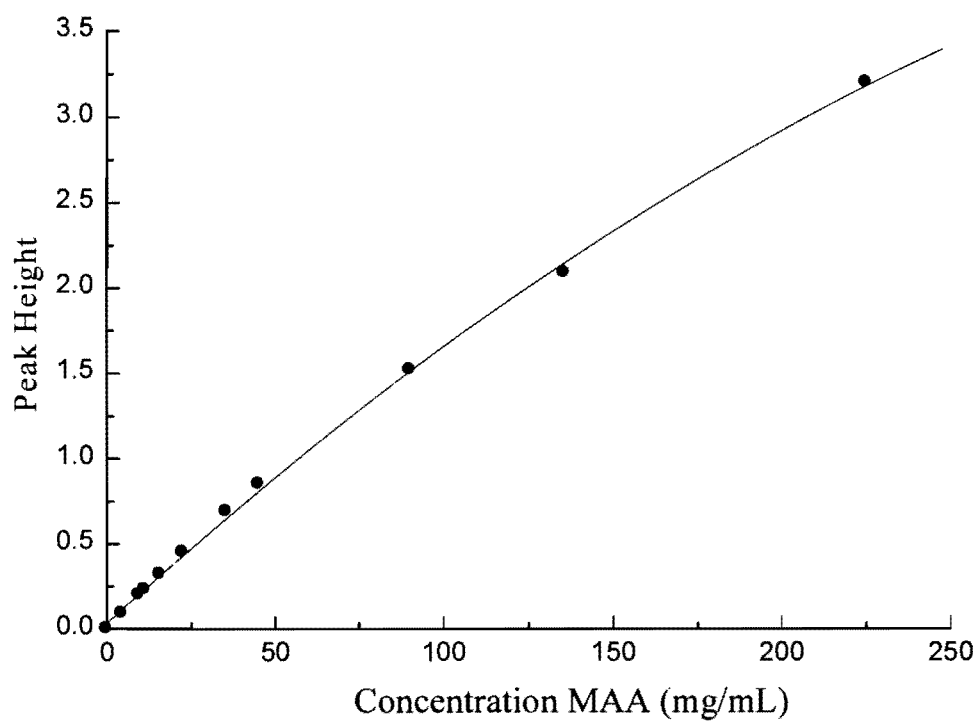
Figure 4-17 Binding Isotherm in the Presence of CRIXIVAN^{TM}. Solvent: chloroform;

Resolution: 1 cm^{-1}; Scans: 200x.

Figure 4-18. Scatchard Plot for Solution Binding of MAA to CRIXIVAN™: Solvent:

chloroform; concentration: 0.1M Crixivan; Resolution: 1 cm^{-1}; Scans: 200x.
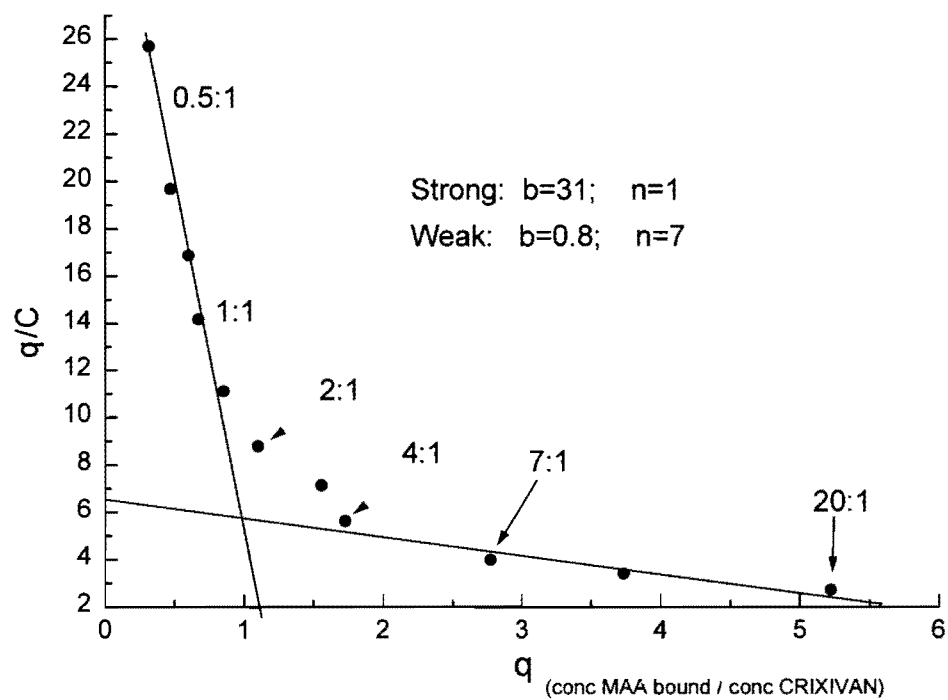
Figure 4-19. Infrared Spectra of the Carbonyl Stretch for MAA in the Presence of Piperazine
and 2-butanol. Solvent: chloroform; concentration: 0.1M; Resolution: 1 cm^{-1};
Scans: 200x.
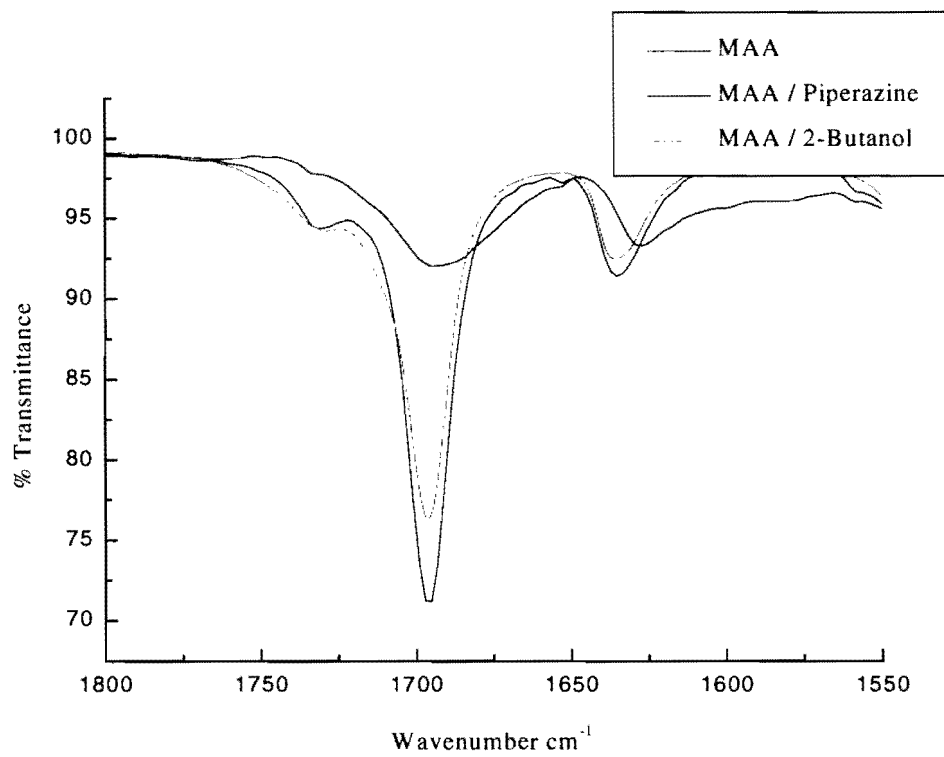
analogues of CRIXIVAN^{TM}. Based on the spectra, there appears to be a significant difference in the strength of the hydrogen bonds that each group forms with MAA. The corresponding spectra for the amide and pyridine analogues suggested that MAA interacts with these groups to extents intermediate to those of the piperazine and alcohol groups.

Closer analysis of the Scatchard plot suggested that it could be divided into two approximate linear portions separated by a curved intermediate region. The first portion corresponded to a MAA concentration range for which the hydrogen bonds are strong (0-2 CRIXIVAN^{TM} equivalents), while the second portion (2-20 equivalents) was indicative of a relatively weak binding region. As shown, the strong binding region (b = 31) corresponds to approximately one binding site (n=1, see x-intercept of plot) on the CRIXIVAN^{TM} molecule. It was rationalized that this binding must occur at the strongest hydrogen bonding fragment of CRIXIVAN^{TM}, the piperazine group. Interestingly, only one binding site is calculated even though the ring contains two nitrogens. It appears that the binding of a single mole of MAA with one of the nitrogen atoms on the piperazine ring hinders (either sterically or electronically) the interaction of a second mole of MAA with the second nitrogen. Alternatively, one mole of MAA may interact very strongly with both nitrogen atoms simultaneously, thereby disallowing the approach of a second mole of MAA toward the ring.

The weak binding region of the Scatchard plot (b = 0.8) was attributed to interactions of MAA with the remaining functional groups on CRIXIVAN^{TM}, thus forming a higher order hydrogen bonded complex. The number of binding sites for this portion was approximately 7, which is slightly larger than the total number of amide and hydroxyl groups on CRIXIVAN^{TM}.

However, it is possible that multiple moles of MAA interact with each group, so this number is, at least, reasonable.

To provide credence for the conclusions made about the Scatchard data, the IR spectra for each MAA-CRIXIVAN^{TM} solution were further analyzed to identify H-bonding shifts for the pyridine, amide, and hydroxyl substituents of CRIXIVAN^{TM}. The portions of the spectra corresponding to the C=C stretch of the pyridine group (1578cm^{-1}) and the C-N stretch of the amides (1515cm^{-1}) at each MAA concentration are presented in Figures 4-20 and 4-21 respectively. As shown, the pyridine stretch shifts smoothly over the entire MAA concentration range from 1578 to 1585 cm^{-1}. Thus, the hydrogen bond equilibrium for this functional group is superimposed upon both the strong and weak binding regions of the Scatchard plot, giving rise to the intermediate region occurring between approximately 2-4 equivalents of MAA. Conversely, the spectra for the amide C-N stretch (1515cm^{-1}, Figure 4-21) showed a relatively abrupt perturbation at MAA concentrations near the beginning of the weak portion of the Scatchard plot (~3 equivalents of MAA), after which a significant shift toward a higher frequency (~1535 cm^{-1}) occurred over the remaining MAA concentration range (3-20 equivalents). This suggests that a higher order structure of the MAA-CRIXIVAN^{TM} complex is formed within the weak the binding region, as MAA begins to interact with the amide groups of CRIXIVAN^{TM}. It was assumed that a weak hydrogen bonding interaction also occurs between MAA and the hydroxyl group of CRIXIVAN^{TM} within this region of the Scatchard plot, although the IR spectra were too complicated to identify a band shift associated with this interaction. The observation that a relatively weak interaction occurs between MAA and the functional surrogate, 2-butanol (see Figure 4-19) is indirect evidence that this interaction indeed occurs.

Figure 4-20. Overlay of the Crixivan Pyridinyl C=C Stretch in the Presence of Varying

Concentrations of MAA: Solvent: chloroform; concentration: 0.1M Crixivan;

Resolution: 1 cm^{-1}; Scans: 200x.
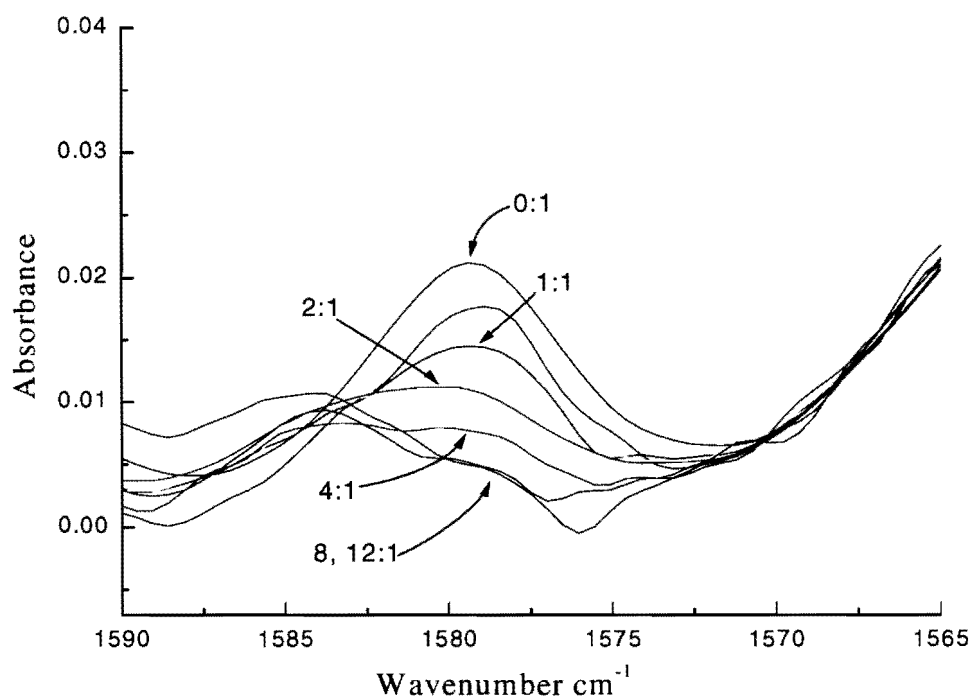
Figure 4-21. Overlay of the Crixivan Amide C-N Stretch in the Presence of Varying

Concentrations of MAA: Solvent: chloroform; concentration: 0.1M Crixivan;

Resolution: 1 cm^{-1}; Scans: 200x.
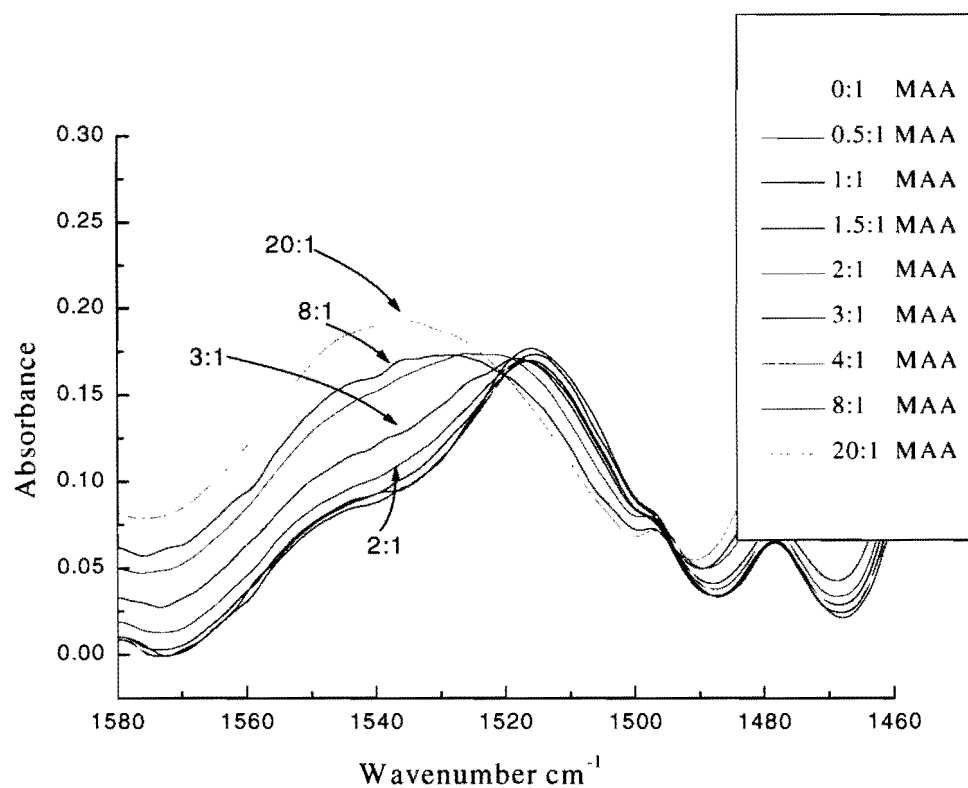
The MAA imprinted polymer used in our initial studies was prepared with a sufficient excess of MAA (7:1 mol/mol MAA/CRIXIVAN^{TM}) to achieve the high order hydrogen bonded complex described by the ATR-IR study above. Accordingly, a scheme representing the structure of the imprinted sites obtained for this polymer (i.e., 7:1 MAA polymer) was deduced and is presented in Figure 4-22. Since the interaction of MAA with CRIXIVAN^{TM} is an equilibrium process, there will likely be an excess of MAA not associated with Crixivan during the polymerization. This excess MAA is presented in its stable dimeric form in Figure 4-22.

As depicted in Figure 4-22, it is likely that each possible hydrogen-bonded form of the MAA is incorporated into the imprinted polymer. The MAA units which are associated with CRIXIVAN^{TM} become part of the imprinted sites, while the remainder of the acid units exist as randomly distributed hydrogen bonded dimers. This is an interesting hypothesis, because it suggests that the randomly distributed 'non-selective' sites on the polymer will be deactivated toward interaction with the analyte, a desirable result. Thus, for the MAA imprinted polymer phase, non-selective adsorption of an analyte far from an imprinted site should be minimal. Based on this assumption, an analyte that cannot access the imprinted sites would be expected to have minimal retention on a column prepared with this polymer. The chromatographic data in Figure 4-13 suggest that this is the case, as the CRIXIVAN™ enantiomer is eluted from the column with a small retention factor (k = 1.0).

To further test the validity of the scheme in Figure 4-22, three other MAA imprinted polymers were prepared using MAA concentrations corresponding to different regions on the

Figure 4-22. Proposed Imprinting Originating from the CRIXIVAN™ -Methacrylic Acid

Hydrogen Bonded Complex.
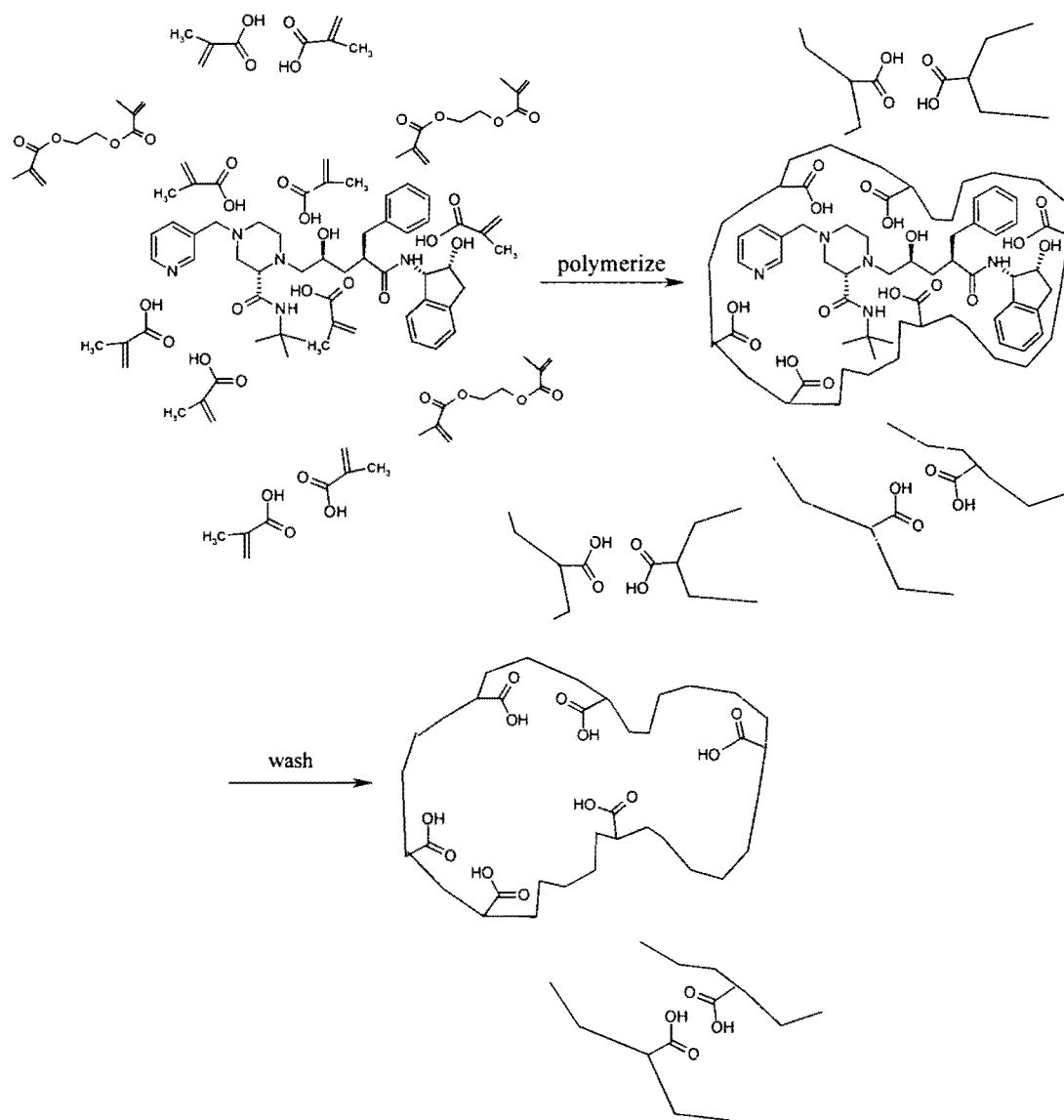
MAA-CRIXIVAN™ Scatchard plot (Figure 4-18). Two of the MIP's were prepared using only 1 and 2 mole equivalents of MAA relative to CRIXIVAN™ (1:1 and 2:1 polymers). Unlike the 7:1 MAA polymer evaluated above, the MAA concentrations used to prepare the 1:1 and 2:1 MAA polymers were too small to effect significant interaction between this monomer and the amide and hydroxyl functions of CRIXIVAN™. As a result, it was expected that the structure of the imprinted sites for these polymers would be determined only by interaction of MAA with the strong H-bonding groups (piperazine and pyridine) on CRIXIVAN™ during the polymerization. Conversely, the third additional polymer was prepared using an excess of MAA substantially greater (21:1 MAA polymer) than that of the original 7:1 MAA polymer. Thus, it was expected that the imprinted sites of this polymer would be defined by a H-bonded complex similar to that of the 7:1 MAA polymer (see Figure 4-22). The retention (k) and selectivity factors (α) for CRIXIVAN™ and its enantiomer are compared for each polymer in Table 4-3.

Comparison of the data for the 1:1 and 2:1 MAA polymers in Table 4-3 (compare columns 1:1[a] and 2:1[a]) indicates that the retention factor (k) of each enantiomer is greater on the 2:1 polymer, while the selectivity factors for these columns are essentially the same. The larger retention factors for the 2:1 polymer is expected, as it possesses twice the number of potential binding sites than the 1:1 polymer. However, the similar selectivity factors suggest that the structure of the imprinted sites are similar for each polymer. Thus, it appears that the structure of the sites formed during the polymerization is independent of the number of points of interaction between MAA and CRIXIVAN™ when these interactions occur at the same region of the template. It is important to reiterate here that the ATR-IR studies above suggested that the hydrogen bonding interactions

Table 4-3. Retention Factors (k') and Selectivity Factor (α) for CRIXIVAN™ /Enantiomer on MAA Imprinted Polymer Columns. Mobile phase: 1-3% acetic acid in chloroform; flowrate: 1.0 mL/min; sample size: 7 µg (1:1, 2:1) or 50 µg (7:1, 21:1) each enantiomer; column Temperature: 30°C; detection: 260nm.

MAA polymer	1:1[a]	2:1[a]	2:1[b]	7:1[b]	7:1[c]	21:1[c]
k'$_{enantiomer}$	0.2	3.4	0.4	1.0	0.4	1.9
k'$_{Crixivan}$	0.7	10.7	0.7	14.5	3.3	15.4
α	3.5	3.1	1.8	14.5	8.3	8.1
SD for α	(0.8)	(0.2)	(0.6)	(1.2)	(1 0)	(0.4)

[a] Mobile Phase: 1% acetic acid in chloroform

[b] Mobile Phase: 2% acetic acid in chloroform

[c] Mobile Phase: 3% acetic acid in chloroform

between CRIXIVAN™ and the first two equivalents of MAA occur solely at the leftmost portion of the template (i.e., at the piperazine and pyridine groups.).

A distinct contrast is seen when the selectivity of the 2:1 and 7:1 MAA polymers are compared (compare columns 2:1[b] and 7:1[b]). The selectivity of the 7:1 MAA polymer (14.5) is nearly one order of magnitude greater than that of the 2:1 MAA polymer (1.8) under the same mobile phase conditions. Apparently, when a sufficient concentration of MAA is present during the polymerization to hydrogen bond with the entire structure of CRIXIVAN™, the resulting polymer possesses well-defined imprinted sites of high selectivity. This premise is further supported by the observation that the selectivity factors for the 7:1 MAA and 21:1 MAA polymers are essentially the same (compare α in columns 7:1[d] and 21:1[d]). It appears that once the hydrogen bonding sites on CRIXIVAN™ become 'saturated' with MAA, further addition of MAA to the polymerization mixture does not improve the selectivity of the imprinted sites. This is reasonable, as it is expected that most of the additional MAA present during the formation of the 21:1 polymer cannot interact with CRIXIVAN™ and therefore becomes randomly incorporated within the polymer. This results in larger non-specific retention of the enantiomers on this column (compare k's in columns 7:1[d] and 21:1[d]).

The data above and Figure 4-22 suggest that a well defined imprint of CRIXIVAN™ is formed when enough MAA is present during the polymerization to assemble around the entire template. This was the case for the 7:1 MAA polymer. While this polymer demonstrated marked selectivity for the CRIXIVAN™ enantiomer, probe analytes that are more similar to the template should provide a more rigorous test of the recognition ability of the imprint.

Accordingly, three isomers that differ from CRIXIVAN™ by the configuration around 1 or 2 of the stereo-centers were also evaluated. The structures of these isomers are presented in Figure 4-23. The selectivity factors of each isomer relative to the CRIXIVAN™ enantiomer are compared in Table 4-4 for the 7:1 MAA and 2:1 MAA polymers.

The data in Table 4-4 supports the assertion that imprinted sites complementary to the entire CRIXIVAN™ structure are formed only when this molecule is completely surrounded by MAA during the polymerization. For these data, the isomers with small selectivity factors (near 1) elute close to the enantiomer and are therefore essentially rejected from the CRIXIVAN™-imprinted sites. Conversely, those which demonstrate a selectivity factor closer to CRIXIVAN™ (~ 8 and 2 for the 7:1 and 2:1 polymers respectively) must have at least limited access to the imprinted sites. For both polymers, the selectivity factors for the R-piperazine and Bis-epi isomers are smaller than the 4-epi isomer, indicating that the 4-epi isomer has better access to the CRIXIVAN™-imprinted sites on both polymers. The poorer 'fit' of the R-piperazine and Bis-epi isomers is likely due to the opposing configuration of the relatively bulky t-butyl amide and phenyl substituents versus the small steric change associated with the opposing hydroxyl group of the 4-epi isomer.

More intriguing, however, is the relative selectivity of each polymer for the 4-epi isomer and CRIXIVAN™. The 7:1 polymer is substantially more selective for CRIXIVAN™ ($\alpha = 8.3$ vs. 2.5), while the 2:1 polymer demonstrates approximately the same selectivity factor for these compounds (α ~2). As mentioned above, the 7:1 polymer likely incorporates a MAA-CRIXIVAN™ complex that leads to a well defined site selective for the entire structure of

Figure 4-23. Structures of Various Isomers of CRIXIVAN™
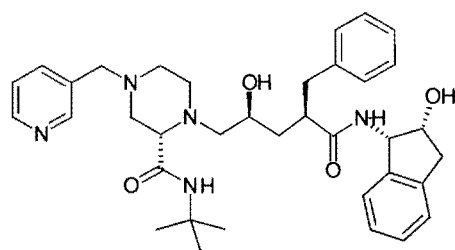
Crixivan
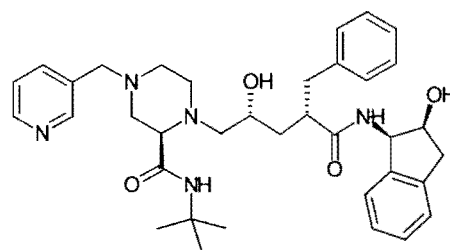
Enantiomer
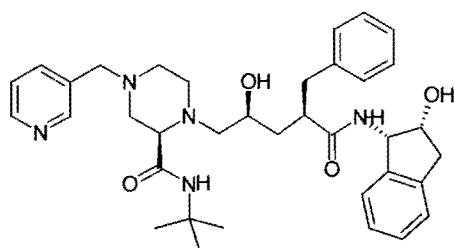
R-piperazine isomer
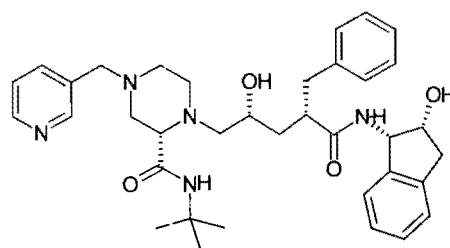
Bis-epi isomer
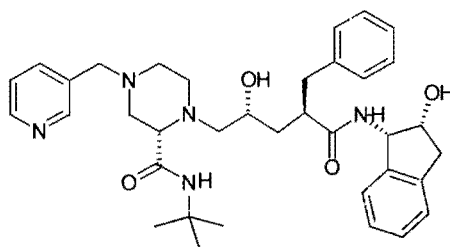
4-epi isomer

Table 4-4. Retention Factors (k) and Selectivity Factor (α) for Various Isomers of

CRIXIVAN™ on the MAA Imprinted Polymer Columns. Mobile phase: 2% (2:1),

3% (7:1) acetic acid in chloroform; flowrate: 1.0 mL/min; sample size: 7μg (2:1)

50μg (7:1) each enantiomer; column Temperature: 30°C; detection: 260nm.

MAA polymer 7:1	k	k enantiomer	α	SD for α
CRIXIVAN™	**3.3**	**0.4**	**8.3**	**(1.0)**
R-piperazine isomer	0.5	0.4	1.3	(nd)
Bis-epi isomer	0.6	0.4	1.5	(nd)
4-epi isomer	**1.0**	**0.4**	**2.5**	**(nd)**

MAA polymer 2:1	k	k enantiomer	α	SD for α
CRIXIVAN™	**0.7**	**0.4**	**1.8**	**(0.6)**
R-piperazine isomer	0.6	0.4	1.5	(0.1)
Bis-epi isomer	0.3	0.4	0.8	(0.1)
4-epi isomer	**0.8**	**0.4**	**2.0**	**(0.4)**

CRIXIVAN™. As a result, significant selectivity is observed between CRIXIVAN™ and the 4-epi isomer even though the latter compound only differs from CRIXIVAN™ by the orientation of a relatively small hydroxyl group. However, for the 2:1 polymer, it was argued that the CRIXIVAN™ template was only 'held' by MAA at the piperazine and pyridine groups during polymer formation. As a result, it is likely that the imprints formed for this polymer are less selective for the remainder of the CRIXIVAN™ molecule. Since CRIXIVAN™ and 4-epi differ by only the configuration of a small substituent in the center of the molecule, the sites of the 2:1 polymer cannot differentiate between these two compounds. The ability of the 2:1 polymer to recognize the bis-epi isomer suggests that the imprinted sites of this polymer possess some shape selectivity for larger substituents. However, it appears that the sites for this polymer are less defined than those of the 7:1 polymer.

Conclusions

Several monomer systems were evaluated for imprinting the HIV Protease Inhibitor, CRIXIVAN™. Attenuated Total Reflectance-Infrared Spectroscopy was used to observe the hydrogen bonding interactions between functional analogues of CRIXIVAN™ and each monomer. The order of selectivity of the resulting imprinted polymers correlated well with the number and strength of the hydrogen bonds occurring between these analogues and each monomer in the polymerization solution. The MAA functional monomer provided an imprint with the best selectivity and was subject to further study by IR spectroscopy. IR spectroscopic studies probing the MAA- CRIXIVAN™ hydrogen bonding equilibrium suggested that a molar excess of MAA near 7:1 relative to CRIXIVAN™ is necessary to achieve an imprint with

maximum selectivity (14.5). This concentration provided a hydrogen-bonded arrangement of MAA around the entire template structure. Imprinted polymers prepared with lower concentrations of MAA (1:1 and 2:1 mol/mol MAA:CRIXIVAN™) demonstrated substantially lower selectivity factors because insufficient amounts of MAA were present during the polymerization to assemble around the template to completely 'capture' all of its structural features. On the other hand, a polymer prepared with substantially larger concentrations, 21:1 mol/mol MAA/CRIXIVAN™ demonstrated similar selectivity to the 7:1 polymer, but greater non-specific binding of the CRIXIVAN™ enantiomers. This likely occurred because the CRIXIVAN™ hydrogen bonding sites are saturated with MAA at concentrations near 7:1 mol/mol MAA/ CRIXIVAN™ and most of the additional 14 equivalents of MAA become randomly incorporated within the polymer.

These studies suggest that an optimal functional monomer and monomer concentration exist for a MIP template to obtain a polymer with maximum selectivity. Thus, for the development of MIP technology, it is desirable to have a convenient method such as IR spectroscopy to assess the strength of the interactions occurring between a template and monomer prior to polymer formation to arrive at an appropriate monomer system for the template of interest.

Chapter 5.

Overall Conclusions

Recent research in molecular imprinting has focused on two primary goals; achieving an unequivocal fundamental description of the imprinting process and applying the technique to a variety of chemical problems. While numerous achievements have been made, the complexity of imprinted polymer systems renders both of these tasks challenging. This dissertation has outlined several studies that are a positive contribution to an expanding research effort focused on understanding the selectivity of MIP systems.

The mechanism of selectivity of an imprinted polymer prepared for dansyl-L-phenylalanine was investigated. The selectivity of the imprint is determined by two factors; the structure of the imprint achieved during polymer formation and the conditions under which the imprint rebinds dansyl-L-phenylalanine. Both of these processes are governed by hydrogen bonding interactions between the template and the functional groups used to prepare the imprinted polymer. For the rebinding of dansyl-L-phenylalanine to its imprint, it appears that selectivity occurs by a cooperative process that involves a correct steric 'fit' of its structure into an imprinted cavity that, in turn, provides for interaction with complementary functional groups inside the cavity. Thus, compounds that differed from the template in shape or functionality could not undergo strong interactions at the imprinted sites and were only weakly bound to the polymer. Further, solvents may be introduced during the rebinding step (the solvent was the mobile phase competitor in this study) that compete with the template for interactions at the imprinted sites and therefore alter the selectivity of the polymer.

Construction of the imprinted sites during the polymerization step, as shown for a CRIXIVAN™ template, requires the presence of strong interactions between the template and the monomers to be incorporated within the polymer. It was shown that the functional monomer must interact with the template at several points around its structure to maximize the selectivity of the resulting polymer. It appears that this requirement results in imprinted sites that are highly defined for the entire template structure. Thus, to achieve an imprint with maximum selectivity, the nature and concentration of the functional monomer in the pre-polymer solution must be optimized for a particular MIP system. Spectroscopic methods such as IR and NMR spectroscopy are useful tools for arriving at an optimal polymer solution for a template molecule of interest.

The field of molecular imprinting has brought exciting challenges to chemical researchers and holds tremendous potential for several areas of chemistry. MIP's are especially valuable to the field of chiral separations. It is our hope that the work presented within provides further motivation to embrace MIP's as practical alternatives to traditional chiral phases.

Literature Cited

1. M.S. Tswett, Tr. Protok. Varshav. Obshch. Estestvoispyt. Otd. Biol; **1905**; p. 14.

2. L.S. Ettre. *J. Chrom. Lib.* **1979**, *17*, 438-505.

3. M.C. Ringo, C.E. Evans *Anal. Chem.* **1998**, *70*, 315-321A.

4. C. Horvath *J. Chrom. Lib.* **1979**, *17*, 151-158.

5. H.A. Strobel, W.R. Heineman Chemical Instrumentation: A Systematic Approach, John Wiley and Sons: New York, **1989**; pp. 927-958.

6. H. Englehardt, H. Elgass in Cs Horvath (Editor), High Performance Liquid Chromatography. Advances and Perspectives Vol. 1, Academic Press: New York, **1980**; p. 208.

7. H. Colin, C. Eon, G. Guiochon *J. Chromatogr.* **1976**, *122*, 223.

8. M. Jaroniec *J. Chromatogr. A* **1993**, *656*, 37-50.

9. C.H. Lochmuller, D.R. Wilder *J. Chromatogr. Sci.* **1979**, *17*, 574.

10. J.G. Dorsey, K.A. Dill *Chem. Rev.* **1989**, 331.

11. P.W Carr, J. Li, A.J. Dallas, D.I. Eikens, L.C. Tan *J. Chromarogr. A.* **1991**, *586*, 1.

12. D.E. Martire, R.E. Boehm *J. Phys. Chem.* **1980,** *84*, 3620.

13. A. Vailaya, Cs. Horvath *J. Chromatogr. A.* **1998**, *829*, 1-27.

14. L.R. Snyder, Principles of Adsorption Chromatography, Marcel Dekker: New York, **1968**.

15. L.R. Snyder, H. Poppe *J. Chromatogr.* **1980**, *84*, 363.

16. A.J.P. Martin *Biochem. Soc. Symp.* **1949**, *3*, 4.

17. W.R. Melander, B. Chen, Cs. Horvath *J. Chromatogr.* **1979**, *185*, 93-109.

18. H. Poppe *J. Chromatogr. A* **1993**, *656*, 19-36.

19. F. Riedo, E. Kovats *J. Chromatogr.* **1982**, *239*, 1.

20. A.J. Muller, P.W. Carr *J. Chromatogr.* **1983**, *318*, 34.

21. T. Fornstedt, P. Sajonz, G. Guiochon *Chirality* **1998**, *10*, 375-381.

22. B. Feibush, N. Grinberg, in Chromatographic Chiral Separations, M. Zeiff, L. Crane, eds., Marcel Dekker, Inc.: New York, **1988**; p 1.

23. W. Schlenk *Experentia,* **1952**, *8*, 337.

24. F.H. Dickey *Proc. Natl. Acad. Sci.* **1949**, *35*, 227.

25. A.H. Beckett, P. Anderson *J. Pharm. Pharmacol.* **1963**, *15*, 253T.

26. G.M. Henderson, H.G. Rule *J. Chem. Soc.* **1939**, 1568.

27. M. Kotake, T Sakan, N. Nakamura, S. Senon *J. Am. Chem. Soc.* **1951**, *73*, 2973.

28. C.E. Dangliesh *J. Chem. Soc.* **1952**, 3940.

29. K.Closs, C.K. Hang *Chem. Ind.* **1953**, 103.

30. L.E. Rhuland, E. Work, R.E. Denman, D.S. Hoare *J. Am. Chem. Soc.* **1955**, *77*, 4844.

31. C.F. Contractor, J. Wragg *Nature* **1965**, *208*, 71.

32. E. Gil-Av, B. Feibush, R. Charles-Sigler, Gas Chromatography; Institute of Petroleum: London, **1967**; p. 227.

33. K. Cabrera, D. Lubba *J. Chromatogr.* **1994**, *666*, 433.

34. R. Thompson et al. *Anal. Chem.* **1995**.

35. W.H. Pirkle *J. Chromatogr.* **1991**, *1*, 558.

36. J. Hermansson, G. Schill, in Chromatographic Chiral Separations; M. Zeiff, L. Crane, eds., Marcel Dekker, Inc.: New York, **1988**; p 245.

37. C. Yu, K. Mosbach *J. Org. Chem.* **1997**, *62*, 4057.

38. Sreenivasan *Die Angew. Makrom. Chem.* **1997**, *65*, 246.

39. D. Spivak, M. Gilmore, K.J. Shea *J. Am Chem. Soc.* **1997**, *119*, 4388.

40. F.H. Dickey *J. Phys. Chem.* **1955**, *59*, 695-707.

41. R. Curtis, U. Colombo *J. Am. Chem. Soc.* **1952**, *74*, 3961.

42. V.V. Patrikeen, A.F. Sholin *Mol. Khromatogr.* **1964**, 66-72.

43. G. Wulff, A. Sarhan *Angew. Chem.* **1972**, *84*, 364.

44. G. Wulff, A. Sarhan *US-A 4 127730* **1978**.

45. G. Wulff, A. Sarhan, K. Zabrocki *Tetrahedron Lett.* **1973**, 4329-4332.

46. G. Wulff, R. Kemmorer, J. Vietmeier *Nouveau J. DeChemie* **1982**, *12*, 681-687.

47. G. Wulff *Angew. Chem Int. Ed. Eng.* **1995**, *34*, 1813.

48. M. Kempe, M. Mosbach *J. Chromatogr.* **1995**, *694*, 3-13.

49. G. Wulff, E. Lohmar *Isr. J. Chem.* **1979**, *18*, 279-284.

50. A. Sarhan, G. Wulff *Makromol. Chem.* **1982**, 85.

51. G. Wulff, W. Vesper *J. Chromatogr.* **1978**, *167*, 171.

52. G. Wulff, S. Schauhoff *J. Org. Chem.* **1991**, *56*, 395.

53. A. Kugimiya, J. Matsui, T. Takeuchi, K. Yano, H. Muguruma, A. Elgersma, I. Karube *Anal. Lett.* **1995**, *28*, 2317-2323.

54. L.I. Andersson, K. Mosbach *J. Chromatogr.* **1990**, *516*, 313.

55. L.I. Andersson, D.J. O'Shannessy, K. Mosbach *J. Chromatogr.* **1990**, *513*, 167.

56. G. Wulff, W. Best, A. Akelah *Reactive Polymers* **1984**, *2*, 167.

57. K. Shea, D. Sasaki *J. Am. Chem. Soc.* **1989**, *111*, 3442-3444.

58. K. Shea, T. Dougherty *J. Am. Chem. Soc.* **1986**, *108*, 1091-109.

59. G. Wulff, B. Heide, G. Helfmeier *J. Am. Chem. Soc.* **1986**, *108*, 1089-1091.

60. G. Wulff, Vietmeier *J. Makromol. Chem.* **1989**, *190*, 1717.

61. K. Shea, D. Sasaki *J. Am. Chem. Soc.* **1991**, *113*, 4109.

62. M. Kempe, K. Mosbach *J. Chromatogr.* **1995**, *691*, 317.

63. D. O'Shannessy, B. Ekberg, K. Mosbach *Anal. Biochem.* **1989**, *177*, 144.

64. M. Kempe, K. Mosbach *Tetrahedron Lett.* **1995**, *36*, 3563.

65. M. Kempe, K. Mosbach *Int. J. Peptide Res.* **1994**, *44*, 603.

66. C.K. Mathews, K.E. van Holde, Biochemistry, Benjamin/Cummings Publishing Co., Inc.: California, **1990**.

67. R.F. Taylor, Protein Immobilization: Fundamentals and Applications, Marcel Dekker, Inc.: New York, **1991**; pp. 263-303.

68. G. Vlatakis, L.I. Andersson, R. Muller, K. Mosbach *Nature* **1993**, *361*, 645-647.

69. L.I. Andersson, Antibody Mimics Obtained by Noncovalent Molecular Imprinting, ACS Symposium Series **1995**, *586*, 89-96.

70. M. Senholdt, M. Siemann, K. Mosbach, L.I. Andersson *Anal. Lett.* **1997**, *30*. 1809-1821.

71. D. Kritz, K. Mosbach *Anal. Chim. Acta* **1995**, *300*, 71-75.

72. S.A. Piletsky, I, Ya. Dubey, D.M. Fedoryak, V.P. Kukhar *Biopolymer and Cell* **1990**, *6*, 55-58.

73. S.A. Piletsky, Y.P. Phrhometz, N.V. Lavryk, T.L. Panasyuk, A.V. El'skaya *Sensors and Actuators B* **1994**, *18-19*, 629-631.

74. D. Kritz, O. Ramstrom, A. Svensson, K. Mosbach *Anal. Chem.* **1995**, *67*, 2142-2144.

75. O. Ramstrom, L.I. Anderson, K. Mosbach *J. Org. Chem.* **1993**, *58*, 7562-764.

76. P. Turkewitsch, B. Wandely, G.D. Darling, W.S. Powell *Anal. Chem.* **1998**, *70*, 2025-2030.

77. S.A. Piletsky, E.V Piletskaya, K.Yano, A. Kugimiya, A.V. Elgersma, R. Levi, U. Kahlow, T. Takeuchi, I. Karube *Anal. Lett.* **1996**, *29*, 157-170.

78. J. Matsui *Anal. Commun.* **1998**, *35*, 225-227.

79. R. Levi, S. McNiven, S.A. Piletsky, S. Cheong, K. Yano, I. Karube *Anal. Chem.* **1997**, *69*, 2017-2021.

80. S. McNiven, M. Kato, R. Levi, K. Yano, I. Karube *Anal. Chim. Acta* **1998**, *365*, 69-74.

81. B. Sellergren *Anal. Chem.* **1994**, *66*, 1578-1582.

82. M. Muldoon, L. Stanker *Anal. Chem.* **1997**, *69*, 803-808.

83. M. Muldoon, L. Stanker *J. Agric. Food. Chem.* **1995**, *43*, 1424-1427.

84. M. Siemann, L.I. Andersson, K. Mosbach *J. Agric. Food. Chem.* **1996**, *44*, 141-145.

85. J. Matsui, Y. Miyoshi, O. Doblhoff-Dier, T. Takehuchi *Anal. Chem.* **1995**, *7*, 4404-4408.

86. L. Ye, O. Ramstrom, K. Mosbach *Anal. Chem.* **1998**, *70*, 2789-2795.

87. L.I. Andersson, A. Paprica, T. Arvidsson *Chromatographia* **1997**, *46*, 57-62.

88. W.M. Mullett, E.P.C Lai *Anal. Chem.* **1998**, *70*, 3636-3641.

89. D.K. Robinson, K. Mosbach *J. Chem. Soc., Chem. Commun.* **1989**, *14*, 969-970.

90. A. Zander, P. Findlay, T. Renner, B. Sellergren *Anal. Chem*, **1998**, *70*, 3304-3314.

91. S.E. Bystrom, A. Borje, B. Akermark *J. Am. Chem. Soc.* **1993**, *115*, 2081-2083.

92. B. Sellergren, K.J. Shea *Tetrahedron* **1994**, *8*, 1403-1406.

93. R. Muller, L.I. Andersson, K. Mosbach *Makromol. Chem.* **1993**, *14*, 637-641.

94. K. Ohkubo *Kobunshi Ronbunshu* **1995**, *52*, 644-649.

95. C. Overberger, M. Morimoto *J. Am. Chem.* **1971**, *93*, 3222.

96. D. J. O'Shannessy, L.I. Andersson, K. Mosbach *J. Mol. Recog.*, **1989**, *2*, 1-5.

97. R. Curti, U. Columbo *J. Am . Chem. Soc.* **1952**, *74*, 3961.

98. G. Wulff, J. Kemmerer, J. Vietmeier, H.G. Poll *Nouveau J. DeChimie.* **1982**, *6*, 681-687.

99. G. Wulff, J. Gimpel *Makromol. Chem.* **1982**, *183*, 2469-2477.

100. B. Sellergren, K.J. Shea *J. Chromatogr.* **1995**, *690*, 29-39.

101. B. Sellergren *Chirality* **1989**, *1*, 63-68.

102. O. Ramstrom, R.J. Ansell *Chirality* **1998**, *10*, 195-209.

103. G. Wulff in Chromatographic Chiral Separations; M. Zeiff, L. Crane, eds., Marcel Dekker, Inc.: New York, **1988**; p.15.

104. A.G. Mayes, L.I. Andersson, K. Mosbach *Anal. Biochem.* **1994**, *222*, 483-488.

105. A. Kugimiya, J. Matsui, T. Takeuchi, K. Yano *Anal. Lett.* **1995**, *28*, 2317-2323.

106. B. Sellergren, A Practical Approach to Chiral Separations by Liquid Chromatography; G. Subramanian (Editor), **1994**; pp. 69-93.

107. O. Ramstrom, I.A. Nicholls, K. Mosbach *Tetrahedron* **1994**, *5*, 649-656

108 J. Matsui, I.A. Nichols, T. Takeuchi *Tetrahedron*, **1996**, *7*, 1357-1361.

109. B. Sellergren, M. Lepisto, K. Mosbach *J. Am. Chem. Soc.* **1988**, *110*, 5853-5860.

110. B. Sellergren, K.J. Shea *J. Chromatogr.* **1993**, *635*, 31-49.

111. G. Mayes, K. Mosbach *Anal. Chem.*, **1996**, *68*, 3769-3774.

112. J. Matsui, T. Takeuchi *Anal. Commun.* **1997**, *34*, 199-200.

113. J. Matsui, Y. Miyoshi, T. Takeuchi *Chem. Lett.* **1995**, *11*, 1007-1008.

114. G.C. Pimentel, A.L. McClellan, The Hydrogen Bond, W.H. Freeman and Company: San Francisco and London, **1960**.

115. T. Neuheuser, B.A. Hess, C. Reutel, E. Weber *J. Phys. Chem.* **1994**, *98*, 6459-6467.

116. S.N. Vinogradov, R.H. Linnell, Hydrogen Bonding, Van Nostrand Reinhold Company: New York, **1971**.

117. G.A. Jeffrey, W. Saenger, Hydrogen Bonding in Biological Structures, Springer-Verlag: Berlin, **1994**.

118. P. Schuster, G. Zundel, C. Sandorfy, The Hydrogen Bond, Vol 1., North-Holland Publishing Company: Amsterdam, **1976**.

119. J. Calvin Giddings, Unified Separation Science, Wiley: Chichester, **1991**.

120. K. Mosbach *Trends Biochem. Sci.* **1994**, *19*, 9.

121. G. Guichon, S.G. Shirazi, A.M. Katti, Fundamentals of Preparative and Nonlinear Chromatography, Academic Press: Boston, **1994**.

122. T. Fornstedt, Z. Guoming, G. Guiochon *J. Chromatogr.* **1996**, *742*, 55.

123. C. Reichardt, Solvent Effects in Organic Chemistry, VCH Verlagsgesellshaft mbH, D-6940: Weinheim, Germany, **1990**; p. 14.

124. P. Schuster (ed.) *Hydrogen Bonds; Top. Curr. Chem.* **1984**, *120*, 1-113.

125. H.S. Andersson, I.A. Nicholls *Bioorg. Chem.* **1997**, *25*, 203-211.

126. C.R. Cantor and P.R. Schimmel, Biophysical Chemistry, W.H. Freeman and Company: New York, **1980**.

127. K. Nakanishi, P.H. Solomon Infrared Absorption Spectroscopy, Holden-Day: Oakland, **1976**; pp.10-56